

Oncogenic KRAS Expression and Signaling

by

Benjamin Logan Lampson

Department of Pharmacology and Molecular Cancer Biology  
Duke University

Date: June 8, 2011

Approved:

---

Christopher M. Counter, Supervisor

---

William F. Marzluff

---

Christopher V. Nicchitta

---

Tso-Pang Yao

Dissertation submitted in partial fulfillment of  
the requirements for the degree of Doctor of Philosophy in the Department of  
Pharmacology and Molecular Cancer Biology in the Graduate School  
of Duke University

2011

ABSTRACT

Oncogenic KRAS Expression and Signaling

by

Benjamin Logan Lampson

Department of Pharmacology and Molecular Cancer Biology  
Duke University

Date: June 8, 2011

Approved:

---

Christopher M. Counter, Supervisor

---

William F. Marzluff

---

Christopher V. Nicchitta

---

Tso-Pang Yao

An abstract of a dissertation submitted in partial  
fulfillment of the requirements for the degree  
of Doctor of Philosophy in the Department of  
Pharmacology and Molecular Cancer Biology in the Graduate School  
of Duke University

2011

Copyright by  
Benjamin Logan Lampson  
2011

## Abstract

RAS is a small GTPase that helps to convert extracellular cues into intracellular actions. It is the most commonly mutated oncogene and is found in an active mutant form in 90% of pancreatic cancers. Therefore, study of how this protein is made and then how this protein signals in the cell could provide the foundation for novel approaches to treat RAS-driven malignancies.

First I demonstrate that the level of protein expressed from the gene *KRAS*, but not the highly homologous gene *HRAS*, is limited in mammalian cells by an abundance of underrepresented (rare) codons in the encoding mRNA. *KRAS* mRNA from both ectopic plasmids as well as from the endogenous cellular gene is subject to slowed translation due to these rare codons within its coding sequence. This has consequences for tumorigenesis, as replacement of the rare codons with commonly used codons accelerates RAS driven tumor growth. This may extend beyond *HRAS* and *KRAS*, as many other homologous gene pairs show a high divergence in codon usage and protein expression, suggesting that this could be a wider phenomenon used by mammalian cells to regulate protein levels.

Second, I demonstrate that *RAS* driven tumors partially depend on eNOS for growth. Using genetically engineered mouse models that recapitulate the spontaneous development of pancreatic cancer, I demonstrate that the protein eNOS is progressively upregulated as tumors develop. I then demonstrate that genetic ablation of *eNOS* partially blocks the development of preinvasive pancreatic lesions in these mice, and trends toward increasing survival in mice that develop lethal pancreatic adenocarcinoma. Furthermore, I then show that inhibition of eNOS using the clinically tested small molecule L-NAME can also slow the development of preinvasive

neoplasia and nonsignificantly increase survival, although not to the level of eNOS genetic ablation. These findings are applicable to a clinical setting, as in conjunction with others I show that L-NAME treatment of human pancreatic cancer xenografts halves their growth, even when the main side effect of L-NAME, hypertension, is treated.

Together, these studies provide a better understanding of how RAS functions within the cell, and thus, ultimately, how RAS driven cancers may be treated.

# Contents

Abstract.....	iv
List of Tables .....	xii
List of Figures .....	xiii
1. Introduction .....	1
1.1 RAS.....	1
1.1.1 RAS: A Small G Protein .....	1
1.1.2 RAS Signaling Pathways.....	1
1.1.3 RAS Family Members.....	4
1.1.3.1 Similarities of the Three RAS Family Members.....	5
1.1.3.2 Molecular Differences Between the Three RAS Family Members.....	6
1.1.3.3 Organismal Differences Between the Three RAS Family Members .....	9
1.1.4 RAS and Cancer .....	11
1.1.5 Methods Used by Tumors to Increase RAS Signaling.....	13
1.1.5.1 RAS Mutations in Cancer .....	13
1.1.5.2 Increased RAS Protein Levels in Cancer .....	14
1.1.5.3 Modulation of Upstream or Downstream Effectors.....	18
1.1.6 Methods of Decreasing RAS Signaling to Block Tumor Growth .....	19
1.1.6.1 Decreasing RAS Protein Level .....	19
1.1.6.2 Decreasing RAS Activity .....	20
1.1.6.3 Decreasing Signaling of Downstream RAS Effectors.....	21
1.2 eNOS.....	26
1.2.1 Nitric Oxide Synthase Structure and Catalysis .....	26

1.2.1.1 Nitric Oxide Signaling Through cGMP .....	28
1.2.1.2 Nitric Oxide Signaling Through S-Nitrosylation.....	28
1.2.2 Nitric Oxide Synthase Family Members .....	29
1.2.2.1 Inducible Nitric Oxide Synthase .....	29
1.2.2.2 Neuronal Nitric Oxide Synthase .....	30
1.2.2.3 Endothelial Nitric Oxide Synthase.....	31
1.2.3 Role of eNOS in Normal Physiology .....	32
1.2.4 Role of eNOS in Cancer .....	34
1.2.4.1 eNOS Mediates RAS Signaling.....	34
1.2.4.2 eNOS Mediates Angiogenesis .....	35
1.2.4.3 eNOS Mediates Notch Signaling .....	36
1.2.5 L-NAME: A NOS Inhibitor.....	37
1.2.5.1 L-NAME Pharmacokinetics and Mechanism of Action .....	38
1.2.5.2 Side Effects of L-NAME Administration .....	40
1.2.5.3 L-NAME Clinical Trials in Humans .....	42
1.3 Translational Control of Gene Expression .....	44
1.3.1 The Process of Translation and Rationale for Regulation .....	44
1.3.2 Regulation of Translation Elongation as a Method of Controlling Protein Expression in Mammals.....	48
1.3.3 Codon Choice as a Possible Mechanism for Control of Translation Elongation?.....	52
1.3.3.1 Studies of Codon Usage in Prokaryotes.....	57
1.3.3.2 Studies of Codon Usage in Yeast.....	58
1.3.3.3 Studies of Codon Usage in Insects .....	59
1.3.3.4 Studies of Codon Usage in Mammals .....	60

1.4 Summary.....	62
2. Materials and Methods.....	65
2.1 Rare Codons Limit KRAS Tumorigenic Activity .....	65
2.1.1 Cell Lines.....	65
2.1.2 Plasmids.....	65
2.1.3 Gene Synthesis .....	67
2.1.4 Protein Analysis.....	68
2.1.5 Metabolic Labeling .....	68
2.1.6 Tumorigenesis Assays.....	68
2.1.7 RT-PCR .....	69
2.1.8 AAV-Mediated Homologous Recombination .....	70
2.1.9 Polysome Profiling.....	71
2.1.10 Statistics .....	72
2.2 Targeting eNOS in Pancreatic Cancer.....	72
2.2.1 Cell Lines.....	72
2.2.2 Mouse Pancreatic Cancer Models.....	73
2.2.3 L-NAME Treatment of Mice .....	74
2.2.4 Grading of ductal lesions and Assessment of Normal Acinar Area.....	75
2.2.5 Mouse squamous papilloma and carcinoma analysis.....	75
2.2.6 Histology and Immunohistochemistry .....	76
2.2.7 PCR of KRas alleles.....	77
2.2.8 Xenograft assays.....	78
2.2.9 Blood pressure measurements .....	78

2.2.10 Statistical Analyses .....	79
3. Rare Codons Limit KRas Tumorigenic Activity .....	81
3.1 Abstract .....	81
3.2 Background.....	81
3.3 Results .....	82
3.3.1 KRas expression is blocked at the level of translation .....	82
3.3.2 Low KRas expression is due to an abundance of rare codons .....	88
3.3.3 Expression of endogenous KRas is limited by codon usage .....	89
3.3.4 <i>KRAS</i> codon usage limits KRas-driven tumorigenesis .....	95
3.3.5 Other gene pairs differ in codon usage and protein expression.....	100
3.3.6 Discussion.....	104
4. Targeting eNOS in Pancreatic Cancer .....	106
4.1 Introduction.....	106
4.2 Results .....	110
4.2.1 eNOS Is Upregulated During PDAC.....	110
4.2.2 Genetic Ablation of <i>eNOS</i> Decreases PanIN Development .....	112
4.2.3 Genetic Ablation of <i>eNOS</i> Decreases Development of Other Oncogenic KRAS-Driven Tumors.....	114
4.2.4 Genetic ablation of <i>eNOS</i> increases the lifespan of mice with lethal PDAC .....	115
4.2.5 L-NAME treatments retard development of preinvasive pancreatic lesions.....	118
4.2.6 L-NAME treatments inhibit other oncogenic KRas-driven tumors .....	119
4.2.7 L-NAME treatments increase the lifespan of mice with lethal PDAC .....	119
4.2.8 L-NAME decreases tumorigenic growth of human PDAC cell lines.....	120
4.2.9 L-NAME reduced PDAC tumor growth in mice treated with an anti-hypertensive ...	124

4.3 Discussion .....	125
5. Conclusion and Future Directions.....	129
5.1 Summary of Studies on the Role of Codon Usage in the Control of KRAS Expression....	129
5.2 Future Areas of Study Concerning the Role of Codon Usage in the Control of Gene Expression .....	132
5.2.1 Studies of KRAS Codon Usage on an Organismal Level.....	132
5.2.1.1 The Effects of KRAS Codon Optimization on Murine Development.....	135
5.2.1.2 The Effects of KRAS Codon Optimization on Murine Tumorigenesis .....	136
5.2.2 Studies of Pathways That May Regulate Expression of Rare Codon Containing Genes .....	138
5.2.2.1 Comparative Quantitative Analysis of mRNA Shifts Upon Polysome Treatment .....	139
5.2.2.2 Analysis of Ratio of KRAS Protein to KRAS mRNA Ratio in Various Tissues.....	141
5.2.2.3 Insulin Control of KRAS Expression .....	142
5.2.2.4 Empirical Testing of Other Stimuli That Are Known to Affect Elongation .....	145
5.2.3 Studies of Other Rare-Codon Containing Gene Pairs.....	147
5.3 Summary of Studies on the Role of eNOS in a Spontaneous Murine Model of Tumorigenesis .....	149
5.4 Future Areas of Study on the Role of eNOS in KRAS-Driven Tumorigenesis.....	152
5.4.1 Testing of L-NAME in Combination with Front-Line Therapy .....	152
5.4.2 Development of a Specific eNOS Inhibitor.....	153
5.4.3 Identify and Inhibit the Other Targets of L-NAME .....	154
5.4.4 Identify the Mechanism by which eNOS Inhibits Tumor Growth .....	157
5.5 Concluding Remarks.....	158
References .....	159

Biography..... 192

## List of Tables

Table 1: Codon Usage Frequency of Amino Acids in <i>Homo sapiens</i> .....	54
Table 2: Homologous Gene Pairs with High Differences in Codon Usage .....	101

## List of Figures

Figure 1: eNOS activation by AKT is required for tumor growth. ....	25
Figure 2: Structure and Function of a Prototypical NOS Enzyme .....	27
Figure 3: Comparison of L-NNA and arginine structure.....	39
Figure 4: Translation of <i>KRAS</i> message is limited by rare codons .....	84
Figure 5: Decreased KRas expression levels are independent of the expression systems used ...	85
Figure 6: Limiting dilution analysis of relative Ras expression levels .....	87
Figure 7: Codon usage controls endogenous KRas expression.....	92
Figure 8: <i>KRAS</i> mRNA has reduced mobility in polysome profiles in HEK-HT cells.....	94
Figure 9: <i>KRAS</i> codon usage limits the growth of tumors driven by oncogenic <i>KRAS</i> .....	98
Figure 10: KRas levels in HEK-HT tumors driven by KRas <sup>G12V</sup> .....	99
Figure 11: Codon usage difference in gene pairs results in expression differences and identifies a unique set of pathways.....	102
Figure 12: eNOS is upregulated during pancreatic tumorigenesis. ....	111
Figure 13: Reduction in area and grade of pancreatic lesions in <i>eNOS</i> <sup>-/-</sup> and L-NAME treated mice .....	113
Figure 14: <i>eNOS</i> <sup>-/-</sup> and L-NAME treated KC mice are resistant to spontaneously arising facial and vulvar tumors .....	116
Figure 15: NOS inhibition provides a survival advantage to KPC mice .....	117
Figure 16: L-NAME decreases the tumorigenic growth of human pancreatic cancer cells, even when its antihypertensive effect is abrogated .....	122
Figure 17: L-NAME broadly decreases the tumorigenic growth of many human pancreatic cancer cell lines.....	123
Figure 18: Exon 3 optimization in the mouse .....	134

Figure 19: Possible interactions between insulin signaling pathway and rare codon containing genes .....	144
Figure 20: Relative expression of PRL genes.....	148
Figure 21: Effects of L-NAME Treatment in <i>eNOS</i> <sup>-/-</sup> Mice .....	155

# **1. Introduction**

## **1.1 RAS**

### **1.1.1 RAS: A Small G Protein**

RAS is a 21 kilodalton small GTP binding protein (G protein) (Takai, Sasaki et al. 2001). Members of this protein family function as molecular switches, toggling between two interconvertible forms: GDP-bound inactive and GTP-bound active states (Takai, Sasaki et al. 2001). Upstream signals stimulate the dissociation of GDP from the G protein by activating a class of proteins known as guanine nucleotide exchange factors (GEFs) (Quilliam, Rebhun et al. 2002). RAS then binds free GTP within the cell. This GTP binding leads to a conformational change in the protein's structure, causing a shift in two switch regions which can then interact with downstream effectors (Karnoub and Weinberg 2008). GTPase acting proteins (GAPs) enhance the otherwise slow intrinsic GTPase activity of RAS proteins, accelerating GTP hydrolysis and promoting a return of the protein to the inactive state (Donovan, Shannon et al. 2002). Thus, RAS proteins can act as signal transducers, converting upstream extracellular signals to downstream intracellular effects.

### **1.1.2 RAS Signaling Pathways**

Activation of cell surface receptors stimulates convergent signals that lead to the activation of RAS by GEFs. RAS serves to both amplify and diversify the incoming information, activating a wide variety of downstream effectors, leading to changes in many different cellular phenotypes.

The classic signals that activate RAS are growth factor receptors with tyrosine kinase activity (reviewed in Malumbres and Barbacid 2003). Phosphotyrosines formed on these

activated receptors serve as docking sites for proteins with SH2 domains. These adaptor proteins (such as GRB2) then in turn recruit RAS GEFs (such as SOS) from the cytosol to the plasma membrane. RAS proteins, anchored in the plasma membrane due to lipid moieties covalently attached to the peptide, can then be directly activated by the recruited GEF.

The extracellular signals that lead to RAS activation are only transient. Thus, once RAS is activated, it must transduce these extracellular signals not only across space but also across time, triggering downstream pathways that lead to long-lasting changes within the cell (Alberts, Wilson et al. 2008). Three classical downstream RAS signaling pathways will be discussed here (Shields, Pruitt et al. 2000).

In the RAF kinase cascade (reviewed in Shapiro 2002; Wellbrock, Karasarides et al. 2004), RAS activates the family of RAF serine/threonine kinases (c-RAF-1, A-RAF, and B-RAF) and also relocalizes them to the plasma membrane. RAF is a MAP kinase kinase kinase, and phosphorylates and activates a MAP kinase kinase (also called MEK). Finally, MEK phosphorylates MAP kinases (also called ERK) on both regulatory threonines and tyrosines. The now active ERK can translocate into the nucleus, and the pathway is complete – an extracellular signal has been transferred to the cell's innermost compartment. Once in the nucleus, ERK phosphorylates and activates mitogenic transcription factors (including, for example, Elk1); this results in the transcription of mitogenic genes (including, for example, cyclins). Since a single upstream kinase protein molecule can phosphorylate many downstream effector molecules before being turned off, these multiple levels in the kinase cascade serve to amplify the signal. Furthermore, since there are many family members of MAPKKKs, MAPKKs, and MAPKs, each step in the pathway can also serve to diversify the signal (Shaul and Seger 2007).

A second downstream RAS signaling pathway is the phosphatidylinositol-3-kinase (PI3K) pathway (reviewed in Vivanco and Sawyers 2002). PI3Ks are heterodimeric lipid kinases composed of a regulatory subunit (p85) and a catalytic subunit (p110). They catalyze the synthesis of phosphatidylinositol-3,4,5-triphosphate (PIP<sub>3</sub>) from the substrate PIP<sub>2</sub>. RAS can directly activate PI3K by binding to the p110 catalytic subunit. Proteins with pleckstrin homology (PH) domains can recognize PIP<sub>3</sub> moieties in the lipid bilayer of the cell and dock there. AKT is a serine-threonine kinase that contains a PH domain and is activated downstream of PI3K (regulation and downstream targets of AKT reviewed in Datta, Brunet et al. 1999; Fayard, Tintignac et al. 2005). The downstream effectors of AKT have roles that fall into the categories of cell survival, cell proliferation, and cell growth. Phosphorylation of BAD and caspase-9 by AKT inhibits their pro-apoptotic functions; furthermore, phosphorylation of members of the Forkhead family of transcription factors prevents their nuclear translocation and induction of transcription of pro-apoptotic proteins. Phosphorylation of glycogen synthase kinase-3 $\beta$  inactivates it and prevents it from degrading cyclin D1. The mammalian target of rapamycin (mTOR) kinase is activated downstream of AKT and causes an increase in cell growth (i.e. cell size). Finally, the eNOS protein (see 1.2 eNOS) is directly phosphorylated by AKT on serine 1177 both *in vivo* and *in vitro* leading to increased enzymatic production of nitric oxide, independent of the typical eNOS need for elevated intracellular calcium (Fulton, Gratton et al. 1999). This PI3K-AKT-eNOS pathway was first demonstrated in vascular endothelial cells, and is responsible for both the continuous, homeostatic formation of vasodilatory nitric oxide in response to the shear stress of blood flow (Dimmeler, Fleming et al. 1999) and also the nitric oxide-mediated angiogenic effects of vascular endothelial growth factor (Fulton, Gratton et al. 1999; Michell, Griffiths et al. 1999).

A third downstream effector of RAS is RALGDS, which is a family of GEFs for the RAS-like G proteins RALA and RALB (reviewed in Katz and McCormick 1997; Ferro and Trabalzini 2010). RALGDS binds directly to RAS in a GTP dependent fashion; this binding promotes translocation of the RALGDS GEFs to the plasma membrane so that they are in proximity to RALA and RALB and can thus facilitate GDP/GTP exchange. The downstream effectors of RALA and RALB include SEC5 and EXO84 (two members of the octameric exocyst complex involved in filopodia formation and polarized sorting of proteins to the basolateral membrane of epithelial cells) as well as RALBP1 (a protein that facilitates endocytosis and which also contains a GAP domain that may be involved in actin dynamics and regulation of RAC and CDC42) (Feig 2003). Additionally, the RAS-RALGDS-RAL pathway activates, through unknown intermediates, transcription factors in the NF- $\kappa$ B and Forkhead families; this may play a role in the pro-proliferative effects that RAL activation has (Feig 2003).

The physiologic roles of the above RAS pathways can be broadly categorized as mitogenic, anti-apoptotic, and pro-cell-survival. Thus, RAS sits at the apex of a signaling hub that, if activated to a pathophysiologic extent, could promote cancer (see 1.1.4 RAS and Cancer). The unique functions of each downstream pathway in normal physiology are also reflected when the RAS pathway is activated to a pathophysiologic degree, as RAS-driven cancers depend on RAS activation of each pathway to different extents (see 1.1.6.3 Decreasing Signaling of Downstream RAS Effectors).

### **1.1.3 RAS Family Members**

By searching for the proteome for structural motifs, over 150 monomeric G proteins can be identified (Wennerberg, Rossman et al. 2005). This “superfamily” can be further divided into

five branches on the bases of similar amino acid sequence and protein function: the RAS, RHO, RAB, RAN and ARF families. The RAS family (Reuther and Der 2000) contains 36 members, and the work here is focused on a subgroup of three closely related proteins within this family, encoded by three separate genes: *HRAS*, *KRAS*, and *NRAS*. Here, the focus is first on the similarities between these three and then on the differences between them at the molecular and at the organismal level.

### **1.1.3.1 Similarities of the Three RAS Family Members**

Eukaryotic organisms beginning with yeast possess RAS-like small G proteins (Barbacid 1987). Invertebrates such as *Drosophila melanogaster*, *Ciona intestinalis*, and *Strongylocentrotus purpuratus* have only one *RAS* gene; vertebrates such as *Danio rerio* up to *Homo sapiens* have three distinct *RAS* genes that can be identified as *HRAS*, *KRAS*, and *NRAS*; (Rotchell, Lee et al. 2001; Diez, Sanchez-Jimenez et al. 2011). In humans, the three genes have a common structure, with an initial noncoding exon followed by four coding exons, although due to variation in intron size the *KRAS* gene covers 46 kilobases while *HRAS* and *NRAS* cover 3.5 kilobases and 10 kilobases, respectively (Lowy and Willumsen 1993). These three family members are 80% identical to one another with the N-terminal 85 amino acids completely identical; *HRAS* is 189 amino acids long while *NRAS* and *KRAS* are 188 amino acids in length. All three members are subject to the same initial post-translational modification. A C-A-A-X motif, present as the last four amino acids in the protein (C-V-L-S in *HRAS*, C-V-V-M in *NRAS*, and C-V-I-M in *KRAS4B*) directs a three step process: (1) irreversible covalent attachment of a lipid farnesyl moiety to the cysteine by farnesyltransferase, (2) cleavage of the A-A-X tripeptide by an endopeptidase present on the cytoplasmic face of the ER, and (3) methylation of the carboxyterminal cysteine

by the ER-resident enzyme isoprenylcysteine carboxymethyltransferase (reviewed in Hancock 2003). While the following intermediate steps do then differ between the isoforms (see 1.1.3.2 Molecular Differences Between the Three RAS Family Members), all three finally reside on the plasma membrane. The switch regions, which interact with downstream effectors, are identical between the three (Lowy and Willumsen 1993). Thus, all can activate the canonical downstream RAF, PI3K, and RALGDS pathways, although *in vivo* they may slightly differ in pathway activation efficiency (Yan, Roy et al. 1998).

### **1.1.3.2 Molecular Differences Between the Three RAS Family Members**

Subtle molecular differences between the RAS proteins do exist, although in general it is unclear how these molecular differences relate to the differences between the proteins seen at the organismal level. The C-terminal 20 amino acid hypervariable domain, responsible for RAS subcellular localization (Hancock 2003), is unconserved between the three (excluding the four amino acid C-A-A-X box at the very end) (Barbacid 1987). After C-terminal carboxymethylation, HRAS and NRAS are transported to the Golgi, where they are palmitoylated on residues within their hypervariable domain (C181 in NRAS, C181 and C184 in HRAS) and then transported via the exocytic pathway through the Golgi to the inner leaflet of the plasma membrane (Hancock 2003). KRAS, on the other hand, is transported from its site of synthesis on the ER to plasma membrane, bypassing the Golgi. A charged string of lysine residues unique within the hypervariable region of KRAS facilitates association with membrane lipids (Hancock 2003). Once in the plasma membrane, HRAS and KRAS slightly differ in their localization, with GDP-bound HRAS present in lipid rafts and shifting to disordered plasma membrane upon GTP loading, while

KRAS is present in disordered membrane independent of activation status (Prior, Harding et al. 2001).

Some post-translational modifications vary between the RAS proteins. KRAS is phosphorylated by protein kinase C within its hypervariable domain, and this phosphorylation event neutralizes the positively charged lysine residues within the hypervariable region, promoting translocation of the protein to the outer mitochondrial membrane. There, it can interact with BCL-XL and promote apoptosis (Bivona, Quatela et al. 2006). HRAS and NRAS are monoubiquitinated, stabilizing their association with endosomes and facilitating transport from the Golgi to the plasma membrane. This monoubiquitination is dependent on the presence of the palmitoylated hypervariable domains and does not occur on KRAS (Jura, Scotto-Lavino et al. 2006).

*KRAS* is alternatively spliced to yield two variants, *KRAS4A* and *KRAS4B* (Barbacid 1987). Since the alternative splicing event involves a choice between two final fourth exons (exons 4A or 4B), these two isoforms differ only in their C-terminal hypervariable region (Barbacid 1987). *KRAS4B* is the dominant isoform present in most cells (Wang and You 2001), and here any mentions of *KRAS* specifically refer to *KRAS4B*. *KRAS4A* is palmitoylated in the same manner as *NRAS* (Omerovic, Laude et al. 2007) and is a non-essential isoform as assessed by murine knockout studies (Plowman, Williamson et al. 2003).

The expression levels of the RAS isoforms are different in cellular exogenous expression assays; *KRAS* in particular is difficult to overexpress (Ellis and Clark 2000). This observation is most noticeable in side-by-side attempts to compare ectopic *KRAS* expression with ectopic expression of the other RAS isoforms (Bivona, Quatela et al. 2006; Kubota, O'Grady et al. 2011). For example, out of eleven RAS family G proteins ectopically expressed in 293 cells, *KRAS*

exhibited the lowest expression (Rodriguez-Viciano, Sabatier et al. 2004). Another attempt to express KRAS in a bicistronic vector with IRES-driven GFP expression found that, while cells expressing high levels of GFP could be sorted out by flow cytometry, a subsequent immunoblot to assess KRAS expression revealed that it was constant and did not correlate with GFP expression. Conversely, expression of the other two RAS family members in this system correlated with GFP expression. Attempts to increase KRAS levels via proteasome inhibition did elevate expression, but not to the levels of HRAS and NRAS (Keller, Franklin et al. 2007). Finally, the degree of difference in ectopic expression of each of the family members is variable, and there are cases in which the difference is only slight or non-existent. The expression of retrovirally introduced KRAS and NRAS proteins were identical in melanocytes (Whitwam, Vanbrocklin et al. 2007). Ectopically introduced dominant negative forms of HRAS, NRAS, and KRAS were similar in COS-7 cells (Matallanas, Arozarena et al. 2003). The expression of retrovirally introduced KRAS and NRAS was slightly lower than HRAS in F9 and PCC4 cells (both types of mouse embryonal carcinoma cell lines) (Quinlan, Quatela et al. 2008); another group found that HRAS, NRAS, and KRAS expression was equivalent in stably infected NIH3T3 fibroblasts but KRAS had slightly lower expression when the same vectors were used to introduce the genes into a myeloid precursor cell line (Parikh, Subrahmanyam et al. 2007). It has also been noted that different expression vectors interact with each *RAS* gene in different ways; the authors suggested empirical determination of the best expression vector for each *RAS* gene in the cell type of interest (Fiordalisi, Johnson et al. 2001).

### 1.1.3.3 Organismal Differences Between the Three RAS Family Members

At an organismal level, the RAS proteins have differing roles both in tumorigenesis and in development (Quinlan and Settleman 2009).

RAS proteins are commonly mutated in cancer (see 1.1.5.1 RAS Mutations in Cancer); about 20% of all cancers have activating mutations in one of the *RAS* genes (Bos 1989; Downward 2003). However, these mutations are not equally distributed between the three isoforms (Lau and Haigis 2009). In fact, about 85% of all *RAS* mutations are in *KRAS*, about 15% in *NRAS*, and 1% in *HRAS* (Downward 2003). Some of this difference may be due to the fact that *KRAS* resides within a genetic locus that is particularly susceptible to mutation, as a transgenic mouse with *Hras* knocked into the *Kras* locus exhibited activating mutations in the *HrasK1* gene upon treatment with urethane, a chemical that typically causes *Kras* mutations (To, Wong et al. 2008). Even in this situation, however, the two genes were not completely interchangeable. A mouse that is heterozygote at the *Kras* locus, with one wild-type *Kras* gene and one *HrasK1* gene, does not exhibit equal distribution of mutations at each allele upon treatment with urethane. Rather, 92% of the time the mutation occurs in the *HrasK1* gene (To, Wong et al. 2008). Additionally, direct comparison of *Hras* and *Kras* retroviruses in rat mammary tumor formation assays indicates that *Hras* is roughly ten-fold more potent than *Kras* at inducing ductal carcinomas (Kim, Lindstrom et al. 2002). In this study, chimeric retroviruses that contained varying segments of the *Hras* and *Kras* genes exhibited fluctuating potencies in mammary tumor formation – even when the switched segments contained no differences at the amino acid level (Kim, Lindstrom et al. 2002). In an example of a molecular difference that leads to a phenotype related to tumorigenesis, it has been shown that activated *KRAS*, but not *HRAS* or *NRAS*, can promote the expansion of an endodermal stem cell population while preventing differentiation,

(as modeled by F9 murine embryonal carcinoma cells, which can undergo differentiation when exposed to retinoic acid) (Quinlan, Quatela et al. 2008). In sum, while the RAS proteins may seem interchangeable in many cellular assays, a preference exists for *KRAS* mutations in human tumors.

Informative studies concerning the differential roles of the RAS proteins in development come from knockout mice and also from developmental disorders in humans. The *Hras* and *Nras* genes are dispensable for embryogenesis as mice without these genes grossly develop normally (Umanoff, Edelman et al. 1995; Ise, Nakamura et al. 2000; Esteban, Vicario-Abejon et al. 2001). Mice missing both the *Hras* and *Nras* genes are viable but appear with a frequency reduced from that expected according to Mendelian ratios (Esteban, Vicario-Abejon et al. 2001). In contrast, *Kras* knockout alone is embryonic lethal (E12.5) with signs of liver apoptosis and anemia (Johnson, Greenbaum et al. 1997). While *Kras* in this respect seems unique, the *Ras* genes do have some functional overlap in their developmental roles, as *Kras*<sup>+/-</sup>;*Nras*<sup>-/-</sup> (but not *Kras*<sup>+/-</sup>*Nras*<sup>+/+</sup>) animals are nonviable (with 70% dying around E10-E12 and the remainder dying perinatally) (Johnson, Greenbaum et al. 1997). Furthermore, triple knockout animals are viable if they also overexpress an *Hras* transgene (Nakamura, Ichise et al. 2008). On the other end of the spectrum, activating mutations of the *RAS* genes also affect development. Activating mutations in *HRAS* cause Costello Syndrome, characterized by heart and facial abnormalities, short stature, mental retardation, and a propensity to develop rhabdomyosarcomas and neuroblastomas (Aoki, Niihori et al. 2005; Schubbert, Shannon et al. 2007). The spectrum of *HRAS* mutations seen in Costello syndrome runs from strongly activating mutations at glycine 12 (similar to those seen in cancer) to weakly activating mutations (such as K117R and A146T, uncommon in cancer) (Schubbert, Shannon et al. 2007). In mice, knock in of a germline activating *HRAS*<sup>G12V</sup> allele

recapitulates the phenotypes seen in Costello syndrome, including high perinatal lethality, high propensity to develop cancer, and craniofacial abnormalities (Schuhmacher, Guerra et al. 2008; Chen, Mitsutake et al. 2009). Germline activating mutations in *KRAS* cause the related Noonan Syndrome, characterized by heart and facial abnormalities, skeletal defects, learning disabilities, and a propensity to develop juvenile myelomonocytic leukemia (Schubbert, Zenker et al. 2006). The spectrum of mutations seen here is more limited; only patients with weakly activating *KRAS* mutations have been discovered (Schubbert, Shannon et al. 2007). Consistent with this, endogenous expression of the strongly activating *KRAS*<sup>G12D</sup> mutation in mice results in cardiomegaly, abnormal brain development, and 100% embryonic lethality by E11.5 (Tuveson, Shaw et al. 2004). Finally, germline activating mutations in *NRAS* have not been found to cause developmental disorders, with the sole account of an activating germline G13D *NRAS* mutation found in a 49 year old male with an autoimmune lymphoproliferative syndrome and a history of childhood leukemia (Oliveira, Bidere et al. 2007).

In sum, *KRAS* is the sole *RAS* gene that is embryonic lethal when either knocked out or when present in a strongly activating germline mutation; *KRAS* is also the most commonly mutated member of the *RAS* gene family. This suggests the existence of unique features of *KRAS* molecular biology, some of which may possibly be exploited to block the cancers that it causes.

#### **1.1.4 RAS and Cancer**

Cancer is a somatic disease broadly characterized by eight cellular abnormalities: sustained proliferative signaling, evasion of growth-suppressive signals, resistance to cell death, replicative immortality, induction of angiogenic signals, activation of invasion and metastasis pathways, reprogramming of energy metabolism, and evasion of immune surveillance (Hanahan

and Weinberg 2000; Hanahan and Weinberg 2011). Cancer is also an evolutionary process in which the cells that most strongly exhibit the aforementioned characteristics survive and divide to create the next generation of tumor cells (Nowell 1976). Thus, signaling pathway alterations that particularly promote some of the above abnormalities, such as hyperactivation of the RAS signaling pathway, are alterations that are commonly accumulated by cancer cells. Pathologic hyperactivation of the RAS-RAF-MEK-ERK cascade, for example, results in constitutive mitogenic signaling and unchecked cell division (Hanahan and Weinberg 2000). The RAS-PI3K-AKT pathway is anti-apoptotic through the inhibitory effects of AKT on caspases and BAD family members; constitutive RAS activation can therefore allow cancer cells to resist apoptotic signals (Vivanco and Sawyers 2002). Thus, hyperactivation of the RAS pathway can endow the cell with not just one but many of the hallmarks of cancer cells.

Understanding how the RAS protein operates within the cell -- how it is made, how it functions and signals, how it is degraded, and how these processes are dysregulated in cancer -- could help to identify potential anticancer therapeutic strategies. For example, identification of post-translational RAS lipidation lead to efforts to develop farnesyltransferase inhibitors to inhibit RAS-driven cancers (see 1.1.6.2 Decreasing RAS Activity) (reviewed in Kloog and Cox 2000). This thesis will explore how the RAS protein is made, particularly, how translation of *KRAS* mRNA is limited in the cell. Furthermore, this thesis will build on previous work (Lim, Ancrile et al. 2008) that identified the RAS-PI3K-AKT-eNOS pathway as critical for RAS-driven xenograft tumor growth. The effect of eNOS inhibition, both genetically and pharmacologically, on tumor formation and host survival in spontaneously arising murine pancreatic cancer models will be assessed. Both of these areas of study contribute to an understanding of RAS protein and how it operates within the cell, and thus hopefully advance toward the ultimate goal of fully

understanding the genesis, maintenance, and possible treatment options for RAS driven cancers.

### **1.1.5 Methods Used by Tumors to Increase RAS Signaling**

The levels of output from the RAS signaling node can be increased in tumors through three non-exclusive mechanisms: increased activity of the RAS protein, increased level of the RAS protein, and increased activation of upstream or downstream effectors.

#### **1.1.5.1 RAS Mutations in Cancer**

*RAS* is the most commonly mutated oncogene in human cancer (Downward 2003; Karnoub and Weinberg 2008). Cancer-causing mutations in *RAS* lock it in the active, GTP-bound state (Downward 2003), although the mechanism by which they do this varies depending on the mutation. Almost all cancer-causing mutations in *RAS* occur in codons 12, 13, or 61 (Bos 1989). Mutation of the glycine in positions 12 or 13 introduces a side chain at this position (glycine is the only amino acid without a side chain), and the resulting bulky group prevents the GAP protein “finger” from inserting itself and stabilizing the transition state in which GTP is hydrolyzed (Scheffzek, Ahmadian et al. 1997). The glutamine in position 61 catalyzes the hydrolysis reaction that results in cleavage of the  $\gamma$ -phosphate of GTP (Krengel, Schlichting et al. 1990). Thus, mutations in any of these residues impair GTP hydrolysis and result in a constitutively GTP-bound, actively signaling version of the protein (Malumbres and Barbacid 2003).

*RAS* mutations are not equally distributed among all types of cancers, and as previously mentioned do not occur with equal frequency in each of the three *RAS* isoforms (see 1.1.3.3 Organismal Differences Between the Three *RAS* Family Members). Activating *KRAS* mutations

are the most common, found in 90% of pancreatic cancers, 35% of lung adenocarcinomas, and 45% of colorectal carcinomas (Smit, Boot et al. 1988; Vogelstein, Fearon et al. 1988; Bos 1989). Activating *NRAS* mutations are the second most common, occurring in 20% of acute lymphoblastic leukemias (Neri, Knowles et al. 1988) and 30% of melanomas (Omholt, Karsberg et al. 2002). *HRAS* mutations occur in 1-10% of bladder cancers (Cattan, Saison-Behmoaras et al. 2000; Downward 2003).

The importance of mutant *KRAS* in tumorigenesis is exhibited not only by the frequency with which mutations occur, but also by the early timing with which mutations occur in tumor development. In colorectal cancer, *KRAS* mutations occur after polyp formation but before malignant transformation (Cho and Vogelstein 1992). In pancreatic cancer, *KRAS* mutations are one of the earliest, if not the earliest, genetic lesion. They are detected in preinvasive neoplastic lesions (Lohr, Kloppel et al. 2005) and introduction of mutant *KRAS* into immortalized pancreatic ductal cells can make them tumorigenic in immunocompromised mice (Qian, Niu et al. 2005). Furthermore, in mouse models, *KRAS* mutations alone are sufficient to drive formation of pancreatic precursor neoplastic lesions that eventually develop into adenocarcinomas (Hingorani, Petricoin et al. 2003). The early appearance of *RAS* mutations in tumors suggested the possibility that cancers may be dependent on *RAS* expression, a hypothesis which has subsequently been confirmed (see 1.1.6.1 Decreasing *RAS* Protein Level); therefore such *RAS*-driven cancers may be susceptible to inhibitors which can block the *RAS* signaling pathway (Downward 2003).

### **1.1.5.2 Increased *RAS* Protein Levels in Cancer**

Higher levels of wild-type *RAS* expression are noted in many types of tumors (reviewed in Zachos and Spandidos 1997), conceding that these studies differ in how overexpression is

defined, how overexpression is detected, and what samples are examined. RAS overexpression could potentially be a secondary effect seen in cells that are highly proliferative; however, reports that *KRAS* gene amplification is common and can occur with together with *KRAS* gene mutation suggest that RAS overexpression may also have a causal role (Yamada, Sakamoto et al. 1986; Liu, Von Lintig et al. 1998; Heidenblad, Jonson et al. 2002; O'Hagan, Chang et al. 2002; Aguirre, Bardeesy et al. 2003; Mita, Toyota et al. 2009; Modrek, Ge et al. 2009; Wagner, Perner et al. 2009; Feldser, Kostova et al. 2010). Perhaps mutation of the *KRAS* gene is not sufficient to maximize its function, and cancer cells which can bypass this unknown impediment to *KRAS* function by amplifying the gene are actively selected. Here the focus is on the possible role that overexpression of mutant RAS may play in RAS cancer signaling.

Higher expression of a mutant *RAS* gene is more tumorigenic. A xenograft study with an immortalized human mammary epithelial cell line found that retrovirally introduced HRAS<sup>G12V</sup> had different potency depending on the levels at which it was expressed. When HRAS<sup>G12V</sup> was introduced at levels similar to the endogenously present HRAS, zero out of twenty-four injected immunocompromised mice formed tumors (Elenbaas, Spirio et al. 2001). In similar studies with immortalized skeletal muscle cell precursors, lines with highly overexpressed retrovirally introduced HRAS<sup>G12V</sup> formed tumors in 100% of injected mice after 4.5 weeks, while lines with lowly expressed HRAS<sup>G12V</sup> formed tumors in 75% of mice after 11 weeks (Linardic, Downie et al. 2005). Comparisons of somatic cell knock in of a *KRAS*<sup>G12V</sup> mutation versus retrovirally mediated *KRAS*<sup>G12V</sup> overexpression found that the stably infected cells had higher levels of *KRAS* protein expression and a higher growth rate in cell culture, formed more colonies in soft agar (Konishi, Karakas et al. 2007) and formed tumors in immunocompromised mice whereas the cells with a knocked in oncogenic mutation in *KRAS* did not (Arena, Isella et al. 2007).

Given that oncogenic RAS overexpression can make cells more tumorigenic, the evidence for mutant *KRAS* gene amplification comes from a wide variety of human tumors and preclinical murine tumor models. Comparative genome hybridization studies have been done on human pancreatic cancer samples and cell lines (where *KRAS* mutations are nearly omnipresent (Bos 1989)) and the results indicate that amplification of a region containing the *KRAS* gene happens in roughly one fourth of samples: 25% of tested cell lines (Bashyam, Bair et al. 2005), 22% of tested cell lines in a different study (Heidenblad, Jonson et al. 2002), 26% of tested tumors and cell lines (Aguirre, Brennan et al. 2004), and 6% of tested primary tumors (Schleger, Arens et al. 2000). Studies of *KRAS* mutations in cancers of different organs also find evidence for *KRAS* amplification. In non-small cell lung cancer, 17% of all samples showed *KRAS* copy number gains, as assessed by quantitative PCR, and the presence of copy number gain was statistically associated with the presence of a *KRAS* activating mutation in the same sample (Modrek, Ge et al. 2009). The authors found that the level of *KRAS* amplification per sample varied, with copy numbers anywhere from 2.5-24 (Modrek, Ge et al. 2009). FISH analysis of non-small cell lung carcinomas by another group found *KRAS* gene amplification in 7% of samples, and 57% of those samples in turn exhibited a *KRAS* mutation (Wagner, Perner et al. 2009). In murine pancreatic and lung cancer models where expression of mutant *KRAS* is driven by its endogenous promoter, *KRAS* gene amplification can be found (Aguirre, Bardeesy et al. 2003; Feldser, Kostova et al. 2010; Junttila, Karnezis et al. 2010). The presence of *KRAS* gene amplification is also important when attempting to inhibit the growth of *KRAS* mutant tumors. Two independent groups have shown that genetic restoration of p53 after *KRAS*-mutant lung tumors have formed does not cause universal tumor regression, only regression of high grade lesions. This was because only higher grade tumors had amplified the *KRAS* gene and thus had

resultant high levels of ERK signaling, which was necessary to activate the restored p53 (Feldser, Kostova et al. 2010; Junttila, Karnezis et al. 2010). Furthermore, *KRAS* amplification is also a cause of resistance to MET (Cepero, Sierra et al. 2010) and MEK (Little, Balmanno et al. 2011) inhibitors.

Further evidence that *KRAS* expression levels are important in cancer arises from findings that cellular mechanisms which naturally exist to limit expression of the *KRAS* oncogene can also limit the growth of *KRAS*-driven tumors, and are downregulated in cancer. For example, *KRAS* is a target of the *let-7* miRNA (Johnson, Grosshans et al. 2005) and reduction of mutant *KRAS* expression via *let-7* overexpression can decrease subcutaneous and orthotopic xenograft growth (Esquela-Kerscher, Trang et al. 2008) as well as tumor burden in a transgenic mouse model of cancer (Kumar, Erkeland et al. 2008). *KRAS* and *let-7* exhibit reciprocal expression patterns in lung cancer specimens (Johnson, Grosshans et al. 2005), and low levels of *let-7* are poor prognostic factors in lung cancer (Takamizawa, Konishi et al. 2004).

In total, these studies provide evidence that *KRAS* expression is important in cancers, even, or perhaps particularly, in those with *KRAS* mutations. Increasing the amount of *KRAS*-encoding DNA is one method to affect *KRAS* protein level; alterations of other steps along the path of protein synthesis may also contribute to high *KRAS* levels. Translational control of gene expression is possible (see 1.3 Translational Control of Gene Expression) and work within this thesis will show that *KRAS* mRNA is poorly translated. Amplification of the *KRAS* gene may be one way that cancer cells proceed around this translation roadblock; restoration of such a roadblock could possibly be exploited for potential therapies in the future.

### 1.1.5.3 Modulation of Upstream or Downstream Effectors

In addition to direct methods of modulating RAS protein activity or expression levels, cancer cells can also modify the activity of downstream KRAS effectors to enhance total output from the RAS signaling pathway. As with RAS, these alterations typically take the shape of either gene mutations or gene amplifications/overexpression (Downward 2003). Upstream of RAS, mutation, amplification, and/or overexpression of the EGFR family of receptors is common in many different types of cancer including breast, colon, lung, head and neck, and stomach (reviewed in Sharma, Bell et al. 2007; Zhang, Berezov et al. 2007). Gene mutations and amplifications are also found in the PI3K (Vivanco and Sawyers 2002) and RAF (Wellbrock, Karasarides et al. 2004) pathways downstream of RAS. Constitutively activating *BRAF* mutations are present in about 60-70% of melanomas and 15% of colon carcinomas (Downward 2003; Wellbrock, Karasarides et al. 2004). The catalytic subunit of PI3K, p110, is amplified in some ovarian cancers, as is its downstream target AKT2 (Cheng, Godwin et al. 1992; Bellacosa, de Feo et al. 1995). PTEN, a lipid phosphatase, is responsible for deactivating the PI3K pathway by converting the PIP<sub>3</sub> docking site into PIP<sub>2</sub> (Simpson and Parsons 2001). Inactivation of *PTEN* is frequent, occurring in 30-40% of all human tumors, making it the most commonly mutated tumor suppressor after *TP53* (Simpson and Parsons 2001). Mutations in *BRAF* are mutually exclusive with mutations in *RAS* in colorectal cancers (Rajagopalan, Bardelli et al. 2002) and melanomas (Garnett and Marais 2004); mutations that result in PI3K pathway activation are mutually exclusive with *RAS* mutations in skin tumors (Mao, To et al. 2004), endometrial carcinomas (Velasco, Bussaglia et al. 2006), and breast cancer cell lines (Hollestelle, Elstrodt et al. 2007). These findings confirm the importance of RAS-RAF and RAS-PI3K connections, and

suggest that in some tumors targeting downstream effectors of RAS could be functionally equivalent to targeting RAS itself.

### **1.1.6 Methods of Decreasing RAS Signaling to Block Tumor Growth**

Here, three different artificial approaches to decreasing the signaling output of the RAS pathway will be discussed: decreasing RAS protein level, decreasing RAS protein activity, and decreasing signaling of downstream RAS effectors. These preclinical studies provide evidence that decreasing RAS pathway signaling in tumors can be a successful anticancer strategy.

#### **1.1.6.1 Decreasing RAS Protein Level**

Tumors initiated by RAS require its expression later in their progression; in other words, RAS-initiated tumors possess an “oncogene addiction” to RAS signaling once tumors have formed (Weinstein and Joe 2008). Supporting this concept, an experiment was done with mice expressing a doxycycline inducible HRAS<sup>G12V</sup> transgene in melanocytes, which caused melanomas to develop with a sixty day latency in an INK4A-null background. One hundred percent of these melanomas regressed within twelve days when doxycycline was withdrawn (Chin, Tam et al. 1999). These results have been extended to KRAS-mutant human pancreatic cancer cell lines as well. shRNA-mediated knockdown of the KRAS<sup>G12V</sup> allele abolishes xenograft tumor formation of human pancreatic cancer cells in immunocompromised mice (Brummelkamp, Bernards et al. 2002). Furthermore, after xenograft tumors of human pancreatic cancer cell lines have been established, inducible knockdown of KRAS<sup>G12V</sup> causes regression of tumor growth (Lim and Counter 2005). These genetic studies in mice provide a proof-of-concept that ablating signaling from RAS can be a successful approach to treating RAS-driven cancers.

### 1.1.6.2 Decreasing RAS Activity

One method of blocking a hyperactive RAS protein would be to block the activity of the enzyme itself. There are difficulties with this approach. Compared to kinases that have a nanomolar affinity for ATP (Ma and Adjei 2009), RAS has a higher affinity for GDP on the order of  $6 \times 10^{11} \text{ M}^{-1} \text{ s}^{-1}$  (John, Sohmen et al. 1990), making the design of drug that could inhibit guanine nucleotide binding, and thus downstream signaling, more difficult (Vigil, Cherfils et al. 2010). Another reason that RAS is considered an “undruggable” enzyme is that its interaction with downstream effectors is mediated through protein-protein interfaces (Downward 2003). These types of interactions are difficult to disrupt with small molecules (Blundell, Sibanda et al. 2006).

One approach to inhibiting RAS activity was to target a post-translational modification of RAS that is absolutely essential for its activity: farnesylation (reviewed in Kloog and Cox 2000; Agrawal and Somani 2009) . As previously mentioned, all three RAS proteins are immediately farnesylated in the endoplasmic reticulum after their synthesis; RAS proteins that are unable to be farnesylated (with the critical cysteine residue replaced by a serine) are inactive and do not transform cells (Willumsen, Christensen et al. 1984). Inhibitors of farnesyltransferase exhibited anti-tumor effects in murine HRAS-driven tumors. Mice expressing HRAS<sup>G12V</sup> driven by an MMTV promoter began treatment with a farnesyltransferase inhibitor (FTI) when their tumors reach  $1000\text{mm}^3$  in size; all tumors regressed (Kohl, Omer et al. 1995). Upon cessation of treatment, the tumors reappeared and then regressed again once the drug was restarted (Kohl, Omer et al. 1995). However, this success could not be recapitulated in human clinical trials. To provide one example, the farnesyltransferase inhibitor tipifarnib was given to twenty treatment-naïve metastatic pancreatic cancer patients for one month. While farnesylation of peripheral blood

biomarker proteins was inhibited, zero complete or partial tumor responses were seen (Cohen, Ho et al. 2003). Despite over 400 patents being filed for FTIs in the span of a decade (Sousa, Fernandes et al. 2008), no FTI has been FDA approved. One hypothesis to explain the difference between preclinical and clinical results is that the preclinical models studied HRAS-driven tumors, while most human tumors are KRAS-driven. KRAS (and NRAS) can be alternatively geranylgeranylated when farnesyltransferase is inhibited (James, Goldstein et al. 1995; Whyte, Kirschmeier et al. 1997; Zhang, Kirschmeier et al. 1997). Thus, the lack of efficacy of FTIs in certain cancers does not imply that the concept of targeting RAS is invalid; rather, it emphasizes the fact that directly blocking RAS activity is extraordinarily difficult. FTIs do exhibit anti-tumor activity in some cancers that are not driven by RAS and are still being tested in clinical trials as general signal transduction inhibitors (Downward 2003); their anti-tumor effects may be mediated through inhibition of farnesylation of other lipidated proteins such as RhoB, CENP-E, and CENP-F (Kloog and Cox 2000).

### **1.1.6.3 Decreasing Signaling of Downstream RAS Effectors**

Given the difficulty in directly inhibiting the RAS protein itself, efforts have also focused on inhibiting the downstream effectors of RAS. Preclinical studies have identified which downstream effectors could be viable clinical targets.

For tumor initiation, active RAF mutants alone (Stanton, Nichols et al. 1989) or an active HRAS variant which can only signal to RAF (White, Nicolette et al. 1995; Hamad, Elconin et al. 2002) is sufficient to transform murine NIH3T3 fibroblasts. Combining RAS variants which can signal only to PI3K and RAF enhances transformation, as assessed by growth in soft agar (Hamad, Elconin et al. 2002). Knockin mice that express a structural variant of the PI3K catalytic

subunit which cannot interact with RAS (but otherwise retains full function) form almost no tumors in a model of spontaneous KRAS-driven lung carcinogenesis, compared to ~40 tumors in controls (Gupta, Ramjaun et al. 2007). However, in human cells, the narrative is different. A variant of HRAS that signals solely to the RALGEF pathway is more transforming than activation of either the PI3K or the RAF pathway alone, and about one-quarter as potent as activation of all the pathways by HRAS<sup>G12V</sup> (Hamad, Elconin et al. 2002).

Once tumors are formed, the signaling requirements from RAS needed for tumor growth change (Lim and Counter 2005). While the RAF and RALGEF pathways are still active in xenograft tumors, the presence of the driving RAS oncogene is not necessary to activate them. In other words, removal of HRAS<sup>G12V</sup> from the system does not affect the fact that elevated phospho-ERK and RAL-GTP levels are present; other signals not originating from RAS are enough to activate these pathways once the tumor has formed (Lim and Counter 2005). However, tumors do regress upon removal of HRAS<sup>G12V</sup> because they still depend on the oncogene to activate the PI3K-AKT pathway (Lim and Counter 2005). For tumor initiation, RAS signaling to RALGEF is particularly important (Hamad, Elconin et al. 2002); for tumor maintenance, RAS signaling to the PI3K-AKT pathway is necessary (Lim and Counter 2005).

The addiction of tumors to RAS is reduced to a PI3K pathway addiction once the tumors have formed. A potential therapeutic target in RAS driven tumors could thus be the two downstream kinases in the PI3K cascade, PI3K itself or AKT. These proteins are kinases and thus, unlike RAS, are druggable targets. Drugs that inhibit this pathway include PI3K inhibitors, AKT inhibitors, mTOR inhibitors, and dual PI3K-mTOR inhibitors; members of each of these four groups have been tested in at least Phase I clinical trials (Engelman 2009). Complicating this issue is the fact that there are at least four different PI3K catalytic subunits and three different

AKT isoforms; broad inhibition of all isoforms may be efficacious but also toxic (Engelman 2009). For example, broad PI3K inhibition leads to immunosuppression as well as glucose intolerance, while AKT inhibitors also exhibit the side effect of hyperglycemia (Rhodes, Heerding et al. 2008; Crouthamel, Kahana et al. 2009). Isoform-selective versions of these drugs may hold promise, particularly in cancers that are reliant on certain isoforms (e.g. cancers with *PI3KCA* mutations and thus a constitutively active p110 $\alpha$  isoform) (Engelman 2009). Furthermore, inhibition of downstream substrates of AKT kinases may also be a method for avoiding the toxic effects of broad, direct PI3K and AKT inhibition.

In this regard, a recent study identified eNOS as a downstream effector of AKT that is important for the maintenance of RAS-driven xenografts (Lim, Ancrile et al. 2008). In HRAS<sup>G12V</sup>-established tumors, targets of AKT were inhibited in a subpopulation of the cells, and the resulting contribution of that subpopulation to overall tumor volume was assessed. This allowed determination of the specific targets of AKT that contribute to tumor maintenance. The AKT substrates IKK $\alpha$ , BCL-X<sub>L</sub>, FOXO3a, TSC2, and eNOS were individually inhibited; knockdown of eNOS gave the greatest reduction in the contribution of that cell population to overall tumor volume. Further xenograft studies indicated that shRNA-mediated knockdown of eNOS in both HRAS<sup>G12V</sup>-driven HEK cell xenografts as well as multiple KRAS<sup>G12V</sup>-driven pancreatic cancer xenografts reduced tumor growth (Figure 1). This reduction in tumor growth could not be rescued by an eNOS<sup>S1177A</sup> mutant, an amino acid alteration which prevents eNOS activation by AKT. Consistent with this, elevated levels of S1177-phosphorylated eNOS are seen in human pancreatic cancer (Lim, Ancrile et al. 2008). To validate these findings in a spontaneously arising model of cancer, it was also shown that *eNOS*<sup>-/-</sup> mice are resistant to DMBA/TPA chemical carcinogenesis (which causes skin papillomas that exhibit HRAS mutations (Quintanilla, Brown et

al. 1986)). Thus, the pathway from RAS to PI3K to AKT to eNOS is important for the maintenance of human pancreatic cancer xenografts and possibly other forms of spontaneous RAS driven cancer (Lim, Ancrile et al. 2008).

In summary, genetic methods to block RAS signaling indicate that it remains an important pathway after tumors are established. Targeting downstream RAS effectors such as eNOS -- a druggable enzyme for which clinically-tested inhibitors already exist -- holds promise in the treatment of RAS driven tumors.

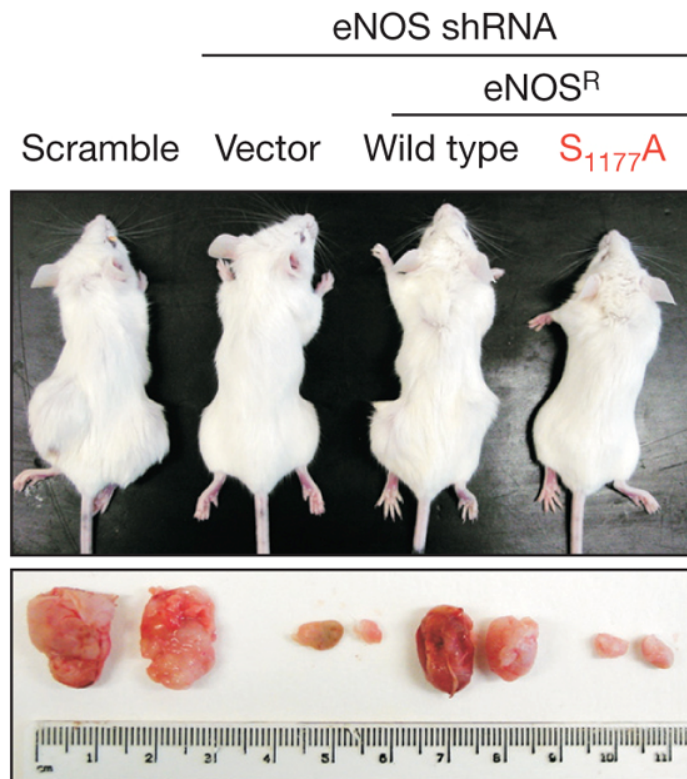


**Figure 1: eNOS activation by AKT is required for tumor growth.**

Representative tumors from immunocompromised mice injected with immortalized HEK cells expressing HRAS<sup>G12V</sup>. Knockdown of eNOS impedes tumor growth and this cannot be rescued with a mutant of eNOS that cannot be phosphorylated by AKT (Lim, Ancrile et al. 2008). Used with permission of the publisher.

## 1.2 eNOS

### 1.2.1 Nitric Oxide Synthase Structure and Catalysis

Nitric oxide synthases (NOSs) are a family of enzymes that produce nitric oxide from oxygen and the amino acid arginine (Figure 2). These enzymes are a combination of two functional domains, an N-terminal oxygenase domain and a C-terminal reductase domain, linked by an inter-domain peptide sequence that binds calmodulin (Zemojtel, Wade et al. 2003). The enzymes all require five cofactors: tetrahydrobiopterin, heme, flavin adenine dinucleotide (FAD), flavin mononucleotide (FMN), and nicotinamide adenine dinucleotide phosphate (NADPH) (Alderton, Cooper et al. 2001). Electrons are donated by NADPH to the reductase domain of the enzyme and proceed via the FAD and FMN carriers to the oxygenase domain, where at the active site of the enzyme they catalyze the reaction of oxygen with L-arginine (Alderton, Cooper et al. 2001). Citrulline and nitric oxide are generated as byproducts. The NOS enzymes function as homodimers, with the electrons being stripped by the reductase domain of one member of the dimer and transferred to the oxygenase domain of the other member (Stuehr 1999).

Nitric oxide (NO) is a gaseous second messenger. It was initially identified as the endothelium-derived relaxing factor produced by the vascular endothelium which causes smooth muscle cells to relax (Ignarro, Buga et al. 1987; Palmer, Ferrige et al. 1987; Furchgott 1999). However, since then, it has been shown to play diverse roles in many systems, from neurotransmitter to antibacterial agent (Stamler, Singel et al. 1992). Two physiologic ways in which NO functions as a second messenger will be discussed here: cyclic GMP (cGMP) dependent mechanisms, and S-nitrosylation dependent mechanisms.

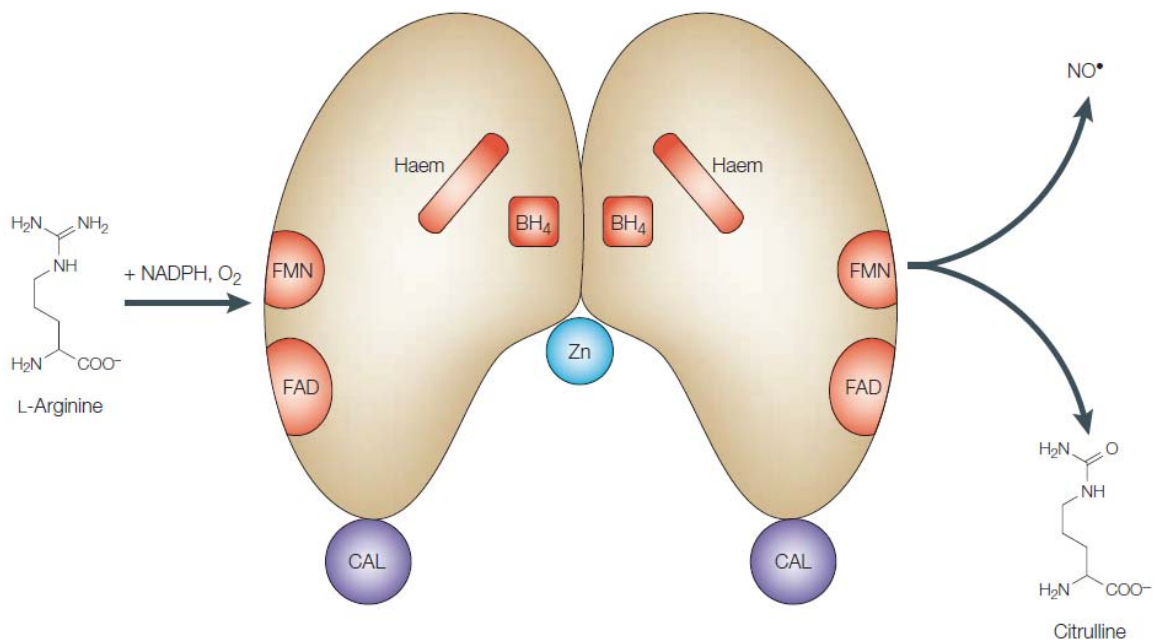


**Figure 2: Structure and Function of a Prototypical NOS Enzyme**

NOS enzymes dimerize and bind the cofactors tetrahydrobiopterin (BH<sub>4</sub>), heme, flavin mononucleotide (FMN) and flavin adenine dinucleotide (FAD). When calmodulin (CAL) is bound, the enzyme can catalyze the conversion of L-arginine to citrulline and nitric oxide (NO); requiring oxygen and NADPH as co-substrates. Each NOS dimer coordinates a single zinc (Zn) atom (Vallance and Leiper 2002). Used with permission of the publisher.

### **1.2.1.1 Nitric Oxide Signaling Through cGMP**

Nitric oxide is released from the endothelium in response to acetylcholine stimulation, causing the neighboring vascular smooth muscles cells to relax and the blood vessel to dilate (Moncada and Higgs 1993). The pathway stimulated by nitric oxide in this case is the cyclic GMP pathway. Since NO can reversibly bind directly to the ferrous iron atom in the porphyrin heme, any heme-containing proteins could potentially be subject to regulation by NO (Cooper 1999). Guanylate cyclase contains a heme group and its maximum catalytic rate upon NO binding to heme is 130-fold that of basal levels (Stone and Marletta 1994). Thus, NO diffuses into the smooth muscle cell, binds to and activates guanylate cyclase, resulting in increased production of cGMP and activation of protein kinase G, which can signal to myosin kinases and cause a relaxation in smooth muscle tissue (Dudzinski, Igarashi et al. 2006) .

### **1.2.1.2 Nitric Oxide Signaling Through S-Nitrosylation**

NO can also signal via post-translational modification of amino acids, a process known as S-nitrosylation (Stamler, Lamas et al. 2001). In a manner analogous to the way in which phosphate groups can be attached to the oxygen atoms in some amino acid side chains, nitric oxide can form a reversible, covalent bond with the sulfur atom in the cysteine side chain (Lane, Hao et al. 2001). Over a thousand proteins are known to be nitrosylated (Seth and Stamler 2011). Nitrosylation can affect protein function in a variety of ways, including inactivating proteins with cysteines at the active site (e.g. caspases, phosphatases, and possibly deubiquitinases) (Mannick, Schonhoff et al. 2001; Yu, Li et al. 2005), increasing the activity of small GTPases such as RAS and DRP1 (Lander, Milbank et al. 1996; Lim, Ancrile et al. 2008; Cho, Nakamura et al. 2009), or causing dimerization of proteins due to oxidation and promotion of

intermolecular disulfide bonds (Akhand, Pu et al. 1999; Cho, Nakamura et al. 2009). Protein denitrosylation is also enzymatically regulated (Benhar, Forrester et al. 2009). Signaling specificity can be achieved by proper localization of the NOS enzyme and its target protein; as only Golgi-targeted eNOS, but not nuclear targeted eNOS, can nitrosylate the Golgi-resident protein *N*-ethylmaleimide-sensitive factor (Iwakiri, Satoh et al. 2006). Additionally, in response to antigen presentation, Golgi-localized eNOS can activate NRAS, which is present on the Golgi in T lymphocytes, but not KRAS, which is not trafficked through the Golgi (Ibiza, Perez-Rodriguez et al. 2008).

## **1.2.2 Nitric Oxide Synthase Family Members**

In vertebrates, the NOS family consists of three genes: endothelial NOS (eNOS), inducible NOS (iNOS), and neuronal NOS (nNOS) (Alderton, Cooper et al. 2001). *Drosophila melanogaster* and other arthropods possess a single NOS isoform (Regulski and Tully 1995), and none can be detected in *Caenorhabditis elegans* or lower eukaryotes (Martinez 1995; Morton, Hudson et al. 1999; Cheung, Arellano-Carbajal et al. 2004). The focus here will be on the three mammalian NOS isoforms.

### **1.2.2.1 Inducible Nitric Oxide Synthase**

In contrast to the other two nitric oxide synthase isoforms, iNOS is a high-output (micromolar amounts of NO), calcium-independent (constitutively bound to calmodulin) enzyme found primarily in the cytosol (Geller and Billiar 1998). The major method of regulation of this enzyme is at the transcriptional level. Multiple inducers of iNOS expression (e.g. cytokines, lipopolysaccharide) converge on the JAK/STAT and/or NF- $\kappa$ B pathways to promote iNOS gene transcription (Kleinert, Pautz et al. 2004). The physiologic roles of iNOS can be deduced from

*iNOS* knockout mice. These mice have increased mortality when infected with pathogens such as *Mycobacterium tuberculosis*, *Listeria monocytogenes*, and *Leishmania major* (Wei, Charles et al. 1995; Nathan 1997). There are conflicting reports concerning whether *iNOS* gene ablation reduces mortality in mouse models of LPS-induced septic shock (Laubach, Shesely et al. 1995; Wei, Charles et al. 1995). Because of a defective inflammatory response, these mice are also protected from the severe inflammatory reactions in settings such as LPS airway challenges (Kristof, Goldberg et al. 1998). These mice also display variable tumor phenotypes depending on the assay, possibly because NO can have the contradictory effects of causing cytotoxicity to tumor cells while also promoting inflammation and radical-induced DNA damage (Fukumura, Kashiwagi et al. 2006; Mocellin, Bronte et al. 2007). In summary, the high levels of NO produced by *iNOS* can be cytotoxic to pathogens and abnormal tumor cells.

#### **1.2.2.2 Neuronal Nitric Oxide Synthase**

The first discovered NOS isoform, nNOS, is a low-output (picomolar amounts of NO), calcium-dependent (reversibly binds to calmodulin) enzyme that is found primarily in the cytosol (Geller and Billiar 1998). While it was initially identified in neurons, it is also expressed in cell types such as pancreatic islets, the macula densa of the kidney, and epithelial cells of the lung, uterus and stomach (Schmidt, Gagne et al. 1992). In the nervous system, NO can serve as a diffusible neurotransmitter that activates the cGMP pathway in neighboring neurons (Snyder 1992). Homozygote nNOS knockout mice exhibit defects that are attributed to the role of NO in central and peripheral neuronal signaling. They display decreased gastric motility and must be maintained on a liquid diet due to pyloric stenosis (Gyurko, Leupen et al. 2002). They have defects in hypothalamic regulated sexual hormone secretion and therefore develop

hypogonadism, preventing them from breeding (Gyurko, Leupen et al. 2002). Finally, they have behavioral abnormalities, including increased aggression (Nelson, Demas et al. 1995).

Another area in which nNOS (and also eNOS) plays a role is in the kidney (Mount and Power 2006). nNOS is expressed in the macula densa (Schmidt, Gagne et al. 1992; Bachmann, Bosse et al. 1995), the portion of the distal tubule that is responsible for feedback regulation of blood flow (and thus total filtration capacity) through the glomerulus. Consistent with this, triple NOS knockout animals are viable but the kidney is unable to retain sodium, resulting in nephrogenic diabetes insipidus, in addition to other signs of kidney dysfunction such as elevated creatinine (Morishita, Tsutsui et al. 2005).

With regards to nNOS and cancer, nNOS has been detected in human central nervous system tumors at levels higher than seen in normal brain tissue (Cobbs, Brenman et al. 1995). The tumor phenotypes of nNOS knockout mice, or studies investigating the effects of nNOS knockdown on tumor growth, have not been published.

### **1.2.2.3 Endothelial Nitric Oxide Synthase**

The enzyme eNOS was first identified in endothelial cells. Analysis of a transgenic mouse with a  $\beta$ -galactosidase reporter driven by 5,200 base pairs of the eNOS promoter confirmed high expression in large and medium sized blood vessels, as well as expression in the vasa recta of the kidney and in hippocampal neurons (Teichert, Miller et al. 2000). eNOS is a low output (picomolar amounts of NO), calcium-dependent (reversibly binds to calmodulin) enzyme that is primarily found associated with the membrane (Dudzinski and Michel 2007). The protein is irreversibly N-terminally myristoylated on glycine 2 and then reversibly palmitoylated on cysteines 15 and 26 (Dudzinski and Michel 2007). These three lipid anchors tether the enzyme in

caveolae (Shaul, Smart et al. 1996). In caveolae, eNOS binds to and is inhibited by caveolin, as caveolin competitively inhibits calmodulin binding to eNOS (Michel, Feron et al. 1997).

Post-translational regulation of eNOS activity occurs through a number of mechanisms. Intracellular calcium levels determine eNOS activity, because binding of calmodulin to the enzyme is required to facilitate transfer of electrons from the reductase to the oxygenase domain for catalysis (Alderton, Cooper et al. 2001). However, phosphorylation of eNOS can also activate the enzyme. Attachment of a phosphate group to serine 1177 prevents calmodulin dissociation from the enzyme and also promotes electron flux through the enzyme (McCabe, Fulton et al. 2000). The roles of eNOS in normal physiology and cancer will be discussed in the next two sections.

### **1.2.3 Role of eNOS in Normal Physiology**

Here, primarily based around studies of *eNOS*<sup>-/-</sup> animals, the functions of eNOS in normal physiology will be summarized, with a focus on the roles of eNOS in cardiovascular homeostasis, kidney function, and metabolism. These studies could indicate some of the side effects that an eNOS inhibitor used for the treatment of cancer may have.

eNOS is the primary source of NO in the endothelium (Lamas, Marsden et al. 1992), and NO causes vasodilation (Moncada and Higgs 1993). Correspondingly, *eNOS*<sup>-/-</sup> mice exhibit a 20% increase in systolic blood pressure over wild type controls (Huang, Huang et al. 1995; Shesely, Maeda et al. 1996). Administration of a non-specific NOS inhibitor to control mice raises blood pressure, while administration of the same inhibitor to *eNOS*<sup>-/-</sup> mice does not affect blood pressure (Kojda, Laursen et al. 1999) or even paradoxically decreases blood pressure (Huang,

Huang et al. 1995), indicating that eNOS is the primary NOS enzyme responsible for maintaining tonic vasodilation.

eNOS is expressed in the kidney and also plays a role there. Eighty percent of adult *eNOS*<sup>-/-</sup> mice exhibit grossly evident renal scars, which were found on histology to be the remnants of degenerated tubules (Forbes, Thornhill et al. 2007). While no lesions were detected in the kidneys of seven day old *eNOS*<sup>-/-</sup> mice, tubular degeneration was found in animals as young as 2 weeks of age. Cells of the renal tubule were undergoing apoptosis, resulting in separation of the filtration unit at the glomerulotubular junction (Forbes, Thornhill et al. 2007). When considering the renal phenotype of *eNOS*<sup>-/-</sup> mice, it is difficult to discern how much of this is due to hypertension-induced renal injury versus injury due to a lack of renal-intrinsic eNOS. eNOS is expressed in afferent and efferent renal arterioles, suggesting that, like nNOS, it could be involved in direct regulation of flow through the glomerulus (Bachmann, Bosse et al. 1995). In general, nitric oxide signaling in the kidney promotes natriuresis (sodium excretion) and diuresis (water excretion) (Mount and Power 2006).

Finally, *eNOS* knockout animals exhibit metabolic abnormalities, including hyperinsulinemia, hyperglycemia, and elevated plasma concentrations of triglycerides, cholesterols and free fatty acids (Duplain, Burcelin et al. 2001). This insulin resistance is not entirely due to the hypertensive effects of *eNOS* ablation, as isolated muscle from an *eNOS*<sup>-/-</sup> animal had lower glucose uptake compared to control when they were perfused under the same pressures (Duplain, Burcelin et al. 2001).

Additionally, about 40% of *eNOS*<sup>-/-</sup> neonates die within one hour of birth due to abnormal lung morphogenesis (Han, Babaei et al. 2004), and female mice exhibit decreased

fertility (Pallares, Garcia-Fernandez et al. 2008), making extensive breeding of these mice difficult.

#### **1.2.4 Role of eNOS in Cancer**

Studies on the role of nitric oxide in cancer biology often give contradictory results (reviewed in Fukumura, Kashiwagi et al. 2006; Mocellin, Bronte et al. 2007). Manipulation of NO signaling can have differential effects on tumor progression depending on the model system that is used, the method with which NO signaling is perturbed, and the particular endpoint (e.g. angiogenesis, metastasis, or tumor growth) that is examined (Fukumura, Kashiwagi et al. 2006; Mocellin, Bronte et al. 2007). Studies that specifically examined the role of eNOS in cancer through the use of genetic methods such as gene knockouts or knockdowns are reviewed below.

##### **1.2.4.1 eNOS Mediates RAS Signaling**

As previously mentioned, eNOS is activated downstream of oncogenic KRAS in pancreatic cancer cells (Lim, Ancrile et al. 2008). Knockdown of eNOS reduced xenograft growth of these cancer cells. Furthermore, *eNOS*<sup>-/-</sup> mice displayed three-fold less skin papillomas per mouse when subjected to a chemical carcinogenesis protocol that causes *HRAS* mutations. Consistent with signaling to eNOS through the AKT pathway, mutants of eNOS that cannot be phosphorylated and activated by AKT do not rescue the eNOS knockdown phenotypes, and elevated phosphorylated eNOS was found in all three tested human pancreatic cancer specimens and seven out of eight cell lines, as compared to normal pancreatic tissue.

The authors of the above study continued to follow the KRAS<sup>G12V</sup>-PI3K-AKT-eNOS pathway in human pancreatic cancer cells to determine the possible targets of eNOS that could

be relevant for tumorigenesis. Informed by a previous study that found RAS itself could be S-nitrosylated on cysteine 118 (Lander, Milbank et al. 1996), they found that the other two isoforms of RAS, HRAS and NRAS, were nitrosylated and activated by eNOS in this system. shRNA and rescue studies showed that these xenograft tumors not only depended on HRAS and NRAS expression for growth, but also needed forms of HRAS and NRAS that could be nitrosylated, as expression of nitrosylation-defective C118S mutants could not rescue the HRAS knockdown phenotype. Thus, the original *KRAS* mutation amplifies and/or diversifies the RAS signal by activating the other two isoforms through eNOS (Lim, Ancrile et al. 2008).

#### **1.2.4.2 eNOS Mediates Angiogenesis**

eNOS plays a role in physiologic angiogenesis. NO donors promote, and NOS inhibitors block, angiogenesis in rabbit cornea models (Ziche, Morbidelli et al. 1994). This can at least be partially attributed to eNOS, as endothelial cells from *eNOS*<sup>-/-</sup> mice show impaired sprouting and proliferation *in vitro*, and *eNOS*<sup>-/-</sup> mice display impaired VEGF-induced angiogenesis in an *in vivo* wound healing assay (Lee, Salyapongse et al. 1999). Later, it was shown that while *eNOS*<sup>-/-</sup> mice have normal levels of endothelial progenitor cells (EPCs) in their bone marrow, they exhibit defective proliferation and release of these EPCs into the circulation upon VEGF stimulation, which is due to the fact that NO-mediated activation of matrix metalloprotease 9 is defective in *eNOS*<sup>-/-</sup> bone marrow (Aicher, Heeschen et al. 2003).

These studies of eNOS in normal vascular angiogenesis raise the possibility that eNOS may also play a role in tumor angiogenesis. Two studies have established that this is the case. Melanoma xenografts were grown in the dorsal skin and cranium under windows so that the vasculature – and the NO within it – could be visualized (Kashiwagi, Izumi et al. 2005). The only

detected eNOS in this model was within the walls of the vasculature. Tumors grown in *eNOS*<sup>-/-</sup> hosts showed significantly reduced total NO concentrations, as well as reduced vessel density and reduced vessel branching. Furthermore, tumor vessels in these *eNOS*<sup>-/-</sup> hosts displayed reduced recruitment of pericytes surrounding the vessel, demonstrating that not just endothelial cell recruitment but also pericyte recruitment is deficient in *eNOS*<sup>-/-</sup> mice. In this model, eNOS was the major contributor to tumor NO, because tumors in *iNOS*<sup>-/-</sup> animals had similar levels of NO and similar vessel morphology to wild-type controls. A second study of eNOS in tumors (Gratton, Lin et al. 2003) took advantage of the fact that caveolin is a naturally occurring inhibitor of eNOS (see 1.2.2.3 Endothelial Nitric Oxide Synthase). A short synthetic peptide named cavtratin was synthesized that contained a portion of the caveolin protein; an antennapedia sequence was coupled to it to facilitate cell uptake. The peptide specifically inhibited eNOS but not the other NOS family members (Bucci, Gratton et al. 2000). Xenograft tumor vascular permeability, which is typically high, was blocked by administration of the cavtratin peptide, and this inhibited tumor growth. To validate the inhibitor studies, the authors also showed that xenograft tumor growth in *eNOS*<sup>-/-</sup> mice was reduced, these tumors displayed little vascular permeability, and cavtratin had no anti-tumor effect on tumor growth in these animals (Gratton, Lin et al. 2003).

#### **1.2.4.3 eNOS Mediates Notch Signaling**

A recent report indicates that eNOS is important for gliomagenesis because it activates the Notch pathway in glioma stem-like cells (Charles, Ozawa et al. 2010). The authors used a mouse model where PDGF-encoding retrovirus is injecting into the ventricular space, resulting in PDGF-driven gliomas. eNOS in these tumors is localized to the blood vessels. The authors found

that the tumor cells surrounding the blood vessels expressed Notch1. Paracrine signaling was responsible for this, as NO produced by the blood vessels diffused into the tumor cells and activated guanylate cyclase/cGMP/PKG, eventually resulting in Notch1 expression. The Notch1 positive cells in this “perivascular niche” were particularly important, as these cells exhibited stem-cell-like characters within the tumor. Thus, eNOS in the vascular endothelium was responsible for maintaining the stem-cell niche in these gliomas, and indeed *eNOS*<sup>-/-</sup> mice displayed increased survival and decreased tumor levels of Notch1 (Charles, Ozawa et al. 2010).

In sum, these studies indicate that eNOS plays different roles in different cancers. However, the data are consistent in that genetic inhibition of eNOS inhibits tumor growth in each model. This indicates that eNOS may be a good target for pharmacologic inhibition; as such a drug may have activity in a wide variety of cancers.

### **1.2.5 L-NAME: A NOS Inhibitor**

An additional reason to investigate the role of eNOS in genetically engineered mouse models of pancreatic cancer is that inhibitors of the enzyme have already been developed and -- in some cases -- used in humans (see 1.2.5.3 L-NAME Clinical Trials in Humans). Therefore, in addition to the upcoming genetic studies of eNOS ablation in pancreatic cancer, a clinically relevant pharmacologic approach has also been taken. However, no *selective* small molecule inhibitors of eNOS have been developed; most available compounds broadly target all three NOS enzymes (Alderton, Cooper et al. 2001). The inhibitor chosen for studies here was L-N<sup>G</sup>-nitroarginine methyl ester (L-NAME). The characteristics of L-NAME and the reasons for choosing this particular drug will be discussed, with emphasis on its clinically relevant aspects: its pharmacokinetics, its off-target effects, and its history of use in humans.

### 1.2.5.1 L-NAME Pharmacokinetics and Mechanism of Action

The majority of NOS inhibitors are analogues of arginine that function by competitively inhibiting access of arginine to the active site (Knowles and Moncada 1994; Alderton, Cooper et al. 2001); L-NAME falls within this category (Figure 3). Upon entry into the cell or into plasma, L-NAME is rapidly cleaved by esterases to yield the active metabolite L-N<sup>G</sup>-nitroarginine (L-NNA). This metabolite inhibits the NOS enzymes with the following IC<sub>50</sub> values: 3.1μM for iNOS, 0.29μM for nNOS, and 0.35μM for eNOS (Alderton, Cooper et al. 2001). Thus, out of the many broad NOS inhibitors, L-NAME shows a partial 10-fold specificity for eNOS and nNOS over iNOS. However, it is unknown if this mild selectivity is relevant *in vivo*.

Another attractive feature of L-NAME is its high solubility and oral bioavailability (Griffith and Kilbourn 1996). While rigorous studies of drug bioavailability have not been published, administration of the drug at a concentration of 1g/L in the drinking water results in blood pressure elevation and thus eNOS inhibition (Trifilieff, Fujitani et al. 2000; Yamashita, Kawashima et al. 2000); in studies here that has been empirically found to result in a dose to the mouse of ~180mg/kg.

In a study where L-NAME was continuously infused into septic patients at the rate of 1mg/kg/h for a span of twelve hours, the half-life of L-NAME in the plasma was 19.2 minutes, while the half-life of L-NNA was 22.9 hours. The maximum plasma concentration of L-NNA reached was 6.2μg/mL, or 28.3μM (Avontuur, Buijk et al. 1998).

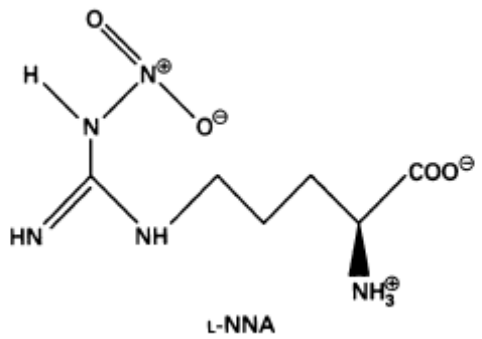
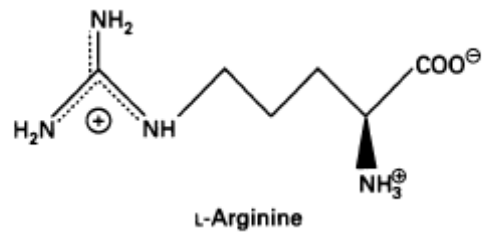


**Figure 3: Comparison of L-NNA and arginine structure.**

This comparison of arginine and the active metabolite of L-NAME, L-NNA, shows the high degree of similarity between the compounds. Adapted with permission (Knowles and Moncada 1994).

### **1.2.5.2 Side Effects of L-NAME Administration**

Acutely, the primary effect of L-NAME is an elevation in systemic vascular resistance and blood pressure. In humans, this met the definition of hypertension in some, but not all, healthy subjects administered L-NAME (Morgan, Silke et al. 2003). In animal studies, the increases in blood pressure become more pronounced the longer the drug is given (Navarro-Cid, Maeso et al. 1996).

Chronic treatment with L-NAME, which might be necessary in an anti-cancer setting, has only been tested in animals and causes chronic hypertension with resultant end-organ damage to the kidney and heart. In one rat study, increased kidney protein excretion (a sign of kidney dysfunction) was found after eight weeks of L-NAME dosing, although there was no effect on plasma creatinine (a more serious sign of kidney dysfunction). This increased proteinuria was prevented by treatment with antihypertensives during the course of the experiment (Navarro-Cid, Maeso et al. 1996). A second rat study looking at a six week dose course also found increased proteinuria in L-NAME treated rats without an increase in plasma creatinine, and confirmed that the renal effects of the drug could be ameliorated by concomitant treatment with the antihypertensive amlodipine (Akuzawa, Nakamura et al. 1998). This study also looked at the histologic changes in the kidney and heart, finding glomerulosclerosis and left ventricular hypertrophy in the L-NAME treated group, but not in any of the rats treated with L-NAME and amlodipine (Akuzawa, Nakamura et al. 1998). A third study also investigated the effects of L-NAME on rat kidney function and additionally examined the kidney after L-NAME withdrawal (Ribeiro, Antunes et al. 1992). Blood pressure continuously rose during the four week course of treatment, reaching 168 mmHg versus 108 mmHg in controls. Renal function was compromised,

as renal vascular resistance rose to over 3 times that of controls, and the glomerular filtration rate dropped to 70% that of controls. Histology showed glomerular lesions and tubular atrophy. The authors demonstrated that treatment with the angiotensin converting enzyme inhibitor losartan could block the effects of L-NAME on blood pressure and renal function. Moreover, after two weeks off of L-NAME, blood pressure began a steady decline towards normal (Ribeiro, Antunes et al. 1992). These studies indicate that while NOS inhibition has effects on the cardiovascular and renal systems, much of these can be prevented by treatment with an antihypertensive, and discontinuation of the drug may also reverse the adverse effects.

Some off-target effects of L-NAME administration can be expected due to inhibition of the other NOS enzymes. The production of NO via iNOS is part of host defense against a broad range of pathogens, including viruses, bacteria, fungi, and parasites (Geller and Billiar 1998). Pharmacologic iNOS inhibition has immunosuppressive effects that allow for re-activation of latent infections. Administration of the partially selective iNOS inhibitor L-NIL to wild-type mice with latent tuberculosis infection resulted in 50% mortality after thirty days, compared to no mortality in the untreated controls (MacMicking, North et al. 1997). A mouse model of herpetic keratitis showed accelerated disease progression when the animals were treated with aminoguanidine, an iNOS inhibitor (Benencia, Courreges et al. 2001). Finally, inhibition of iNOS with L-NIL exacerbated *Toxoplasma gondii* protozoal infection to the point of lethality in mice (Schluter, Deckert-Schluter et al. 1999). Such effects would be undesirable in a cancer patient population that may already be immunosuppressed due to chemotherapy.

Finally, if either nNOS or iNOS enzymes play a role in pancreatic cancer, then any results with the drug L-NAME will be confounded by those effects. Studies of L-NAME in *eNOS*<sup>-/-</sup> mice can address this issue.

### 1.2.5.3 L-NAME Clinical Trials in Humans

Since NOS inhibitors cause an increase in blood pressure, they were developed for the treatment of cardiogenic and septic shock. L-NAME is one of only two NOS inhibitors to have been tested in phase II trials in humans. The studies discussed below involve L-NAME and another arginine mimetic NOS inhibitor, L-N<sup>G</sup>-monomethyl arginine (L-NMMA). These trials used intravenous infusion of the drugs over a short period of time in an acute intensive care setting; this is different from the long-term, orally dosed approach that may be used in cancer patients.

One of the earliest trials of NOS inhibitors in humans was an open-label trial of L-NMMA for the treatment of septic shock (Grover, Zaccardelli et al. 1999). Blood pressure in patients with shock is maintained using drugs such as norepinephrine; this study showed that L-NMMA was a potent vasoactive agent in humans and could be used to reduce the dose of norepinephrine needed to maintain blood pressure, mainly by increasing systemic vascular resistance (Grover, Zaccardelli et al. 1999). This was followed by a randomized, double-blind, placebo controlled phase III study of L-NMMA for the treatment of septic shock; subjects received L-NMMA for up to fourteen days, with additional vasoactive drugs allowed if L-NMMA alone could not maintain blood pressure. The study was stopped early due to an increase in mortality in the L-NMMA treatment arm (59% versus 49% at 28 days after study enrollment); this was primarily attributed to a higher proportion of cardiovascular-related deaths in the treatment group (Lopez, Lorente et al. 2004). Subsequently, studies of L-NMMA in cardiogenic shock also produced negative results. The final large scale study of any NOS inhibitor in humans was the TRIUMPH study, a phase III, randomized, double-blind, placebo-controlled trial of L-NMMA for the treatment of cardiogenic shock (Alexander, Reynolds et al. 2007). The drug was given as an initial bolus, infused over a five hour period, and then discontinued; all-cause

mortality at 30 days was the primary objective. Despite a significant elevation of blood pressure in the intervention group, the study was again terminated early based on pre-specified futility criteria. No difference was found between mortality rates in the two arms (Alexander, Reynolds et al. 2007).

Clinical trials with L-NAME in humans were also performed. An open-label trial of continuous 12 hour L-NAME infusion in patients with septic shock showed that it was a potent vasoconstrictor (Avontuur, Tutein Nolthenius et al. 1998). A 30 subject, phase II, randomized, open-label, placebo-controlled study of L-NAME in the treatment of cardiogenic shock was stopped early because of impressive positive results (Cotter, Kaluski et al. 2003). As in the TRIUMPH study, the drug was infused as a bolus followed by a five hour treatment period. L-NAME treated patients had a one month survival rate of 73% versus 33% in the control arm (Cotter, Kaluski et al. 2003). However, development of the drug was dropped due to the negative results with L-NMMA in both cardiogenic and septic shock that were starting to appear at the time.

In addition to these major studies involving many subjects, there are over one hundred smaller studies where L-NAME has been given to subjects with a variety of conditions, including tetraplegia (Wecht, Weir et al. 2007; Wecht, Weir et al. 2008), diabetes (Sokolnicki, Roberts et al. 2007), and asthma (Gomez, Barbera et al. 1998), as well as healthy volunteers (Morgan, Silke et al. 2003; Muldowney, Davis et al. 2004; Young, Fisher et al. 2009). Typically these are studies are not treatment-oriented, but rather are designed to examine the role of nitric oxide in various physiologic and pathophysiologic processes.

In sum, despite the negative results in phase III trials showing that NOS inhibitors do not reduce mortality from cardiogenic and septic shock, such studies lay the groundwork for administering these drugs, particular L-NMMA and L-NAME, to humans.

## **1.3 Translational Control of Gene Expression**

As previously discussed, the levels of RAS proteins in cancer cells correlate with tumorigenic potential. Work within this thesis examines how translational elongation may control RAS protein levels. Other instances in which translation elongation regulates gene expression will be examined first.

### **1.3.1 The Process of Translation and Rationale for Regulation**

Information contained within the DNA polymer is transcribed into messenger RNA, and the information contained with that mRNA instructs protein synthesis. The process of translation is the process of converting the information within mRNA into a protein.

The initial step of protein synthesis is recognition of the mRNA and the translation start site by the ribosome, a process called translation initiation (reviewed in Sonenberg, Hershey et al. 2000). The initiation process consists of five key steps: (1) identification of the 5'-methyl guanosine ( $m^7G$ ) cap by eukaryotic initiation factors, (2) assembly of the initiating methionine amino acid with the 40S small ribosomal subunit, (3) joining of the assembled small ribosomal subunit with the message, (4) scanning and location of the start codon, and (5) binding of the large ribosomal subunit. Over 25 polypeptides take part in this process, only a few of which will be discussed here. First, the identification of the  $m^7G$ -cap is the responsibility of the protein eukaryotic initiation factor 4E (eIF4E). eIF4E is the limiting initiation factor in cells, and is also regulated by eIF4E binding proteins (eIF4E-BPs), which bind directly to the site where the  $m^7G$ -

cap is recognized. Phosphorylation of eIF4E-BPs is a major mechanism of translational control; for example, the complex of mTOR and raptor can directly phosphorylate (and inactivate) eIF4E-BP (Hara, Maruki et al. 2002), thereby stimulating protein synthesis. This regulation of eIF4E is a supportive example of the hypothesis that the majority of regulation of translation takes place at the initiation step (Kozak 1999). eIF4E combines with eIF4G, a scaffolding protein, which increases eIF4E affinity for the m<sup>7</sup>G-cap. At the same time, a GTP-bound form of the GTPase eIF2 recognizes specific initiating methionine-bound tRNAs, met-tRNA<sub>i</sub>, which possess unique base pair structures that distinguish them from regular methionine bound tRNAs. In a highly regulated step, the eIF2-tRNA<sub>i</sub> complex binds to the small 40S subunit (which is bound to yet another initiation factor, eIF3) to create the second macromolecular structure needed for translation initiation. The scaffolding protein eIF4G recognizes eIF3, and thus a protein bridge is created, linking the mRNA to the 40S ribosomal initiation complex. Then, scanning for an initiating ATG codon begins, in the 5' to 3' direction along the mRNA. Again, this step is highly regulated, as strong secondary structure, 5' UTR length, nucleotide context surrounding the proximal ATG, and bound proteins can all affect this scanning process. Only once the ATG is recognized is the large 60S ribosomal unit recruited. The protein eIF5, which is bound to the large ribosomal subunit, serves as a GAP for eIF2, meaning that once the large ribosomal subunit is docked, GTP hydrolysis – and thus protein synthesis – can begin (reviewed in Sonenberg, Hershey et al. 2000).

During the elongation phase of protein biosynthesis (reviewed in Sonenberg, Hershey et al. 2000), the ribosome selects an aminoacyl-tRNA complex (aa-tRNA) that pairs with the exposed codons in the mRNA, at which point a peptide bond is catalyzed between the growing peptide chain and the incoming amino acid. Again, this can be greatly simplified into a series of

steps: (1) “charging” of a tRNA with the proper amino acid, (2) recruitment of the charged aa-tRNA to the active site of the ribosome, (3) peptide bond formation, and (4) translocation of the mRNA by three nucleotides so that the next codon-anticodon pair can be made. Charging of the tRNA is carried out by the tRNA synthetase enzyme; there are at least twenty tRNA synthetase enzymes, one per amino acid that must be recognized. The synthetase catalyzes a two step reaction in which the amino acid is first conjugated to an ATP molecule, and then transferred to the tRNA. The proper pairing of amino acid and tRNA is required to maintain the fidelity of the genetic code, and – like DNA polymerase – tRNA synthetases have evolved proofreading activity to ensure a correct match (Sankaranarayanan and Moras 2001). Next, a complex forms between the aa-tRNA and the GTPase eukaryotic elongation factor 1A (eEF1A); note the parallel here with the GTPase eIF2 involved in translation initiation. When the eEF1A-aa-tRNA complex enters the A site of the ribosome, an attempt is made to match the codon of the mRNA with the anticodon on the tRNA. If the match is successful, the ribosome facilitates GTP hydrolysis by eEF1A, and eEF1A-GDP leaves the ribosome. (The protein eEF1B is a GEF that recharges eEF1A into a GTP-bound state.) The ribosome then catalyzes the formation of a peptide bond between the incoming tRNA and the growing peptide chain. Next, another GTPase, eEF2, enters the ribosome and catalyzes the GTP-dependent translocation of the peptidyl-tRNA chain from the A site to the P site. The cycle is complete and can begin anew with the next codon (reviewed in Sonenberg, Hershey et al. 2000).

To complete the process of protein synthesis, translation must be terminated (reviewed in Stansfield, Jones et al. 1995; Nakamura, Ito et al. 1996). The signal for termination is the appearance of one of three particular codons in the mRNA: UAA, UAG, or UGA. The overall process of termination is similar to that of elongation, except that instead of the codons being

recognized by a tRNA molecule, the stop codons are recognized by the protein eukaryotic releasing factor 1 (eRF1). The crystal structure of eRF1 indicates that it acts as a “molecular mimic” of tRNAs; that is, a portion of it resembles an anticodon (that can match all three stop codons), and a second portion resembles the stem of the tRNA molecule. This stem facilitates ribosome-mediated catalysis of the peptide-tRNA ester bond of the growing peptide chain in the P site. Just as in elongation and initiation, eRF1 binds to a GTPase, eRF3 (analogous to eEF1A and eIF2). When eRF1 successfully finds a stop codon in the A site, eRF3-GTP undergoes GTP hydrolysis and leaves eRF1 in the ribosome. Thus, the peptide-tRNA bond can be cleaved and the process of protein synthesis is complete (Stansfield, Jones et al. 1995; Nakamura, Ito et al. 1996).

Translational regulation of gene expression has benefits that control at other levels of gene expression, such as transcription, do not have (reviewed in Sonenberg, Hershey et al. 2000). First, translational control of protein expression is rapid. Transcriptional control affects the first step in protein synthesis, and is slow compared to the immediate consequences of altering translation. Translational regulation is also direct. Affecting the transcription of a gene changes an early step in the process, leaving the possibility that variations in other steps of gene synthesis (e.g. capping, polyA tailing, or mRNA export) could obscure the initial action and desired effect. On the other hand, there are no intermediate steps between translating an mRNA and making a protein. Just like transcription, regulation of translation could be a global event, affecting all translation, or a specific event, affecting only translation of certain mRNAs (as dictated by nucleotide sequence). Translational regulation can also provide spatial control of gene expression. An example of this occurs in the patterning of the *Drosophila* embryo. Nanos protein is required in the posterior of the embryo to direct the formation of abdominal

segment; it must be absent from the anterior of the embryo, where it could suppress head development. To achieve this protein localization, the *nanos* mRNA is localized, but this is inefficient, so in addition the mRNA is also translationally repressed at the steps of both initiation and elongation (Dahanukar and Wharton 1996; Andrews, Snowflack et al. 2011).

Finally, it should be noted that the magnitude of translational control on a certain gene need not be great; that is, regulation of translation may only be a fine-tuning effect (Sonenberg, Hershey et al. 2000).

### **1.3.2 Regulation of Translation Elongation as a Method of Controlling Protein Expression in Mammals**

As mentioned above, the majority of translational regulation is thought to occur at the initiation step (Kozak 1999; Sonenberg, Hershey et al. 2000). Regulation of translation initiation, as opposed to elongation or termination, allows the benefits of translational control without inefficiently committing energy and amino acids to the synthesis of proteins which may not be completed. Nevertheless, in eukaryotes, there are a number of examples of regulation at the elongation step. A few of these examples will be examined to inform the latter studies concerning regulation of KRAS mRNA elongation.

One method of regulation of translation elongation would be to slow ribosome movement across the message, which could serve as a fine-tuning method affecting protein levels. Isolation of nascent hemoglobin peptides from rabbit reticulocytes shows not a smear of sizes (as would be expected if the translation rate were constant) but rather a discrete banding pattern, indicating that ribosomes may pause at certain sites (Protzel and Morris 1974). Similarly, using the fact that ribosomal footprints protect about 30 nucleotides from nucleases, one would expect uniform distribution of mRNA fragments after nuclease protection assays if

the ribosome translation rate is constant. This is not the case, at least during *in vitro* translation of bovine preprolactin mRNA in both wheat germ extract and rabbit reticulocyte lysate (Wolin and Walter 1988). In addition to ribosomal pausing at the initiation and elongation steps, one study found two pause sites within the message, both at GGC codons. As the leading ribosome stalled at these points, ribosomes behind it stacked up (Wolin and Walter 1988).

The protein eEF2, which is involved in moving the nascent peptide chain from the A site to the P site, is phosphorylated at threonine 56, which inhibits its ability to bind ribosomes (see 1.3.1 The Process of Translation and Rationale for Regulation) (Carlberg, Nilsson et al. 1990). It has been shown that this results in a decrease in polyU directed phenylalanine synthesis (Ryazanov and Davydova 1989). Therefore, processes that increase this protein's phosphorylation could inhibit the translation rate of endogenous cellular mRNAs. The activity of eEF2 kinase, of which eEF2 is the only known substrate (Browne and Proud 2002), is regulated by a number of mechanisms. eEF2 kinase activity is stimulated by increases in both cellular calcium levels (Ryazanov 1987) and protein kinase A (Redpath and Proud 1993) activity. The former effect has been shown to be important in the protection of neurons from glutamate toxicity (Marin, Nastiuk et al. 1997). Excessive levels of glutamate stimulation increase neuronal intracellular calcium levels, causing an increase in eEF2 kinase activity. This causes a decrease in protein translation, an effect which actually decreases neuronal toxicity; the authors hypothesized this was because eEF2 phosphorylation allowed shunting of energy to more immediate, protective needs (Marin, Nastiuk et al. 1997). On the other end of the spectrum, mTOR signaling inhibits eEF2 kinase activity via S6 kinase, which phosphorylates eEF2 kinase and inhibits it (Wang, Li et al. 2001). This results in more active eEF2 and provides an explanation for why insulin, amino acids, and glucose – all of which can signal through mTOR – cause a decrease

in eEF2 phosphorylation and an increase in protein translation (Morley and Traugh 1993; Diggle, Redpath et al. 1998; Campbell, Wang et al. 1999; Traugh 2001). Regulation of eEF2 via this mechanism links the activity of translation to the nutrients which surround the cell (Browne and Proud 2002).

MicroRNAs (miRNAs) may also act the level of translation elongation by repressing ribosomal movement through an unclear mechanism (Jackson and Standart 2007). MicroRNAs with perfect complementarity to their target promote degradation through endonucleolytic cleavage; however, the majority of miRNAs are imperfect matches to their target and cause a lesser decrease in target message abundance in addition to a large decrease in protein abundance. It has been shown that miRNAs associate with translating mRNAs in the polysome fraction in cells, and that this association reduces the mobility of messages in polysomes (Maroney, Yu et al. 2006). These authors showed that *KRAS* mRNA exhibits reduced mobility in polysomes, and this was attributed to miRNA regulation, given the previous reports of *KRAS* regulation by *let-7* (Johnson, Grosshans et al. 2005). However, no experiments were done to show that relief of *let-7* inhibition restored polysome mobility; in other words, the link between miRNA regulation and reduced *KRAS* mobility was not established. This leaves open the possibility that the slow translation of *KRAS* message could be due to other means.

The two final examples in this section will deal with examples of how the process of translation elongation is pathologically altered in cancer. First, a recent study highlights a novel mechanism by which translation of specific messages may be regulated (Hussey, Chaudhury et al. 2011). Typically, the expression of two genes involved in epithelial-to-mesenchymal transition, *DAB2* and *ILE1*, is inhibited because of a nucleotide element in their 3' UTR termed the BAT element. The authors discovered that hnRNP1 E1 binds to this BAT element and loops

back to bind eEF1A1 at the same time. The binding of hnRNP E1 to eEF1A1 prevents eEF1A1 release from the ribosomal A site following GTP hydrolysis, and thus expression of the messages is inhibited. Transforming growth factor- $\beta$ , which is known to promote epithelial-to-mesenchymal transition, mediates phosphorylation of hnRNP E1, causing dissociation of the hnRNP E1-eEF1A1 complex. The messages are free to translate. Abolition of this regulation via knockdown of hnRNP E1, or rescue of the knockdown with a mutant that cannot be phosphorylated, causes epithelial-to-mesenchymal transition of certain cell types and tumor growth. Thus, eEF1A1, in addition to eEF2, may be a target for translational regulation.

In addition to regulating proteins involved in elongation, expression of the tRNAs involved in protein synthesis can be regulated. Transcription of the tRNA genes is driven by the RNA polymerase III machinery (White 2011), which is often activated above normal levels in cancer (White 2005). The first demonstrated example of hyperactive RNA polymerase III in cancer was an examination of four different ovarian tumors that revealed elevated tRNA expression and corresponding elevated expression of TFIIC (a component of the RNA polymerase III transcriptional apparatus) in all samples (Winter, Sourvinos et al. 2000). RB can bind RNA polymerase III regulatory subunits and block transcription; this regulation is lost in RB deficient tumor cells, fibroblasts from RB knockout mice, and E1A-transformed cells (White, Trouche et al. 1996). Overexpression of BRF1, a protein necessary for recruitment of RNA polymerase III to its transcription sites, causes increased synthesis of tRNAs and is sufficient to transform cells (Marshall, Kenneth et al. 2008). All mice injected with BRF1 transformed cells had tumors by 10 weeks' time, as compared to RAS transformed control cells, which formed tumors in four weeks. However, this is not entirely due to effects on just translation elongation,

as in this system tRNA<sub>i</sub><sup>met</sup>, also a product of RNA polymerase III and a necessary part of translation initiation, was weakly transforming as well.

Reasons for specifically regulating translation elongation include the following (reviewed in Sonenberg, Hershey et al. 2000; Browne and Proud 2002). Translation elongation is an energy intensive process, and under conditions where cells must conserve energy or divert it to other processes, control of elongation may be appropriate. The effects of altering translation elongation are even more immediate and direct than altering translation initiation, which still requires assembly or disassembly of a multi-protein complex. Translation elongation rate may be increased in settings where translation initiation is also increased, in order to avoid a limitation in translation due to slow elongation. Additionally, slowing translation increases the fidelity of the process, and thus cells may modulate elongation to balance a demand between protein output and nascent peptide quality (Carr-Schmid, Durko et al. 1999; Carr-Schmid, Valente et al. 1999). These hypotheses provide supportive rationale for examining translational regulation of *KRAS* mRNA.

### **1.3.3 Codon Choice as a Possible Mechanism for Control of Translation Elongation?**

Due to the fact that there are 64 possible three letter codes but only 20 amino acids, the genetic code is redundant. Multiple different codons can encode for the same amino acid. Does it matter which codon is used? More specifically, in the process of translation elongation, does codon choice matter? There is not an even distribution of codon usage in human genes (see Table 1) (Nakamura, Gojobori et al. 2000). This uneven distribution results in rare codons and common codons, and for this thesis a rare codon is any codon in Table 1 that is not the most commonly used codon. However, the uneven distribution of codon usage does not demonstrate

that certain codons are preferred over others in the process of translation elongation. Codons used by a gene reflect more than just their role in elongation (Chamary, Parmley et al. 2006); there are at least three other mechanisms *in mammals* that could explain how an uneven distribution in codon usage could arise without any role for codon usage in translation elongation (Chamary, Parmley et al. 2006; Plotkin and Kudla 2011).

**Table 1: Codon Usage Frequency of Amino Acids in *Homo sapiens***

Codon	Amino Acid	Frequency (%)
ATG	M	100%
TGG	W	100%
TTT	F	46%
TTC	F	54%
TAT	Y	44%
TAC	Y	56%
CAT	H	42%
CAC	H	58%
CAA	Q	27%
CAG	Q	73%
AAT	N	47%
AAC	N	53%
GAT	D	46%
GAC	D	54%
GAA	E	42%
GAG	E	58%
TGT	C	46%
TGC	C	54%
AAA	K	43%
AAG	K	57%
ATA	I	17%
ATT	I	36%
ATC	I	47%
GTA	V	12%
GTT	V	18%
GTC	V	24%
GTG	V	46%

Codon	Amino Acid	Frequency
GGT	G	16%
GGA	G	25%
GGG	G	25%
GGC	G	34%
CCG	P	11%
CCA	P	28%
CCT	P	29%
CCC	P	32%
ACG	T	11%
ACT	T	25%
ACA	T	28%
ACC	T	36%
GCG	A	11%
GCA	A	23%
GCT	A	27%
GCC	A	40%
CTA	L	7%
TTA	L	8%
TTG	L	13%
CTT	L	13%
CTC	L	20%
CTG	L	40%
TCG	S	5%
AGT	S	15%
TCA	S	15%
TCT	S	19%
TCC	S	22%
AGC	S	24%
CGT	R	8%
CGA	R	11%
CGC	R	18%
CGG	R	20%
AGG	R	21%
AGA	R	21%

Codon usage data retrieved from (Nakamura, Gojobori et al. 2000)

First, the nucleotide sequence of a gene is a property of the genomic region in which it sits. Isochores are large domains of relatively homogenous GC content in mammals (Sharp, Averof et al. 1995). The GC content of a gene at synonymous sites (GC3) strongly correlates with the isochores in which the gene resides (Aota and Ikemura 1986). In other words, for unknown reasons, mutational biases in certain regions of the genome favor (or disfavor) guanines and cytosines, and this favoritism is evident in both the noncoding DNA surrounding the gene and the coding DNA sequence at synonymous sites (Sharp, Averof et al. 1995; Chamary, Parmley et al. 2006). A gene positioned in an isochores with a high GC content will have a high GC3 percentage, and thus appear to “prefer” certain codons (Chamary, Parmley et al. 2006). However, it is possible to statistically correct for the background GC content, and even when this corrected for, highly expressed (but not lowly expressed) genes still exhibit preference for certain codons and thus codon bias (Urrutia and Hurst 2003).

A second factor explaining part of the variation in codon usage in the above table is also a product of a biased mutational process. In mammals, the cytosine in CpG dinucleotides can be methylated; this cytosine then has a relatively high chance of spontaneously deaminating to become a thymidine (Wang, Kuo et al. 1982). This “hypermethylability” of CpG dinucleotides means that they appear with reduced frequency in mammalian genomes (Josse, Kaiser et al. 1961); this is reflected in the fact that codons in Table 1 which end in CG are greatly underrepresented.

Additionally, codon usage can affect gene expression in at least two ways without directly affecting the process of translation (Chamary, Parmley et al. 2006). First, there is a reduced rate of synonymous mutations around intron/exon junctions and within elements in exonic DNA that control splicing. Synonymous mutations – and thus usage of particular codons -

- are therefore under selection in certain areas of the gene because they affect intron removal. This is supported by the fact that single nucleotide polymorphisms decrease in frequency towards the ends of exons (Majewski and Ott 2002), and also by the identification of examples of synonymous mutations that cause disease because they affect the splicing process (Cartegni, Chew et al. 2002). Second, there is evidence that the GC content of an mRNA affects its overall stability. Mammalian mRNA sequences exhibit a higher average thermodynamic stability than a collection of random mRNA sequences encoding for the same amino acids (Chamary and Hurst 2005). The authors hypothesized that this may be due to a higher-than-expected appearance of cytosines at fourfold degenerate sites, which can form base pairs with guanosines in the second codon position to form stable RNA structures that may be protected from RNAses (Chamary and Hurst 2005). Furthermore, changing codons of the dopamine receptor D2 (DRD2) in humans affects ectopic transcript levels and stability; creation of synthetic mRNAs that encode the same protein but have a higher incidence of C|G dinucleotides (where | indicates the boundary between two codons) results in a 1.2 fold increase in RNA levels and a 33% increase in mRNA half-life (Duan and Antezana 2003). Thus, certain codons may be enriched because they affect splicing and/or transcript stability.

These explanations for how codon bias could arise in mammalian genes are not mutually exclusive with a hypothesis that also posits a role for codon usage in translation rate. As discussed below, existing data support a role for codon usage in regulating translation elongation, at least in prokaryotes and lower eukaryotes. In mammals, the data are less clear.

### 1.3.3.1 Studies of Codon Usage in Prokaryotes

In certain species of prokaryotes, codon choice does play a role in expression of endogenous genes (Ikemura 1985). Common codons in highly expressed genes correlate with highly abundant tRNAs (Ikemura 1985; Tuller, Waldman et al. 2010). This is corroborated by the fact that genes from heterologous organisms must often be codon optimized to achieve high expression in bacteria, or alternatively expression can be improved by ectopic expression of the rare tRNA (Burgess-Brown, Sharma et al. 2008).

Recent data, however, modified the above findings by reflecting the fact that codon usage may be particularly important in the early 5' region of the coding sequence. The tRNA adaptation index (tAI) is a measure of the translational efficiency of a particular codon which takes into account not only the amount of tRNA in the cell that can perfectly pair with that codon, but also the amount of tRNA present that can imperfectly pair with the codon, due to variation in the wobble position (Tuller, Carmi et al. 2010). An analysis of the tAI along the length of all *E. coli* genes found that the tAI for the first ~20 codons was generally lower than the tAI for the rest of the gene; in eukaryotes, the tAI was also low at the beginning and at the end of the gene as well. This was posited to serve as a translational "ramp," meant to minimize ribosomal traffic jams and abortive protein synthesis by gradually allowing ribosomes to reach their maximum speed, and sterically hindering following ribosomes from attaching to the message until the previous ribosome is moving. Additionally, the ribosomes recognizing the suboptimal codons in these ramps may be particularly sensitive to tRNA and nutrient abundance in the cell, sterically preventing more translation of the message if conditions are not ideal. The presence of a translation ramp was found not only in *E. coli* but in all other species tested, including yeast and humans (Tuller, Carmi et al. 2010).

A second group examined the expression in *E. coli* of 154 synthetic GFP genes that all varied in synonymous codon content, and then statistically identified factors within the coding region of the mRNA that accounted for the wide expression differences seen. The factor controlling the majority of protein expression was mRNA folding energy near the start codon; mRNAs with weak 5' secondary structure had higher expression (Kudla, Murray et al. 2009). Thus, in *E. coli*, codon usage is important for overall expression of a gene, and its modification of ribosomal kinetics in the 5' portion of the message may be particularly important for ensuring efficient translation.

### **1.3.3.2 Studies of Codon Usage in Yeast**

The process of transcription is physically separate from translation in eukaryotes, and studies indicate that in this eukaryotic setting codon choice can also affect translation rate. In yeast as in bacteria, the relationship between codon usage and tRNA abundance (as measured by tRNA gene copy number) is not linear but is skewed, indicating both a preference for optimal codons and an avoidance of suboptimal codons (Ikemura 1985; Akashi 2003).

Codon order is also important for expression in yeast (Cannarozzi, Schraudolph et al. 2010). The genes of eukaryotes from yeast to flies to humans show evidence for codon recycling. When one particular codon is used to encode for an amino acid, the next time that amino acid appears in the protein sequence, it is more likely to be encoded for by the previously used "recycled" codon than any other isoaccepting codon. Two GFP mutants were constructed with the same codons and expressed in yeast. However, in one gene the codons were highly correlated (for example, all the GTA valine codons occurred in succession, then all the GTG codons, etc.) and in a second GFP gene the codons were highly anti-correlated (the GTA valine

codon was followed by a GTG valine codon which was followed by a GTA codon, etc.) The correlated GFP gene had a higher expression than the anti-correlated GFP gene. The authors estimate an increase in translation speed of 30%, and hypothesize that the mechanism underlying this phenomenon is binding of outgoing tRNAs to the ribosome and subsequent recycling (Cannarozzi, Schraudolph et al. 2010).

### 1.3.3.3 Studies of Codon Usage in Insects

An early example indicating that codon usage could be relevant to translation elongation and protein expression involved the silk producing glands of *Bombyx mori*. The fibroin protein, one of the major components of silk, is partially made up of tandem repeats of the amino acid sequence Gly-Ala-Gly-Ala-Gly-Ser (Mita, Ichimura et al. 1994). Over 95% of the codons used to encode for glycine in this portion of the protein are GGT, and similar biases in codon usage exist for the alanines and serines in the sequence (Mita, Ichimura et al. 1994). When the larva enters the portion of its life where these glands must produce silk in high quantities, the tRNA content of the silk-producing cells shifts to match that of the exact tRNAs needed to produce fibroin (Chevallier and Garel 1979).

Studies of codon usage in *Drosophila* show that the codons of the aldehyde dehydrogenase (*Adh*) gene control protein levels and function. Replacement of 10, 6, or even 1 of the leucine codons in *Adh* (a 192 amino acid protein) with unpreferred leucine codon(s) resulted in a significant decrease in aldehyde dehydrogenase level (Carlini and Stephan 2003) and in fly ethanol tolerance (Carlini 2004). Correspondingly, replacement of seven suboptimal leucine codons in the *Adh* gene with their optimal counterpart resulted in increases in protein activity and function in larva (Hense, Anderson et al. 2010).

#### 1.3.3.4 Studies of Codon Usage in Mammals

In bacterial, yeast, and insect systems, as opposed to mammals, the question of whether codons play a role in translation elongation is easier to answer because in these simpler systems endogenous genes can be readily modified, tRNA content can be determined, and certain features that complicate the situation and are specific to mammals, such as isochores, are lacking. Furthermore, in mammals, an evolutionary argument can be made against selective pressure promoting the use of translationally optimal codons. (The absence of selective pressure shaping coding usage does not necessarily imply that codon choice plays no role in translation; however, the case for codon importance in translation elongation is much easier to make if such a selective pressure can be demonstrated, as in lower eukaryotes and bacteria.) The argument against selective forces acting on synonymous sites in mammalian genes is known as the nearly neutral theory (Sharp, Averof et al. 1995; Chamary, Parmley et al. 2006). This posits that a mutation will only be selected for/against if the effect of the mutation on organism fitness multiplied by the effective population size is large. For example, consider a nonsense mutation in DNA polymerase of a single bacterium. This will be selected against because the effect on fitness is large and the pool of other competing bacteria is large. The product of these two numbers will thus be large as well. A *synonymous* mutation in bacterial DNA polymerase may have a much smaller effect on organism fitness, but since the competition is so great, this too will be selected against. With mammals, however, both the effective population size and the expected effect on organism fitness of a synonymous mutation are quite small. Therefore, their product is small and the mutation will not be selected for or against. Thus, one may not see the signature of selective pressure on mammalian codon usage (Chamary, Parmley et al. 2006), even if it has an effect on translation.

Some studies have been done that suggest codon choice in mammals may have effects on translation elongation. The aforementioned studies of Protzel and Wolin suggest that elongation rate is not constant (Protzel and Morris 1974; Wolin and Walter 1988). The previously mentioned studies of correlated codons in yeast (Cannarozzi, Schraudolph et al. 2010) and the 5' ramp in bacteria (Tuller, Carmi et al. 2010) found that such features also exist in human transcripts, suggesting that codon choice could have functional consequences in mammals.

There are also certain anecdotal observations of instances in mammals where codon choice has consequences. Deoptimization of codon pairs can decrease infectivity of poliovirus; this is relevant because the virus uses the mammalian host machinery to synthesize its proteins (Burns, Shaw et al. 2006; Coleman, Papamichail et al. 2008). Synonymous SNPs within the coding region of the human transporter protein MDR1 alter its protein folding and subsequent transport function (Kimchi-Sarfaty, Oh et al. 2007). Another example involves two actin isoforms,  $\beta$ -actin and  $\gamma$ -actin. Despite the fact that their N-terminal amino acids are nearly identical, only  $\beta$ -actin is arginylated. It was shown that the codons used by the  $\gamma$ -actin isoform slow translational speed (through an unknown mechanism), and even though  $\gamma$ -actin is co-translationally arginylated too, the slower translation speed gives the ubiquitination machinery time to recognize and degrade it. The codons used by an mRNA direct a post-translational modification of the protein (Zhang, Saha et al. 2010).

Finally, the expression of heterologous genes ectopically introduced into mammalian cells can be limited by their codon choice. For example, codon optimization of jellyfish GFP increases its expression in human cells (Zolotukhin, Potter et al. 1996). Codon optimization can increase expression of ectopically introduced mammalian genes in mammalian cells (Fath, Bauer

et al. 2011). For example, the RNA splicing protein nPTB1 has frequent rare codons which cause ribosomal stalling in *in vitro* assays. Ribosomal stalling and low expression of the protein could be rescued when a codon optimized variant of the protein was expressed (Robinson, Jackson et al. 2008). The demonstration that codon choice alters expression of ectopically introduced genes does not necessitate that endogenous mammalian genes are also subject to this regulation, because the mRNA of an overexpressed transgene may be present in the cell at levels many thousand-fold higher than those of normal transcripts (Plotkin and Kudla 2011). At this high level, elongation may become the rate limiting step because the cellular machinery is overwhelmingly swamped with identical mRNAs. The principles that govern the expression of ectopically introduced genes may not govern the expression of endogenous genes (Plotkin and Kudla 2011).

In sum, there is data supporting the fact that codon usage could control the expression of endogenous mammalian genes. Experiments within this thesis confirm that changing the codons of an endogenous mammalian gene does indeed alter expression levels.

## 1.4 Summary

This two part thesis focuses first on how the KRAS protein is made, and second on one way that KRAS signaling can be inhibited to reduce tumor growth.

In **Chapter 3**, I investigate the role that codon usage plays in expression of the RAS protein. As RAS protein levels are important in development and cancer, mechanisms that regulate the translation of the *RAS* genes could have biological significance. I show that *KRAS* has more rare codons than *HRAS* and that this is responsible for the lower KRAS protein levels seen in ectopic expression assays. I then optimize the codons of the endogenous cellular *KRAS*

gene and demonstrate that this results in increased KRAS protein expression and enhanced KRAS-driven tumorigenesis. Furthermore, I demonstrate that these consequences are due to increased translation rate of a normally slowly translated mRNA. Working with Joey Prinz and David MacAlpine, I then identify other gene pairs that exhibit the same high homology that the RAS genes do, as well as their corresponding codon usage differences. I then show that these predicted gene pairs do exhibit the divergence in expression levels that is predicted by their divergent codon usage, implying that the mechanism of translational slowing that controls KRAS expression may broadly be a feature controlling expression of many other genes.

With these studies, the computational identification of highly homologous gene pairs with a wide difference in codon usage was the work of Joey Prinz and David MacAlpine. In particular, they are responsible for the gene list generated in Table 2, the identification of the gene pairs whose relative expression levels were tested in Figure 11A, and the identification of signaling pathways, such as the ones depicted in Figure 11B and Figure 19, which contain a higher-than-expected-by-chance number of genes with rare codons.

In **Chapter 4**, I investigate the role that eNOS inhibition plays in slowing RAS driven tumorigenesis. As detailed above, eNOS has been identified in xenograft assays as an important downstream mediator of RAS signaling (Lim, Ancrile et al. 2008). With the help of Brooke Ancrile, I further tested inhibition of this target in genetically engineered mouse models with a genetic and a pharmacologic approach in order to discern whether eNOS blockade could be a viable option for the treatment of pancreatic cancer in humans. I first tested the consequence of *eNOS* knockout on two separate mouse models of pancreatic KRAS driven neoplasia. Then I tested the effect that pharmacologic inhibition of eNOS using the clinically tested general NOS inhibitor L-NAME has on pancreatic cancer in these same models. In the first mouse model that

investigates early stage pancreatic lesions, I showed that *eNOS* knockout results in a significant reduction of preinvasive pancreatic lesions, as well as a reduction in two other off-target KRAS-driven tumors that appear in these mice. I also showed that L-NAME has a similar but smaller and non-significant effect on early pancreatic lesion development. In the second mouse model that fully recapitulates the development of metastatic, lethal, pancreatic ductal carcinoma, I demonstrated that both *eNOS* knockout and L-NAME treatment cause a 25% and 13% increase in lifespan, respectively, although this does not reach the level of significance. In conjunction with Disean Kendall and Meghan Morrison, these results are brought closer to the clinic by demonstration that L-NAME also has an effect on human pancreatic cancer xenograft growth, and that the major side effect of L-NAME, elevated blood pressure, can be managed with an antihypertensive without erasing its effects on tumor growth.

With the genetically engineered mouse models, Brooke Ancrile developed genotyping protocols for the *LSL-Kras<sup>G12D</sup>*, *Pdx-1-Cre*, and *eNOS* alleles; she also bred all the KC mice used in the study and began crossing the *LSL-Trp53<sup>R172H</sup>* gene into the model. Disean Kendall and Meghan Morrison performed the studies investigating the role of L-NAME on xenograft growth and generated the data in Figure 15B, Figure 16, and Figure 17. Disean Kendall also quantified the normal pancreatic area remaining in the tissue of KC mice, as depicted in Figure 13B and Figure 21B. Michael Shealy and Diana Cardona assessed ductal lesions in the KC mice and are responsible for the data in Figure 13C and Figure 21C.

## 2. Materials and Methods

### 2.1 Rare Codons Limit KRAS Tumorigenic Activity

#### 2.1.1 Cell Lines

HEK-HT cells, generated as previously described (Armbruster, Banik et al. 2001), were used for the transient and stable exogenous RAS studies. HEK-HT cells were maintained at 37°C in 5% CO<sub>2</sub> in DMEM (Sigma) supplemented with 10% fetal bovine serum (Gibco) and 100U/mL penicillin and streptomycin. Pancreatic cancer cell lines (ATCC) were maintained in RPMI (Sigma) with identical supplements, and HCT116 colon cancer cells (ATCC) were maintained in McCoy's 5A media (Gibco/Invitrogen) with identical supplements.

#### 2.1.2 Plasmids

All constructs undergoing PCR at any step were sequenced to verify the contents. pBabePuro and pBabeBleo constructs containing HRAS and KRAS and their oncogenic mutants were generated as previously described (Lim, Ancrile et al. 2008), and were used for all transient and stable expression studies, except when indicated otherwise. pDCR-KRAS, pDCR-HRAS, pCGN-KRAS, and pCGN-HRAS for studies of RAS expression in alternative vectors were kind gifts from Adrienne Cox. The chimeric KRAS\* plasmid was generated by three piece ligation of PCR amplified, BamHI-SpeI cut HRAS N-terminus (forward primer 5'-AGGCCGAGCTCGGATCCACGCGTCCGCCATGGACTACAAGGACGACGATGACAAG-3' and reverse primer 5'-CACGCACTAGTGTGTAGAAGGCATC-3' which inserts a SpeI site with a synonymous mutations at T158) and SpeI-SalI cut KRAS C-terminus (forward primer 5'-GATGCCTTCTATACTAGTTCGAG-3' also introduces a SpeI site at T158 and reverse primer 5'-gacgcgtcgacTTACATAATTACACACTTTG-3') into BamHI-SalI digested pBabepuro. The following

mutations were then made with five rounds of site directed mutagenesis to create an N-terminus that exactly matched KRAS at the amino acid level: Q95H (CAG to CAT), D107E (GAT to GAG), A121P and A122S (GCTGCA to CCTTCA), E126D and S127T and R128K (GAATCTCGG to GACACTAAG), Y141F (TAC to TTC), E153D (GAG to GAT). To create the GST-RAS fusion proteins, a Sall-NotI digest of pCIneo-GST (Armbruster, Banik et al. 2001) was used as the backbone for ligation of the following Sall-NotI digested PCR products: GST-HRAS -- 5'-GGAATTCCCGGGTCTGACTCACGGAATATAAGCTTGTG-3' (forward), 5'-GGTAGGTTGCGGCCGCTCAGGAGAGCACACTTGCAGCTC-3' (reverse); GST-STOP-HRAS -- 5'-GGAATTCCCGGGTCTGACTCtgaGAATATAAGCTTGTG-3' (forward) and GST-HRAS reverse primer; GST-KRAS -- 5'-GGAATTCCCGGGTCTGACTCACTGAATATAAACTTGT-3' (forward), 5'-GGTAGGTTGCGGCCGCTTACATAATTACACTTTG-3' (reverse); GST-STOP-KRAS -- 5'-GGAATTCCCGGGTCTGACTCtgaGAATATAAACTTGT-3' (forward) and GST-KRAS reverse primer; GST-KRAS\* -- GST-HRAS forward primer and GST-KRAS reverse primers were used; GST-STOP-KRAS\* -- GST-STOP-HRAS forward primer and GST-KRAS reverse primers were used. To create the AAV targeting construct, the following components were assembled into BluescriptKS in this order: (1) 5' homology arm from HCT116 genomic DNA (5'-ATGGTTTACCCGCGCCGCGTGCCCGGCTCACTTGCATCTCTTAACAGCTG-3' forward and 5'-CCAACTACCACTAGTTTATATTCAGTCATTTTCAGCAGGC-3' reverse) inserted with SacI and SpeI digestion, (2) 3' homology arm from HCT116 genomic DNA (5'-ACGAAGTTATGTCGACAGCTGTGAAATCTAGAACAGG-3' forward and 5'-GGGAACAAAAGCTGGGTACCGCGGCCGCACTCACTGTAAGTGGGAG-3' reverse) inserted with Sall-KpnI digestion, (3) either a *KRAS*<sup>G13D</sup> codon optimized cDNA (see Gene Synthesis section, below) or a *KRAS*<sup>G13D</sup> cDNA with regular codons with a BGH polyA tail fused via overlap extension PCR,

using a SpeI-BamHI digest, and (4) a shortened neomycin resistance cassette from pNeDaKO (Kohli, Rago et al. 2004) without the zeocin resistance cassette (5'-GAACCAGCTGGGGATCCAACAAAAGCTGGAGCTCCACC-3' forward primer and 5'-AGAATCGTCGACCCCCAGCTGGTTCTTCCGCCTCAGAAGCCATAG-3' reverse primer) using a BamHI-Sall digest of both vector and insert. After all pieces were assembled and verified by sequencing, the entire cassette was moved into pAAV-MCS (Stratagene) using NotI non-directional cloning.

### 2.1.3 Gene Synthesis

For optimized constructs with many silent mutations (*KRAS* incremental codon replacement, *KRASop*, *CFL2op*, *ORMDL1op*), a gene synthesis approach was used. An Excel macro was employed to codon optimize each gene by replacing each suboptimal codon with the most commonly used synonymous codon (according to Table 1) and then to split the resulting construct into 60-mer oligonucleotides that overlapped by 12-15 base pairs. These oligonucleotides were diluted to 500nM and mixed with 10 $\mu$ M flanking forward and reverse primers and PCR was carried out using Platinum Taq (Invitrogen) at a gradient of annealing temperatures. The reaction at the annealing temperature which gave the most robust product of an appropriate size was gel purified and ligated into pBluescriptKS. The resulting constructs were sequenced to verify accuracy; the frequency of products containing mutations (typically at the oligonucleotide junctions) was proportional to the length of the construct (1/8 correct products for *KRASop*, 2/3 correct products for *ORMDL1op* and *CFL2op*).

### **2.1.4 Protein Analysis**

For all immunoblots, cells were lysed in 25mM Tris pH 7.4, 150mM NaCl, 5mM EDTA, 1% Triton X-100, 1mM DTT, and 1mM PMSF, and then resolved by SDS page. Membranes were blotted with anti- $\beta$ -tubulin 1:1000 (Sigma), anti-FLAG 1:1200 (Sigma), anti-KRAS 1:100 (Santa Cruz), anti-GST 1:500 (Santa Cruz) or anti-myc 1:5000 (Invitrogen); all antibodies were diluted in 5% non-fat dry milk in TBS-Tween.

### **2.1.5 Metabolic Labeling**

A 6cm plate of 80% confluent cells was preincubated with methionine- and cysteine-free RPMI (Sigma) with 15% dialyzed FBS (Invitrogen) for one hour. Then, 200 $\mu$ Ci of EXPRESS Protein Labeling Mix (Perkin-Elmer) was added; cells were labeled for 15min, collected and washed with PBS, resuspended in 400 $\mu$ L lysis buffer (see 2.1.4 Protein Analysis) and lysed on ice for 30min. The samples were then centrifuged at 13000g for 10 minutes, the supernatant collected, and aliquots set aside for input lanes. The rest of the sample was used for immunoprecipitation with M2 anti-FLAG resin (Sigma). After overnight immunoprecipitation the beads were washed three times with lysis buffer, an equal volume western loading buffer was added and sample was boiled for 10 minutes to release the bound proteins. After SDS-PAGE electrophoresis the gel was fixed in 7% acetic acid and 25% methanol in water for thirty minutes, washed, soaked in a 1% glycerol, 5% polyethylene glycol (MW 5000) (Sigma) solution for thirty minutes and then dried. After a 15 hour exposure the gel was developed.

### **2.1.6 Tumorigenesis Assays**

All studies were done according to protocols approved by the Duke University Institutional Animal Care and Use Committee. For HEK-HT tumorigenesis studies,  $1 \times 10^7$  cells

mixed with Matrigel (BD Biosciences) were injected subcutaneously into the flanks of 4 SCID/beige mice per cell line, after which tumor volumes were determined at regular intervals as described previously (O'Hayer and Counter 2006). For HCT116 tumorigenesis studies,  $1 \times 10^6$  cells resuspended in 100 $\mu$ L PBS were injected subcutaneously into the flanks of 6 SCID/beige mice per cell line. Results shown are representative of duplicate experiments. Tumors were removed and photographed when one of the lines reached maximal volume.

### 2.1.7 RT-PCR

The reverse transcription reaction was done with the Omniscript RT kit (Qiagen) according to the manufacturer's instructions. For direct studies of total RAS transcript levels, two micrograms of total RNA, isolated with RNAzolB (Tel-Tech) according to manufacturer's instructions, was used for the reverse transcription with oligo-DT priming. The resulting cDNA was diluted 1:25 and assessed by qPCR using SybrGreen PCR mastermix (BioRad). For exogenous RAS studies the following pBabe MCS specific primers were used: 5'-CTCAATCCTCCCTTTATCCAG-3' (forward) and 5'-CTGGTTGCTGACTAATTGAGATGC-3' (reverse). For quantitation of total KRAS in the HCT116 knockin clones, the following KRAS 5'UTR primers were used: 5'-GAGCGAGCGCGGCAGGCACTG-3' (forward) and 5'-AGTTTATATTCAGTCATTTTC-3' (reverse). Reference primers directed against GAPDH: 5'-GAAGGTGAAGGTCGGAGTCAA-3' (Forward) and 5'-GCAGAGGGGGCAGAGATGAT-3' (Reverse) were used as controls. Measurements were done on the BioRad iCycler iQ (v3.1), with 40 amplification cycles. No RT control cDNA was included to ensure against contaminating transcript. For each sample, qPCR reactions were done in triplicate, and the entire analysis was done twice independently. For polysome studies RNA was isolated as indicated in the section Polysome Profiling and then the entire fraction of purified

RNA was used as a template for cDNA synthesis. The following primers were used to detect each of the indicated transcripts: HRAS 5'-CAGGAGACCCTGTAGGAGGA-3' (forward) and 5'-ATCCAGGATGTCCAACAGGC-3' (reverse) semi-quantitative at 22 cycles for HCT116 cells and 26 cycles for HEK cells; KRAS endogenous allele only 5'-GGCTCAGCGGCTCCCAGGTG-3' (forward) and 5'-ATATCCAAGAGACAGGTTTC-3' (reverse) semi-quantitative at 23 cycles for HCT116 cells and 26 cycles for HEK cells; KRAS knockin allele only 5'-GGCTCAGCGGCTCCCAGGTG-3' (forward) and 5'-cACcAcCtGCTTtCTGTAgctg-3' (reverse, lowercase letters anneal only to bases present in optimized KRAS sequence).

### **2.1.8 AAV-Mediated Homologous Recombination**

The procedure of Rago et al. (Rago, Vogelstein et al. 2007) was generally adhered to with the following details. The targeting vector, pHelper, and pAAV-RC (Stratagene) were introduced into 293 cells with Fugene 6 (Roche) transfection reagent. Cells were scraped into 1mL PBS forty-eight hours later and virus was harvested with three cycles of freeze-thaw in an ethanol-dry ice bath. The lysates were clarified and 350µL added directly to a 60% confluent 10cm plate of HCT116 cells along with 4mL of McCoy's 5A growth media. After a three hour incubation, 8mL of growth media were added and cells incubated for 48 more hours. The cells were then trypsinized and resuspended in 3mL PBS. Thirty microliters of this suspension was then added to 200mL of McCoy's 5A plus 400µg/mL neomycin and cells were seeded in twenty 96-well plates. Ten to fourteen days later colonies were scored; generally about 10-13 colonies appeared per plate. Colonies were transferred and replica plated into two 96-well plates. Two days later, DNA was isolated from one plate using the Wizard SV96 genomic DNA purification system (Promega) according to the manufacturer's instructions. The screening primers used spanned the 3' homology arm to give 1393bp product: 5'-ATCAATTCTCTAGAGCTCGCTGAT-3'

forward and 5'-TTTTTACAATAACATGGAGTCAGCA-3' reverse. Step-down PCR was performed with Platinum Taq (Invitrogen) with four cycles each at annealing temperatures of 64°C, 61°C, 58°C, and then thirty cycles at an annealing temperature of 55°C. Positive clones were then expanded and tested for presence and mRNA expression of the recombined allele via RT-PCR and sequencing of the product obtained with the KRAS knockin detection primers detailed in the RT-PCR section. Determination of the allele on which knock in occurred was done by PCR amplification and sequencing of the remaining codon wild-type KRAS allele.

### **2.1.9 Polysome Profiling**

A 10cm plate of 50-60% confluent cells was treated for five minutes with 200µM cycloheximide. For indicated conditions, pactamycin (kind gift of Christopher Nicchitta) was added to 200nM for five minutes prior to cycloheximide addition. Cells were washed with PBS plus 200µM cycloheximide and then 1mL lysis buffer (400mM KOAc, 25mM KHEPES pH 7.2, 15mM Mg(OAc)<sub>2</sub>, 1% NP-40, 0.5% sodium deoxycholate, 1mM DTT, 1mM PMSF, 200µM cycloheximide, and 40U/mL RNaseOut [Invitrogen]) was applied directly to the plate for ten minutes on ice. Collected lysates were centrifuged for ten minutes at 12000g and the supernatant was carefully layered on top of a 15-50% sucrose gradient. Samples underwent ultracentrifugation for three hours at 35000rpm in a Beckman L8-80M ultracentrifuge (SW40Ti rotor). The gradients were fractionated using an ISCO gradient fractionator with a continuous absorbance monitor into 34 to 36 fractions of volume 330µL. For RNA isolation, first 2µL PelletPaint (Novagen) was added to each fraction, and then 2.5 volumes GT buffer (4M guanidine thiocyanate, 25mM sodium citrate pH 7.0, 0.5% N-lauryl sarcosine, 5mM EDTA, and 0.1M beta-mercaptoethanol) was added and samples were rotated for fifteen minutes at room

temperature. Then, 220 $\mu$ L chloroform was added, samples were shaken vigorously and separated by centrifugation at 12000g for 15 minutes. The upper aqueous phase was removed (700 $\mu$ L) and mixed with equal volume isopropanol and 0.1 volumes 3M sodium acetate pH 5.2. After overnight incubation at -20°C, RNA was pelleted via centrifugation at 13000g for 20 minutes. The pellet was washed with 75% ethanol and resuspended in 30 $\mu$ L DEPC treated water.

### **2.1.10 Statistics**

For xenograft studies, we compared tumor weights and tumor volumes of all mice in each arm on the final day of the experiment using a two sided unpaired t test. For mRNA quantitation, fold changes were calculated using the  $\Delta\Delta$ Ct method. The  $\Delta$ Ct of each sample equals Ct(target) minus Ct(GAPDH control), and fold changes were determined by calculating  $2^{\Delta\text{Ct}(\text{control average}) - \Delta\text{Ct}(\text{sample})}$ . A two sided unpaired t test was used to compare mRNA fold changes. All statistical analyses were performed using Graphpad Prism v5 (Graphpad Software).

## **2.2 Targeting eNOS in Pancreatic Cancer**

### **2.2.1 Cell Lines**

The pancreatic cancer cell lines AsPC-1, CAPAN-1, CFPac-1, HPAC, HPAF-II, MiaPaCa-2, PANC-1 and SW-1990 were obtained from American Type Cell Culture and cultured in RPMI media supplemented with 10% fetal bovine serum (Gibco Invitrogen). Cell lines were derived from KPC mice by mincing tumor tissue in collagenase V (Sigma-Aldrich) for 30 minutes at 37°C, pelleting cells, and then resuspending and plating the cells in FBS-containing DMEM media. Resultant cell lines were passaged four times before analysis to enrich for tumor cells devoid of stroma.

## 2.2.2 Mouse Pancreatic Cancer Models

*Pdx-1-Cre* (Hingorani, Petricoin et al. 2003) and *LSL-Trp53<sup>R172H</sup>* (Olive, Tuveson et al. 2004) mice were obtained from the Mouse Models of Human Cancers Consortium Mouse Repository. *LSL-Kras<sup>G12D</sup>* (Jackson, Willis et al. 2001) and *eNOS<sup>-/-</sup>* (Shesely, Maeda et al. 1996) mice were purchased from Jackson Laboratories. Heterozygote *Pdx-1-Cre<sup>tg/+</sup>*; *eNOS<sup>+/-</sup>* were interbred with *LSL-Kras<sup>G12D</sup>*; *eNOS<sup>+/-</sup>* to generate *LSL-Kras<sup>G12D/+</sup>*; *Pdx-1-Cre<sup>tg/+</sup>*; *eNOS<sup>-/-</sup>* (*eNOS<sup>-/-</sup>* KC) mice and their corresponding wild type (*eNOS<sup>+/+</sup>*) KC littermate controls. *LSL-Kras<sup>G12D/+</sup>*; *Pdx-1-Cre<sup>tg/+</sup>*; *LSL-Trp53<sup>R172H/+</sup>* (KPC) mice were generated in a similar manner except that the final step consisted of crossing littermates that were either wild type or null at the *eNOS* allele.

Genotyping primers and protocols were as follows. For detection of the *LSL-Kras<sup>G12D</sup>* allele, Platinum Taq was used in 12 $\mu$ L reactions containing buffer and dNTPs at manufacturer's recommended concentrations, with primers 5'-GTCTTTCCCAGCACAGTGC-3', 5'-CTCTTGCCTACGCCACCAGCTC-3', 5'-AGCTAGCCACCATGGCTTGAGTAAGTCTGCA-3' that detect both the wild-type *KRAS* allele and the *LSL-KRAS<sup>G12D</sup>* allele if present. Cycling conditions were 95°C for 2 minutes, followed by thirty four cycles of 95°C for 30 seconds, 61°C for 30 seconds, 72°C for 45 seconds, followed by one step at 72°C for 10 minutes and then cooling to 4°C. For detection of the *LSL-Trp53<sup>R172H</sup>*, RedTaq (Sigma) was used in 12 $\mu$ L reactions containing buffer and dNTPs at manufacturer's recommended concentrations, with primers 5'-AGCTAGCCACCATGGCTTGAGTAAGTCTGCA-3' and 5'-CTTGGAGACATAGCCCACTG-3' which only detect presence of the *LSL-Trp53<sup>R172H</sup>* allele. Cycling conditions were 94°C for 3 minutes, followed by thirty cycles of 94°C for 1 minute, 60°C for 90 seconds, 72°C for 2 minutes, followed by one step at 72°C for 5 minutes and then cooling to 4°C. The *eNOS* wild-type and knockout alleles were detected using 12 $\mu$ L Platinum Taq reactions and primers 5'-

AATTCGCCAATGACAAGACG-3', 5'-AGGGGAACAAGCCCAGTAGT-3', and 5'-CTTGTCCCCTAGGCACCTCT-3'. Cycling conditions were 94°C for 3 minutes, followed by thirty-five cycles of 94°C for 30 seconds, 66°C for 45 seconds, 72°C for 45 seconds, followed by one step at 72°C for 7 minutes and then cooling to 4°C. The *Pdx-1-Cre* transgene was detected using 12µL Platinum Taq reactions and primers 5'-CTGGACTACATCTTGAGTTGC-3' and 5'-GGTGTACGGTCAGTAAATTTG-3'. Cycling conditions were 94°C for 3 minutes, followed by thirty-seven cycles of 94°C for 30 seconds, 60°C for 30 seconds, 72°C for 30 seconds, followed by one step at 72°C for 7 minutes and then cooling to 4°C. Primers for all genotyping reactions were suspended in water upon purchase from IDT Oligos and dispensed into single use aliquots which were discarded after each use.

Untreated, *eNOS*<sup>-/-</sup> or L-NAME-treated KC mice were euthanized at 330±7 days of age. Untreated, *eNOS*<sup>-/-</sup> or L-NAME-treated KPC mice were individually handled, observed, and weighed three times weekly and euthanized if they displayed excessive inactivity, 20% weight loss, or ascites. All procedures utilizing mice were performed according to Duke Institutional Animal Care and Use Committee-approved protocols.

### **2.2.3 L-NAME Treatment of Mice**

As KC and KPC mice were identified by genotyping they were randomly assigned to either received untreated water or water treated with L-NAME (Sigma-Aldrich) (Seligsohn and Bill 1993; Trifilieff, Fujitani et al. 2000; Yamashita, Kawashima et al. 2000) at a concentration of 1g/L beginning after weaning (three weeks of age) until the termination of the experiment, during which time water was replaced three times weekly. Measurement of water intake and

corresponding mouse body weight indicates that this is equivalent to an average daily dose of about 180mg/kg.

#### **2.2.4 Grading of ductal lesions and Assessment of Normal Acinar Area**

Histologic sections (5 $\mu$ m) of formalin-fixed and paraffin-embedded tissue stained with hematoxylin and eosin were reviewed by two pathologists blinded to the experimental groups. Examined slides consisted of a single longitudinal section of pancreas (head to tail) with adjacent small intestine and spleen from each mouse. Quantification of murine pancreatic intraepithelial (mPanIN) lesions was accomplished by first determining the total number of anatomic pancreatic lobules per specimen. Lobules were counted and subsequently evaluated if they contained at least a single identifiable duct and surrounding circumscribed pancreatic acini and/or fibrosis. Within each lobule, the highest grade mPanIN lesion (normal, 1A, 1B, 2 or 3) was identified in accordance with prior literature (Hruban, Adsay et al. 2006).

To quantify the percent normal acinar tissue remaining in the pancreas, five random photomicrographs of H&E stained pancreata were taken per mouse for sixteen total mice in each group. Normal acinar tissue was outlined in Adobe Photoshop which then calculated total area circled relative to total area depicted on the slide.

#### **2.2.5 Mouse squamous papilloma and carcinoma analysis**

Vulvar papillomas were excised from KC mice at time of necropsy (330 $\pm$ 7 days of age) and weighed. The pedunculated tumor tissue could be grossly identified and separated from adjacent normal tissue. Facial papillomas were tallied throughout the course of the experiment when they reached a size of 2mm by 2mm. Some facial papillomas were removed by electrocautery from anesthetized mice to prevent interference with food and water intake.

Facial papillomas that recurred in the same area as one that had been previously removed were not counted a second time. The number of face papillomas per mouse was thus recorded as the number of independent papillomas that appeared over the course of the ~330 day experiment.

## **2.2.6 Histology and Immunohistochemistry**

Tissues were fixed in formalin for 24 hours and transferred to 70% ethanol. Tissues were paraffin embedded by Duke pathology and 5 $\mu$ m sections were made. For H&E staining, sections were rehydrated by incubating in Hemo-De xylene substitute (Electron Microscopy Sciences) for 10 minutes followed by a second 10 minute incubation in fresh Hemo-De. Slides were then incubated successively in 100% ethanol, 95% ethanol, and 70% ethanol for 5 minutes each. Slides were then transferred directly into Harris Modified Hematoxylin (Fischer Chemical) for five minutes, and then rinsed in running water until clear. Slides were dipped 2-3 times in acid alcohol (100mL 70% ethanol and 1mL concentrated hydrochloric acid), rinsed in water for one minute, and then placed for five minutes in an eosin-phloxine mixture. A stock eosin solution was made by dissolving 1g eosin Y (Fischer Chemical) in 100mL water, and a stock phloxine solution was made by dissolving 1g phloxine B (Fischer Chemical) in 1000mL water. To create the eosin-phloxine mixture used to stain slides, 10mL of the stock eosin solution, 1mL of the stock phloxine solution, 78mL 95% ethanol, and 400 $\mu$ L glacial acetic acid were mixed. After incubation in the eosin-phloxine mixture, slides were dehydrated by following the reverse of the hydration procedure outlined above. Coverslips were then mounted using Cytoseal XYL mounting media (Electron Microscopy Sciences).

Immunohistochemical staining was done following the protocol of Vectastain Elite ABC kits (Vector Labs) used for peroxidase-based detection. In sum, specimens were

deparaffinized and rehydrated by two 10 minute incubations in xylene, followed by two incubations of 5 minutes each in 100% ethanol, followed by single incubations of 5 minutes each in 95%, 80%, 60% and 30% ethanol; specimens were then transferred to distilled water. Antigen retrieval was then performed by incubating the slides for 4 minutes in boiling 10mM sodium citrate, pH 6.0 buffer. After antigen retrieval, slides were washed in PBS for 5 minutes and then samples were circled using a Liquid Blocker Super Pap pen (Electron Microscopy Sciences). Endogenous peroxide activity was quenched by incubation in 0.3% H<sub>2</sub>O<sub>2</sub> (diluted in water) for 30 minutes at room temperature, followed by a 5 minute wash in PBS. Samples were blocked with the blocking sera provided by the Vectastain kit, appropriately matched to the species of the primary antibody. Samples were then incubated for 30 minutes with the primary antibody diluted in PBS at the following concentrations:  $\alpha$ -iNOS 1:200 (Santa Cruz sc-651),  $\alpha$ -eNOS 1:70 (Assay Designs 905-386), or  $\alpha$ -nNOS (1:200, Cell Signaling #4231). After two five minutes washes in PBS, the secondary antibody from the Vectastain kit was applied, followed by the tertiary reagent. Staining was developed using the DAB substrate kit (Vector Labs); samples were incubated with the substrate for 2 minutes before immediately quenching in water to stop the reaction. Slides were counterstained with hematoxylin for 30 seconds and then dehydrated by following the reverse of the rehydration procedure outlined above. Coverslips were then mounted using Cytoseal XYL mounting media (Electron Microscopy Sciences).

### **2.2.7 PCR of KRas alleles**

Pancreatic, facial papilloma, or vulvar tumor tissue (~10mg) collected at necropsy was incubated in 500 $\mu$ l DNA lysis buffer (10mM Tris pH8.0, 10mM EDTA, 100mM NaCl, 0.5% SDS, 1mg/ml proteinase K) at 55°C overnight. The following day, 250 $\mu$ l saturated NaCl was added and

particulate matter was removed by centrifugation at 12000g for 10min. Supernatant was collected and mixed with equal volume isopropanol. DNA was precipitated by centrifugation at 12000g for 10 minutes and washed with 70% ethanol. The pellet was resuspended in 200 $\mu$ l water and 2 $\mu$ l was used for PCR to detect presence of the wild type and recombined *Kras* alleles. Detection of the recombined allele was done using the same primers and protocol used for *Kras* genotyping as outlined in 2.2.2 Mouse Pancreatic Cancer Models; however, if recombination is present the reaction will yield a third band that is 32 base pairs high than the wild-type band (due to the single 32 base pair lox site remaining behind after neomycin excision).

### **2.2.8 Xenograft assays**

Ten million cells suspended in 100 $\mu$ l of Matrigel (BD Biosciences) were injected subcutaneously into the flanks of severe combined immunodeficient/beige mice (Charles River) and randomly assigned to a treatment group after which resultant tumors were measured three times weekly as previously described (Hamad, Elconin et al. 2002). Depending on the experiments, mice were treated with 180mg/kg oral L-NAME (see above) beginning on the day of xenograft injection, or once tumors reached a size of 0.75cm<sup>3</sup>, with 120mg/kg intraperitoneal injections of gemcitabine (Eli Lilly) twice weekly for two weeks once tumors reached a size of 0.75cm<sup>3</sup>, or with 10mg/kg intraperitoneal injections of amlodipine (Sigma) five times weekly as previously described (Yu, Liang et al. 2001), beginning on the day of xenograft injection. As a control for all intraperitoneal injections, an equal volume of PBS was injected in control mice.

### **2.2.9 Blood pressure measurements**

Blood pressures were measured five days a week in conscious mice using a computerized tail cuff monitor (Hatteras Industries) as previously described (Krege, Hodgin et al.

1995). Mice were familiarized with the apparatus and measurement procedures for a three week period prior to initiation of the experiment. During the experiment, blood pressures for each mouse were measured five times a week by the same operator at the same time each day in the following manner. Fifteen total measurements were taken per mouse. The first five measurements were discarded as the animals acclimated to the apparatus. Ten measurements were kept per mouse, and the average of these ten measurements represented the blood pressure for that mouse each day, and is graphed in Figure 16C.

### **2.2.10 Statistical Analyses**

For two cohort xenograft studies, we compared tumor volumes of untreated and treated mice on the final day of the experiment using a two sided unpaired t test. A *P* value of less than 0.05 was considered statistically significant. For xenograft studies with multiple arms, one way ANOVA was used with Tukey's Multiple Comparison Test and a *P* value of less than 0.05 was considered statistically significant. For comparison of individual arms in blood pressure studies, for comparison of individual arms in studies analyzing the area of normal acinar tissue remaining in KC pancreata, and for comparison of facial papilloma appearances in the mice, a two sided unpaired t test was again used. For comparison of vulvar papillomas the Mann-Whitney U test was performed, with a two-tailed *P* value less than 0.05 considered significant. For analysis of normal ducts and PanIN-1A lesions, chi-squared analysis was performed to compare each arm to the control untreated mice. Ducts were grouped into two groups (e.g. normal versus abnormal, or PanIN-1A versus all other) and chi-squared analysis was performed. Kaplan-Meier survival curves were generated for each of the KPC mice cohorts and *P* values

were calculated using the log-rank (Mantel-Cox) test. All statistical analyses were performed using Graphpad Prism v5 (Graphpad Software).

## 3. Rare Codons Limit KRas Tumorigenic Activity

### 3.1 Abstract

KRas is a member of the Ras small GTPase family of oncogenes composed of the nearly identical KRas, NRas and HRas proteins. While KRas is commonly mutated in human cancers to promote tumorigenic phenotypes, accumulating evidence suggests that elevation in the level of this oncoprotein also plays a role in tumorigenesis. Here, we report that despite an 82% amino acid identity between KRas and HRas, when expressed from the same vector the level of KRas protein was twenty-fold lower compared to HRas. This reduction was a result of a bias in underrepresented (rare) codons in KRas. In fact, changing rare codons to common codons not only increased both ectopic and endogenous KRas expression, but also its tumorigenic activity. The divergence in codon usage between nearly identical proteins was not limited to the Ras family, as genome-wide analysis identified gene pairs with opposing codon bias that not only manifested in a difference in protein expression, but were also specifically enriched for key signaling molecules and pathways. Thus, codon bias limits the oncogenic potential of KRas and may represent a broader regulatory switch in cell signaling.

### 3.2 Background

KRas, HRas, and NRas comprise a family of highly homologous small GTPases (Takai, Sasaki et al. 2001; Downward 2003; Karnoub and Weinberg 2008). Mutations altering amino acids G12, G13 and Q61 of *KRAS*, and less commonly *HRAS* or *NRAS*, render the encoded protein constitutively GTP-bound and active (Bos 1989; Downward 2003; Karnoub and Weinberg 2008). While it is well described that such mutations promote cancer (McCormick 1999), accumulating evidence suggests that the level of KRas protein in tumors is also important. Specifically, over-

expressed mutant KRas is more tumorigenic than the endogenous mutant *KRAS* gene (Arena, Isella et al. 2007; Konishi, Karakas et al. 2007). Mechanisms that increase KRas protein levels are also seen in tumors, such as down-regulation of the *let-7* miRNAs that block KRas expression (Takamizawa, Konishi et al. 2004; Kumar, Erkeland et al. 2008), amplification of the *KRAS* pseudogene which accelerates cell growth by competing for miRNA binding (Poliseno, Salmena et al. 2010), and finally, amplification of the oncogenic allele of *KRAS* itself, a common feature of *KRAS*-mutant tumors (Yamada, Sakamoto et al. 1986; Radinsky, Kraemer et al. 1987; Liu, Von Lintig et al. 1998; Heidenblad, Jonson et al. 2002; O'Hagan, Chang et al. 2002; Aguirre, Bardeesy et al. 2003; Mita, Toyota et al. 2009; Modrek, Ge et al. 2009; Wagner, Perner et al. 2009; Sasaki, Hikosaka et al. 2011). Importantly, the level of the oncogenic protein appears to have therapeutic implications, as amplification of the *KRAS* gene determines the responsiveness to restoration of the tumor suppressor p53 (Feldser, Kostova et al. 2010; Junttila, Karnezis et al. 2010) and is a cause of resistance to MET (Cepero, Sierra et al. 2010) and MEK (Little, Balmanno et al. 2011) inhibitors.

### **3.3 Results**

#### **3.3.1 KRas expression is blocked at the level of translation**

In the course of comparing the expression of identically FLAG epitope-tagged *HRAS* and *KRAS* cDNAs in SV40-transformed and hTERT-immortalized HEK-HT cells, we detected a twenty-fold reduction in the level of KRas compared to HRas protein, as noted in a subset of previous studies (Figure 4A) (Ellis and Clark 2000; Rodriguez-Viciano, Sabatier et al. 2004; Bivona, Quatela et al. 2006; Keller, Franklin et al. 2007; Kubota, O'Grady et al. 2011). This difference was rather unexpected given the high homology between KRas and HRas (Figure 4B), and was seen despite

the fact that both proteins were expressed from the same vector, detected with the same antibody, and all regulatory untranslated regions (UTR) were absent (Figure 4A). The difference was observed regardless of the method of DNA introduction into cells (Figure 5A), the type of cells (Figure 5B), the expression construct, promoter, exogenous UTRs (Figure 5C), the absence or presence of an intron in the vector (Figure 5D), the epitope tag (Figure 4E), the mutational status of Ras (Figure 5A), or even the membrane targeting of Ras and thus protein activity (Figure 5E).

To determine if this difference was a property of the KRas protein or mRNA, we separated these two variables by creating an artificial construct encoding KRas protein from a completely different mRNA, termed KRas\*. Taking advantage of the fact that KRas and HRas proteins are nearly identical except for the terminal 30 amino acids of the hypervariable region (Figure 4B), the 5' region of *HRAS* cDNA, mutated at ten nucleotides to exactly match the KRas amino acid sequence, was fused in frame with the KRas hypervariable domain to create *KRAS\**. We found that stable expression of this *KRAS\** cDNA in HEK-HT cells restored expression of KRas, almost to the level of HRas (Figure 4A). Again, this rescue was observed regardless of methods of DNA introduction, cell type, vectors encoding different promoters, UTRs, or introns, the epitope tag or membrane targeting (Figure 5A,B,D and E). Thus, the dramatic difference in the expression of KRas compared to HRas is due to differences in nucleotide but not amino acid sequence.

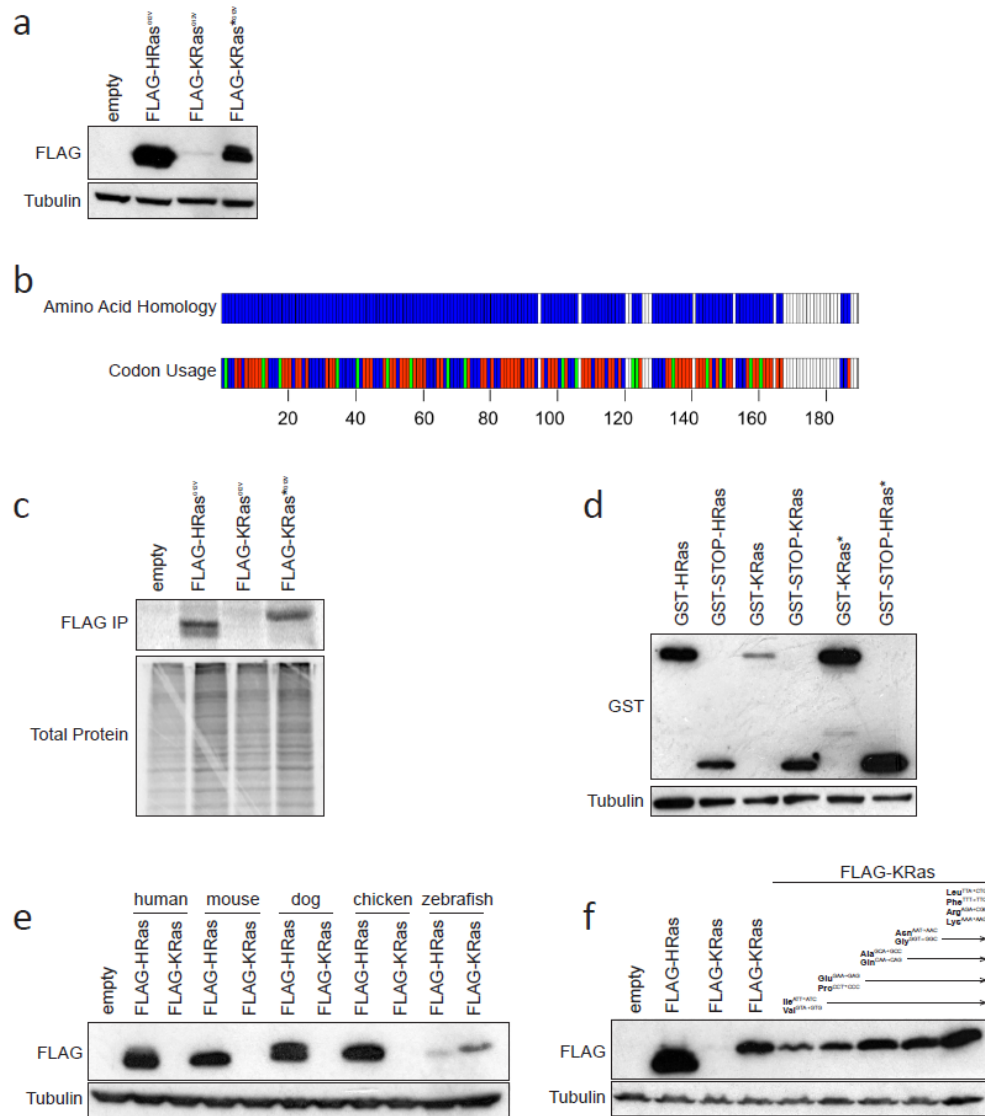


**Figure 4: Translation of KRAS message is limited by rare codons**

(a) Relative levels of RAS expression in HEK-HT cells stably infected with the indicated constructs. (b) The amino acid homology of HRAS and KRAS is represented in the upper bar, with identical amino acids represented in blue and nonidentical amino acids represented in white. Each box represents one amino acid. The codon usage of HRAS and KRAS is represented in the lower bar, with red boxes indicating an instance where KRAS uses a rarer codon, green boxes indicating instances where HRAS uses rarer codons, blue boxes indicating instances where they use identical codons, and white boxes representing instances where the amino acids are not identical. Each box represents one codon. (c) Metabolic labeling of RAS protein and total protein synthesized in 15 minutes in HEK-HT cells stably overexpressing each of the indicated constructs. (d) Relative protein expression levels of HEK-HT cells stably expressing the indicated GST-RAS fusion constructs. (e) Relative expression levels of heterologous RAS proteins from the indicated species transiently transduced into human 293 cells. (f) Expression levels of KRAS constructs with the sequential optimization of the indicated codons.

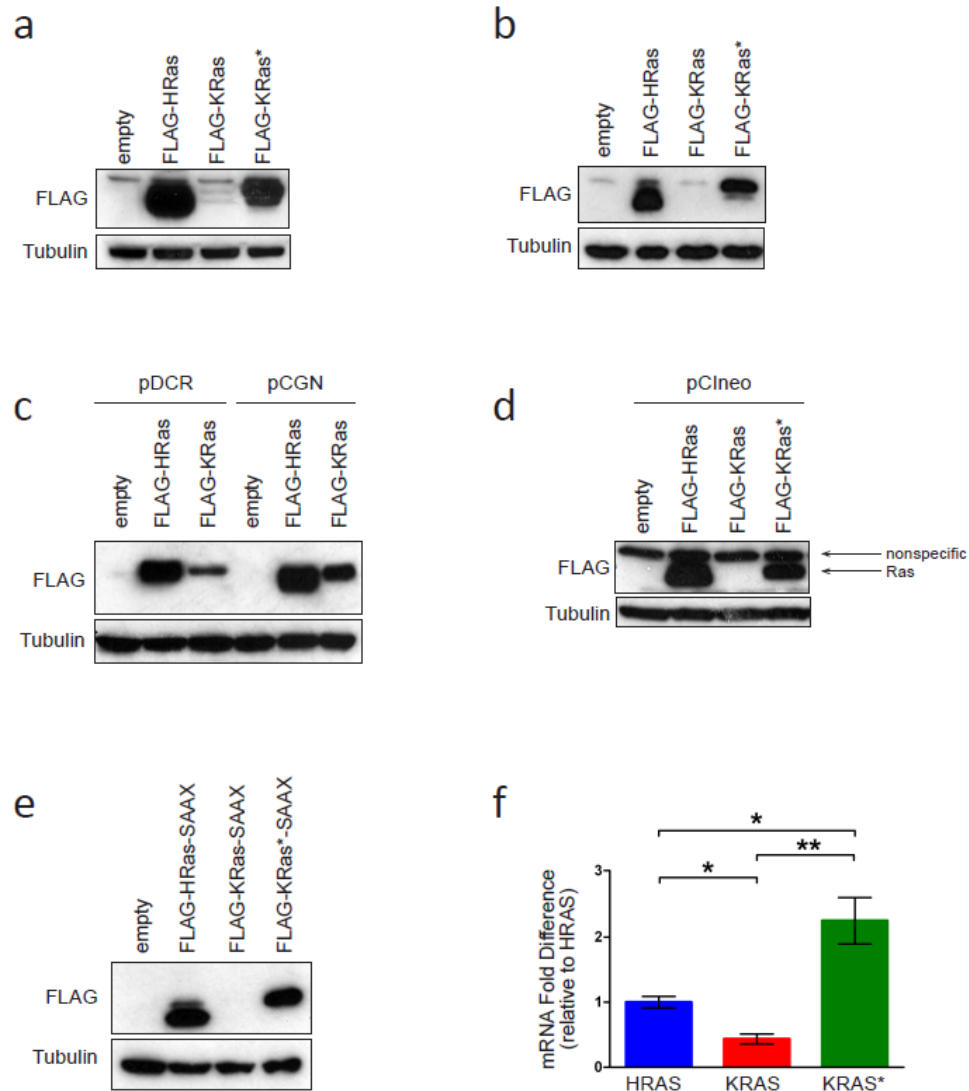


**Figure 5: Decreased KRas expression levels are independent of the expression systems used**

(a) Relative expression levels of the various Ras isoforms when transiently transfected into 293 cells. (b) Relative expression levels of ectopic Ras when the indicated isoforms are stably introduced into HCT116 cells. (c) Relative expression levels of HRas and KRas when transiently transfected into 293 cells using the indicated vectors to drive expression. (d) Expression levels of Ras constructs when transiently transfected into 293 cells using pCIneo, a vector which contains an intron in the 5' UTR, to drive expression. (e) Expression levels of Ras mutants carrying cysteine to serine mutations at the prenylation site after stable introduction into HEK-HT cells. (f) Relative levels of mRNA encoding for ectopically expressed Ras isoforms, as determined by quantitative RT-PCR of cDNA created from HEK-HT cells stably expressing the indicated Ras constructs. \*  $P < 0.05$ , \*\*  $P < 0.005$ .

The nucleotides responsible for limiting KRas expression may act at the steps of transcription, translation, or degradation. To assess whether the difference lied at the level of transcription or mRNA stability, the steady state level of exogenous KRas versus HRas mRNA was measured in HEK-HT cells stably expressing KRas or HRas. While the encoded KRas mRNA was present at about half the level of HRas mRNA (Figure 5F), consistent with a low GC content reducing mRNA stability (Duan and Antezana 2003; Chamary and Hurst 2005; Chamary, Parmley et al. 2006), this difference nevertheless failed to account for the far more dramatic twenty-fold reduction of KRas protein (Figure 6), pointing towards a translation defect. In agreement, brief metabolic labeling of proteins in HEK-HT cells stably expressing HRas, KRas or KRas\* revealed that HRas protein was readily detected while KRas was not, and moreover, that the latter level was restored in KRas\*-expressing cells (Figure 4C). This reduction in the translation of KRas lies at the level of translation elongation. Specifically, a chimeric GST-KRas cDNA encoding GST fused at the C-terminus in frame with KRas was poorly expressed in HEK-HT cells, suggesting stalling of ribosomes upon entering the KRas sequence. Indeed, the simple addition of a STOP codon between GST and KRas (GST-STOP-KRas), such that an essentially identical mRNA was produced but ribosomes were prevented from entering the KRas sequence, restored protein expression (Figure 4D). In fact, GST-STOP-KRas was expressed as well as GST-STOP-HRas (Figure 4D). Similarly, expression was restored, regardless of the absence or presence of a STOP codon, when the *KRAS* mRNA sequence was replaced with that of *KRAS\** (Figure 4D). We conclude that poor translation elongation of *KRAS* mRNA accounts for the low expression of the encoded protein.

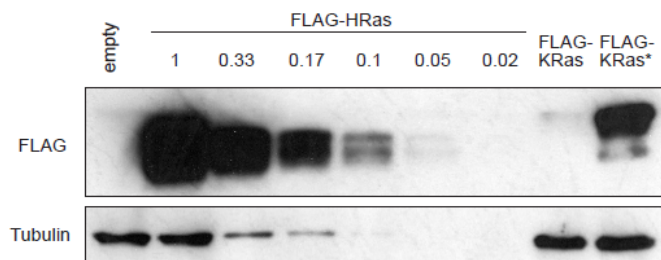


**Figure 6: Limiting dilution analysis of relative Ras expression levels**

Lysates from HEK-HT cells stably expressing FLAG-HRas were diluted in the indicated ratios and expression of ectopic HRas was compared to expression of ectopic KRas.

### 3.3.2 Low KRas expression is due to an abundance of rare codons

Interestingly, we failed to identify any one region of KRas that accounted for this reduced expression. Instead, chimeric *HRAS-KRAS* constructs that contained increasing amounts of *KRAS* nucleotide sequence had decreasing amounts of expression. This suggests that sequences reducing translation occur throughout the entire *KRAS* mRNA. In this regard, the presence of underrepresented (rare) codons can limit the ectopic expression of proteins in mammalian cells, and optimization of codon usage can elevate expression of ectopically introduced genes (Zolotukhin, Potter et al. 1996; Robinson, Jackson et al. 2008; Fath, Bauer et al. 2011). Although admittedly the impact of rare codons on the endogenous expression of mammalian genes has not been reported, we nevertheless evaluated the codon usage of *KRAS* and *HRAS*. Based on human genome-wide analysis of the relative frequencies that degenerate codons are used to encode for the same amino acid (Nakamura, Gojobori et al. 2000), we found that *KRAS* consistently used rarer codons than *HRAS*, despite encoding for the same amino acids. Specifically, out of the 160 amino acids in common between KRas and HRas, *KRAS* uses a rarer codon than *HRAS* 83 times, *HRAS* uses the rarer codon 18 times, and 59 times they use the same codon (Figure 4B). This suggested the possibility that *KRAS* translation is slow due to a bias of rare codons.

Five pieces of independent evidence indicate that rare codons account for the poor expression of KRas compared to HRas. First, the rare codons are lost in *KRAS\**, which correspondingly expresses high levels of KRas protein (Figure 4A). Second, the identification of rare codons throughout *KRAS* is consistent with the finding that no one region could account for the poor expression of KRas. Third, evolutionary analysis of KRas and HRas revealed that the

bias towards rare codons observed in murine, canine and avian KRas equated with much lower expression of KRas compared to HRas (Figure 4E). However, zebrafish KRas and HRas had similar codon usages with respect to each other and correspondingly were expressed at similar levels (Figure 4E). Fourth, changing the bias towards common codons can increase expression in mammalian cells of heterologous proteins from not only other species (Zolotukhin, Potter et al. 1996), but also from mammals (Robinson, Jackson et al. 2008; Fath, Bauer et al. 2011). In this regard, changing all the rare isoleucine and valine codons (nine each) scattered throughout *KRAS* to their common counterparts (*e.g.* Ile<sup>ATT→ATC</sup> and Val<sup>GTA→GTG</sup>) increased the amount of KRas protein detected by immunoblot (Figure 4F). Moreover, progressively converting more and more of the rare codons to common codons proportionally increased KRas expression (Figure 4F). In conclusion, rare codons limit KRas translation.

### **3.3.3 Expression of endogenous KRas is limited by codon usage**

Ectopically expressed mRNAs, which can be present at many thousands of times their normal cellular level, could potentially overwhelm the translational machinery. It thus remained possible that the limiting nature of certain codons may only arise in this artificial context (Plotkin and Kudla 2011). To determine if the principles governing expression of the ectopic mammalian *KRAS* cDNA also applied to the expression of the endogenous mammalian *KRAS* gene, we assayed whether changing rare codons of the human *KRAS* gene to their more common counterparts increases the level of endogenous KRas protein. Specifically, recombinant adeno-associated virus (rAAV) gene targeting (Rago, Vogelstein et al. 2007) was used to replace one *KRAS* allele of the human colon cancer cell line HCT116 with a codon optimized version of *KRAS* containing 142 silent mutations in 130 codons of this 188 amino acid protein. The targeting

vector consisted of 28 base pairs of normal exon 1 sequence followed by an in-frame codon-optimized oncogenic KRas4B<sup>G13D</sup> cDNA (KRas<sup>G13D</sup>op), a bovine growth hormone polyadenylation sequence, a neomycin resistance marker, and flanking *KRAS* intronic sequences (Figure 7A). Successful homologous recombination would knock the KRas<sup>G13D</sup>op cDNA into exon 1 of one allele of the endogenous *KRAS* gene. Thus the entire gene could be codon-optimized to overcome the widespread distribution of rare codons throughout *KRAS* that limits protein expression. Additionally, KRas<sup>G13D</sup>op would not only be expressed from the endogenous *KRAS* promoter, but also spliced to an upstream noncoding exon, thereby retaining unchanged all of the 5' UTR of the endogenous gene plus the first 17 coding nucleotides, minimizing effects on translation initiation. As a control, an identical targeting vector encoding a wild-type KRas4B<sup>G13D</sup> (KRas<sup>G13D</sup>wt) cDNA was constructed to knock a wild-type KRas4B<sup>G13D</sup> cDNA (KRas<sup>G13D</sup>wt) into the *KRAS* locus.

After infection with either of the two AAV targeting vectors, HCT116 cells were selected in neomycin. ~1,800 neomycin-resistant clones were assayed by genomic PCR across the 3' homology arm for successful homologous recombination events, which were confirmed by RT-PCR and direct sequencing of the spliced, knocked in *KRAS* mRNA. Six total clones were identified in this manner, two with KRas<sup>G13D</sup>wt and four with KRas<sup>G13D</sup>op cDNA successfully knocked into one allele of the *KRAS* gene. Immunoblot analysis revealed equally poor expression of endogenous KRas in the two KRas<sup>G13D</sup>wt knock-in clones and in two control clones exhibiting a random integration event, on par with the level observed in the parental HCT116 cells. However, every one of the four clones in which the KRas<sup>G13D</sup>op was successfully knocked into the *KRAS* locus exhibited high levels of endogenous KRas protein compared to the control KRas<sup>G13D</sup>wt knock-in cell lines (Figure 7B). RT-PCR analysis revealed that the level of *KRAS* mRNA

in the KRas<sup>G13D</sup>op knock-in clones was on average about twice that detected in KRas<sup>G13D</sup>wt knock-in clones or the parental cell line (Figure 7C). These results mirrored the results from exogenously expressed *KRAS* cDNA, suggesting a similar reduced rate of translation is imposed by rare codons in the endogenous *KRAS* gene.

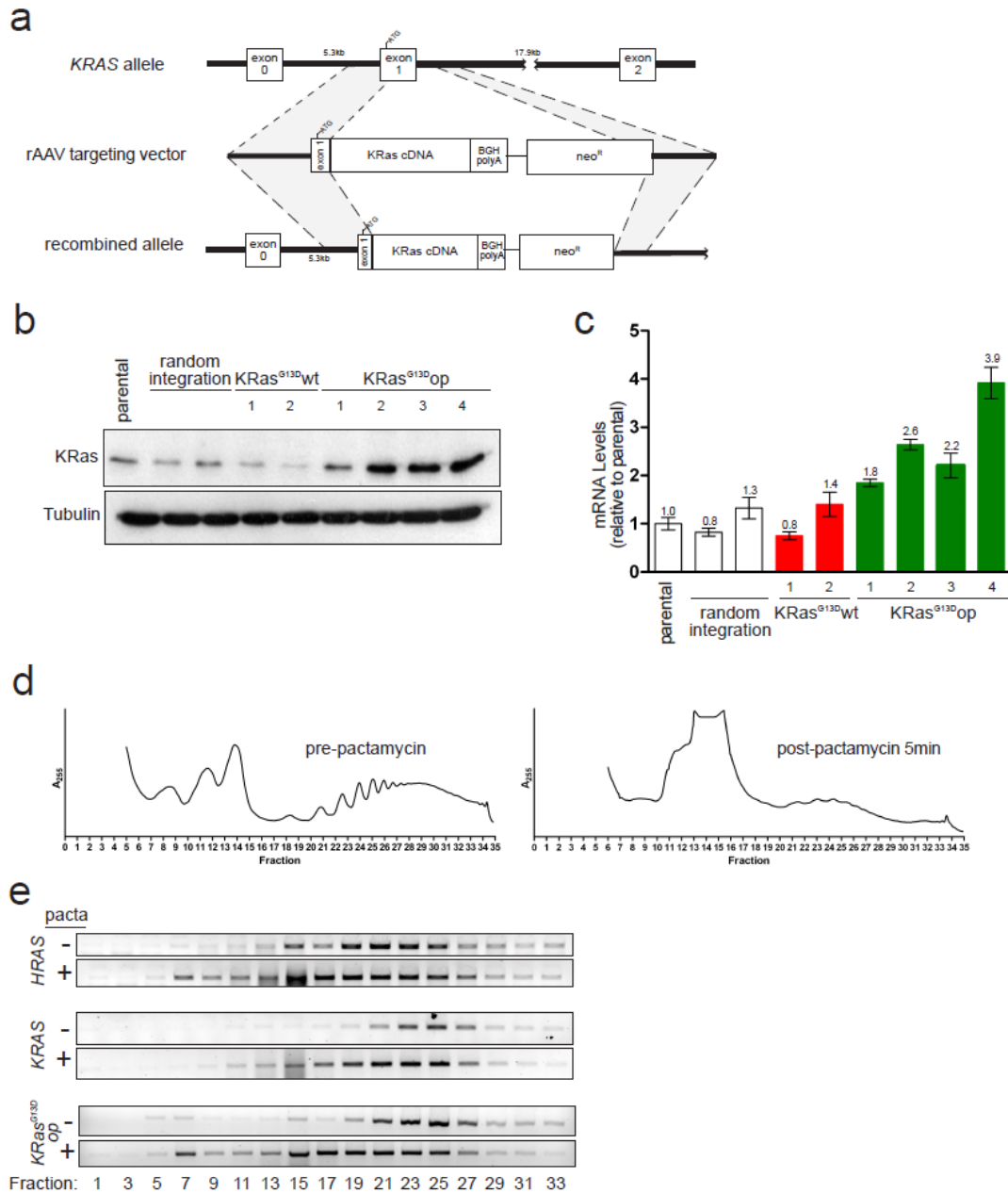


**Figure 7: Codon usage controls endogenous KRas expression**

(a) Targeting strategy to replace the endogenous *KRAS* gene in human HCT116 colon cancer cells with a codon optimized form. (b) KRas expression levels in the parental HCT116 cell line, two clones with non-homologous integration of the neomycin resistance gene, two clones with homologous integration of the *KRAS*<sup>G13D</sup>wt gene with standard codon usage, and four clones with homologous integration of the *KRAS*<sup>G13D</sup>op gene with optimized codon usage. (c) Total *KRAS* mRNA levels in the clones depicted in (b). (d) Polysome profiles of *KRAS*<sup>G13D</sup>op HCT116 cells before and after pactamycin treatment. (e) Semiquantitative RT-PCR analysis of the sedimentation of *HRAS*, *KRAS*, and *KRAS*<sup>G13D</sup>op mRNAs in the profiles depicted in (d).

To assess whether the mRNA encoded from the endogenous *KRAS* gene is poorly translated, we performed polysome profiling of one of the *KRas*<sup>G13D</sup>*op* knock-in HCT116 clones to identify the relative positions within the gradient of the endogenous *HRAS* mRNA, mRNA derived from the knocked-in *KRas*<sup>G13D</sup>*op* allele, and mRNA derived from the remaining unaltered *KRAS* allele. Analysis of the baseline position of the mRNAs by RT-PCR within the gradient revealed that they all accumulated in polysome fractions (fractions 19-27), consistent with the transcripts bound to multiple ribosomes (Figure 7D,E). To assess the ribosome movement along these transcripts, the same cells were treated with pactamycin to inhibit translation initiation, as confirmed by the loss of ribosomal RNA in the heavy fractions (Figure 7D), then shortly thereafter fractionated and subjected to RT-PCR analysis. Pactamycin treatment led to an accumulation of *HRAS* mRNA in the free fractions of the gradient (fractions 7 and less), consistent with ribosomes completing translation of *HRAS* mRNA and then being blocked from re-initiating translation, leading to an accumulation of ribosome-free transcripts. Conversely, profiles of pactamycin treated cells showed only a minimal shift of endogenous *KRAS* mRNA in the gradient, with the bulk of the message still appearing in the polysomal fractions (Figure 7E). This result was confirmed in a different cell line; similar differences in *HRAS* and *KRAS* mRNA polysome profile mobilities were shown in human HEK-HT cells following pactamycin treatment (Figure 8). Lastly, polysome profiling of the *KRas*<sup>G13D</sup>*op* mRNA revealed that the transcripts shifted from the polysome fractions to the free fractions after pactamycin treatment, demonstrating that the slow translation of *KRas* mRNA is reversed by changing the rare codons to common codons. Rare codons therefore limit the translation of endogenous *KRAS* mRNA.

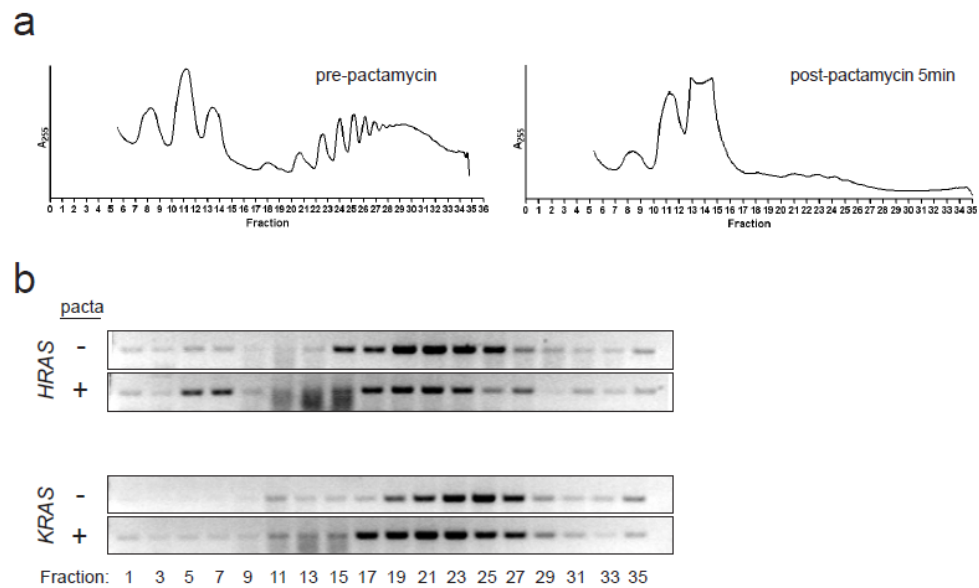


**Figure 8: *KRAS* mRNA has reduced mobility in polysome profiles in HEK-HT cells**

(a) Polysome profiles of HEK-HT cells before and after pactamycin treatment. (b) Semiquantitative RT-PCR analysis of the sedimentation of *HRAS* and *KRAS* mRNAs in the profiles depicted in (a).

### 3.3.4 KRAS codon usage limits KRas-driven tumorigenesis

Codon choice can alter protein expression and function in lower eukaryotes. For example, highly expressed yeast genes contain optimal codons (Sharp, Tuohy et al. 1986; Sharp and Cowe 1991) and targeted replacement of codons in the *Drosophila* alcohol dehydrogenase gene with either suboptimal (Carlini and Stephan 2003; Carlini 2004) or optimal (Hense, Anderson et al. 2010) codons can respectively decrease or increase ADH activity and alcohol tolerance. We therefore addressed the impact of the rare codon bias on the biological function of KRas. It is well established that expression of oncogenic Ras imparts tumorigenic growth to cells, and hence we tested whether changing rare codons to common codons increased the ability of oncogenic KRas to promote tumorigenesis. To this end, ectopic expression of oncogenic Ras is required for HEK-HT cells to form tumors when injected into immunocompromised mice (Hahn, Counter et al. 1999). Thus, HEK-HT cells were stably infected with a retrovirus encoding positive control oncogenic HRas (HRas<sup>G12V</sup>), no transgene as a negative control (vector), wild-type KRas<sup>G12V</sup> (KRas<sup>G12V</sup>), or the aforementioned oncogenic KRas\* (KRas\*<sup>G12V</sup>) that lacks rare codons and is robustly expressed (Figure 4A). The four cell lines were injected subcutaneously into four immunocompromised mice each and monitored for tumor growth. As previously reported (Hahn, Counter et al. 1999; O'Hayer and Counter 2006), positive control HRas<sup>G12V</sup>-expressing HEK-HT cells readily formed tumors, reaching endpoint size after eleven days, whereas very small or no masses were detected at the injection site of negative control HEK-HT cells at the same time point (Figure 9A-C). Also, at the same time point, KRas<sup>G12V</sup>-expressing HEK-HT cells largely failed to form masses beyond those detected in negative control

vector HEK-HT cells (Figure 9A-C); although in a lengthier experiment these cells eventually did form tumors which, intriguingly, had elevated levels of KRas expression (Figure 10). This 90-fold difference in tumor mass was completely rescued if the rare codons in KRas<sup>G12V</sup> were changed to common codons, as KRas\*<sup>G12V</sup>-expressing HEK-HT cells formed tumors with nearly identical kinetics to positive control HRas<sup>G12V</sup>-expressing HEK-HT cells (Figure 9A-C). Thus, HEK-HT cells ectopically expressing the identical driving oncogene with the identical activating mutation formed tumors of differing aggressiveness, depending on the codons used to encode KRas.

To address whether rare codons also limit the tumorigenic potential of the endogenous *KRAS* gene, we assayed the tumorigenic growth between the aforementioned HCT116 cells in which a wild-type versus a codon optimized KRas<sup>G13D</sup> cDNA was knocked into the endogenous *KRAS* gene. One allele of the *KRAS* gene in the parental HCT116 cells contains a G13D mutation while the other allele remains wild-type. To make the most direct comparison, we thus chose knock-in clones in which homologous recombination of the wild-type and optimized KRas<sup>G13D</sup> targeting vector both occurred in the same wild-type *KRAS* allele. Two KRas<sup>G13D</sup>wt (clones 1 and 2) and one KRas<sup>G13D</sup>op (clone 3) knock-in clones met this criteria, and were subcutaneously injected into four immunocompromised mice each and monitored for tumor growth. The KRas<sup>G13D</sup>op HCT116 cells that exhibit high levels of endogenous KRas protein (Figure 7B) readily formed tumors, reaching the tumor size endpoint by 25 days (Figure 9D). Conversely, each of the two KRas<sup>G13D</sup>wt HCT116 clones that exhibited poor KRas protein expression (Figure 7B) had significantly slower tumor growth kinetics that manifested in an average tumor weight of 2.6 (clone 2) to 30 (clone 1) times less than KRas<sup>G13D</sup>op HCT116 cells (Figure 9E). Thus, rare codons retard the tumorigenic potential of the endogenous *KRAS* gene, indicating that codon usage has a biological impact on KRas function.



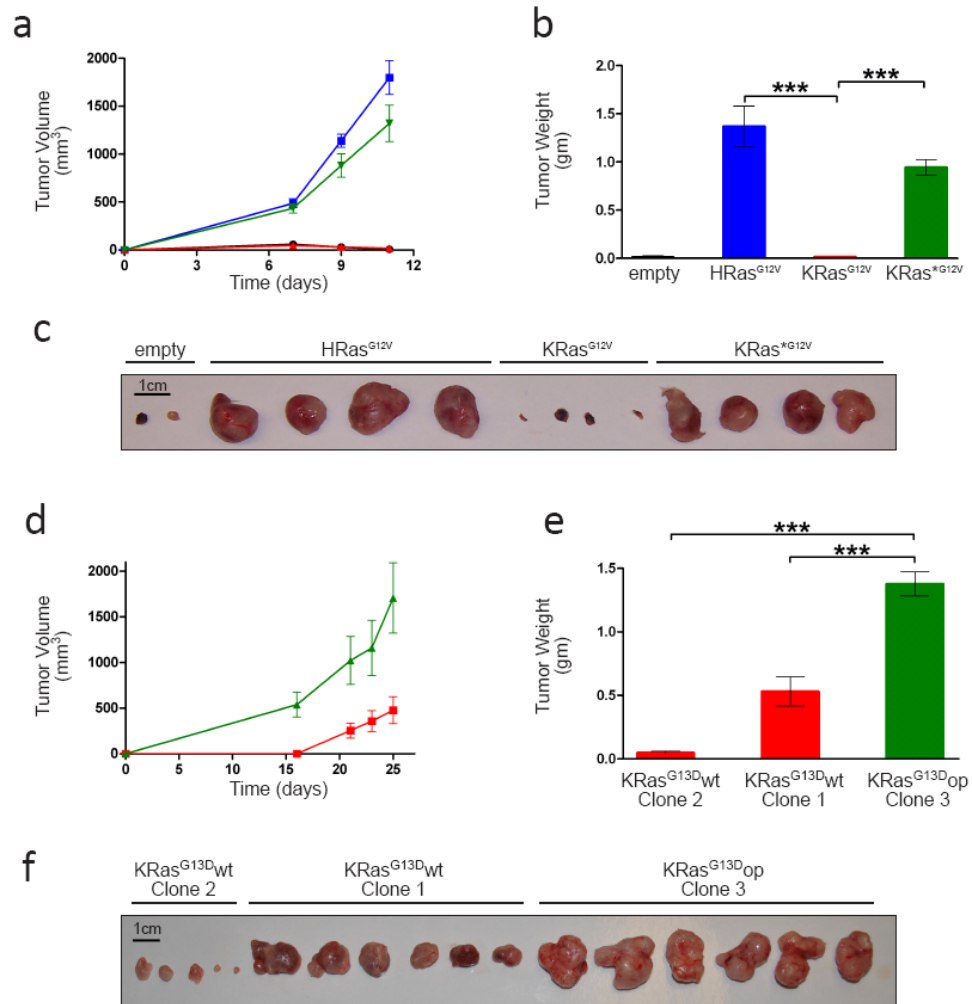


**Figure 9: KRAS codon usage limits the growth of tumors driven by oncogenic KRAS**

(a) Mean size  $\pm$  SEM of subcutaneous tumors derived from HEK-HT cells expressing the following oncogenic Ras isoforms: ● empty vector, ■ HRas<sup>G12V</sup>, ▲ KRas<sup>G12V</sup>, and ▼ KRas<sup>G12V</sup>, measured in cohorts ( $n=4$ ) of mice. (b) Mean tumor weight  $\pm$  SEM of subcutaneous tumors driven by HRas<sup>G12V</sup>, KRas<sup>G12V</sup>, KRas<sup>G12V</sup>, or lacking a driving oncogene (empty); tumors were isolated from mice at the endpoint of the experiment depicted in (a). (c) Photograph of subcutaneous tumors isolated from mice from the experiment depicted in (a). (d) Mean size  $\pm$  SEM of subcutaneous tumors derived from HCT116 clones driven by ▲ KRas<sup>G13D</sup>op (clone 3) or ■ KRas<sup>G13D</sup>wt (clone 1) injected into cohorts ( $n=6$ ) of mice. (e) Mean tumor weight  $\pm$  SEM at endpoint of subcutaneous HCT116 tumors driven by the indicated oncogenes. (f) Photograph of subcutaneous tumors derived from the indicated clones. \*\*\* $P<0.001$ .

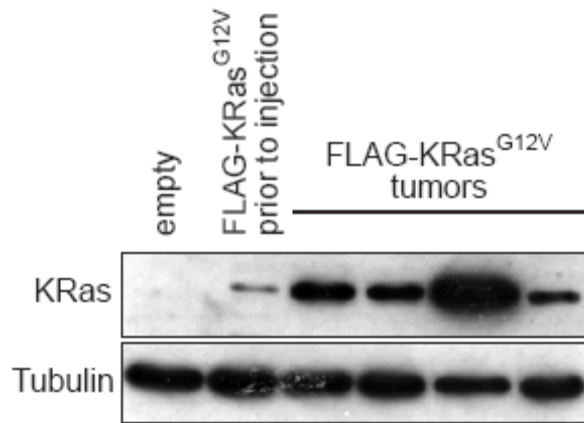


**Figure 10: KRas levels in HEK-HT tumors driven by KRas<sup>G12V</sup>**

HEK-HT cells expressing FLAG-KRas<sup>G12V</sup> (lane 2) were injected into four immunocompromised mice. After 3 months, tumors formed and cells from the individual tumors were isolated, grown in culture, and then analyzed for KRas expression (lanes 3-6).

### 3.3.5 Other gene pairs differ in codon usage and protein expression

Ras proteins are integral components of multiple cell signaling networks. Given that translational regulatory mechanisms can be utilized to modulate cellular processes or signaling pathways (Hamilton, Stoneley et al. 2006), we sought to identify and characterize other homologous gene pairs, such as the Ras genes, that differ in codon usage and similarly exhibit a difference in protein expression. The identification of such pairs on a genome-wide scale may indicate a widespread regulatory role for differential codon usage. A genome-wide analysis was performed to identify homologous gene pairs, which were then analyzed for codon usage differences using the GC content at synonymous sites (GC3) as a proxy for codon usage, as rarer codons typically end in adenine or thymine (Nakamura, Gojobori et al. 2000). Using *KRAS* and *HRAS* as a benchmark, which are 82% identical and have a log ratio of GC3 content of 1.28, we rank ordered gene pairs that were at least 80% identical at the amino acid level and possessed a log ratio of GC3 content of 0.8. To determine whether the different codon usage reflected a difference in protein expression, as observed in KRas and HRas, we further refined this search to genes pairs encoding cDNAs less than 1.5 kbp in size to facilitate cloning and expression analysis. Of the 37 gene pairs identified in this manner (Table 2), 12 were randomly assayed for protein expression. Specifically, the cDNAs for the 12 gene pairs with low versus high rare codon bias (*UBE2D4* versus *UBE2D2*, *RAB1B* versus *RAB1A*, *GNPDA1* versus *GNPDA2*, *NEK6* versus *NEK7*, *RAB11B* versus *RAB11A*, *CFL1* versus *CFL2*, *EEF1A2* versus *EEF1A1*, *CSNK1G2* versus *CSNK1G3*, *GNAI2* versus *GNAI2*, *ORMDL3* versus *ORMDL1*, *AKT1* versus *AKT3*, and *PRKAR1A* versus *PRKAR1B*) were Myc epitope-tagged and cloned into the same expression vector, which was then transiently transduced into 293 cells.

**Table 2: Homologous Gene Pairs with High Differences in Codon Usage**

<u>Gene 1</u>	<u>Gene 2</u>	<u>Percent Homology</u>	<u>GC3 Log Ratio</u>
CALM3	CALM2	100	1.23
UBE2D4	UBE2D2	93.2	0.8
RAB1A	RAB1B	93.07	0.89
PRKACA	PRKACB	92.88	0.89
UBE2V1	TMEM189-UBE2V1	92.86	0.91
EEF1A2	EEF1A1	92.62	0.89
UBE2D1	UBE2D4	91.84	1.02
RAB11A	RAB11B	91.28	1.32
GNB4	GNB1	91.02	0.81
PPP1CA	PPP1CC	90.66	0.95
UBE2V2	TMEM189-UBE2V1	90.21	1.08
ARF5	ARF4	90	0.89
PPP1CB	PPP1CA	88.79	1.12
GNPDA1	GNPDA2	88.24	1.24
CSNK1G2	CSNK1G3	88.19	1.45
GNAI2	GNAI1	87.89	0.91
AP1S1	AP1S2	87.82	1.06
RAB4B	RAB4A	87.32	0.8
RAB5A	RAB5C	87.04	1.13
PSMA7	PSMA8	86.76	1.04
CAMK2A	CAMK2D	86.08	0.87
SMAD3	SMAD2	84.9	1.05
CALML3	CALM2	84.56	1.63
ORMDL1	ORMDL3	84.31	1.18
ORMDL2	ORMDL1	83.01	0.84
AKT3	AKT1	82.71	1.21
ACTL6B	ACTL6A	82.28	1.07
GMFG	GMFB	82.27	1.08
GDI2	GDI1	82.21	0.82
HDAC1	HDAC2	82.17	1
KRAS	HRAS	82.01	1.28
PELI2	PELI1	81.43	0.83
PRKAR1A	PRKAR1B	81.36	0.87
NEK6	NEK7	81.23	1.24
MAT1A	MAT2A	81.01	0.8
CFL2	CFL1	80.72	1.24
ASF1B	ASF1A	80	1.18

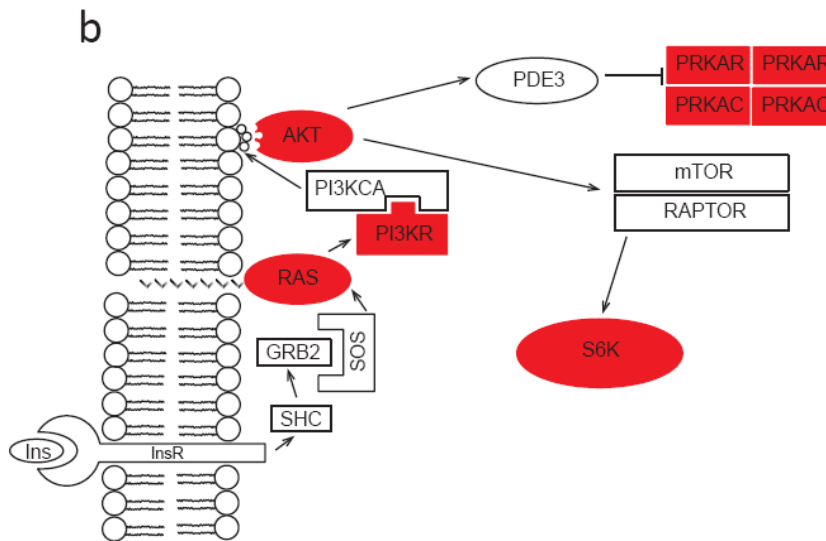
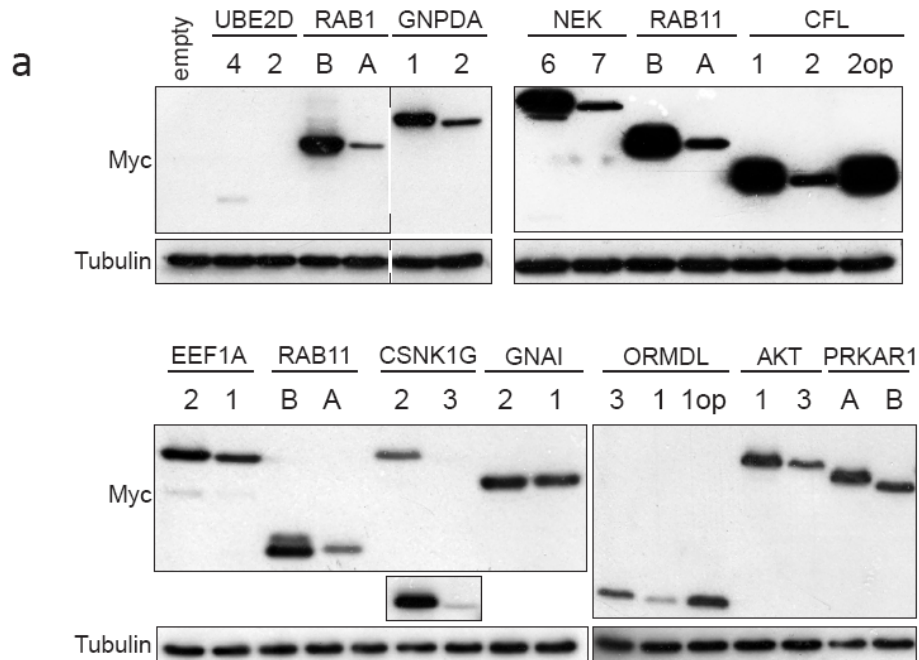


**Figure 11: Codon usage difference in gene pairs results in expression differences and identifies a unique set of pathways**

(a) Highly homologous gene pairs with different codon usages were transiently expressed in 293 cells and resulting protein levels were evaluated by immunoblot. In each case the member of the gene pair with common codons is listed first, and the member with more rare codons is listed second. (b) Simplified diagram of the relevant proteins within the insulin signaling pathway. Genes with multiple highly homologous family members with wide differences in codon usage are highlighted in red.

Immunoblot analysis revealed that in every case, the gene characterized by rare codons expressed lower levels of protein compared to the counterpart with more common codons (Figure 11A). We confirmed that the differences in protein expression between members of the gene pairs were due to codon usage. Specifically, cDNA versions of Myc epitope-tagged *CFL2* and *ORMDL1* were synthesized such that all the rare codons were changed to common codons. Immunoblot analysis of 293 cells transiently transduced with expression vectors encoding these optimized cDNAs revealed that the loss of rare codons in *CFL2op* and *ORMDL1op* restored protein expression to the level observed with *CFL1* and *ORMDL3* (Figure 11A). This direct comparison of highly homologous gene pairs revealed that rare codon bias limits the expression of mammalian genes.

We next assessed whether there was any overarching relationship of gene pairs exhibiting differences in codon bias. KEGG pathway analysis was performed with an expanded list of gene pairs to determine if such gene pairs lied in a particular pathway, which could reflect cellular situations in which rare codons may play a functional role. The insulin signaling ( $p = 8.8 \times 10^{-12}$ ), oocyte meiosis ( $p = 1.2 \times 10^{-10}$ ), and long-term potentiation ( $p = 5.3 \times 10^{-9}$ ) pathways were found to be enriched with gene pairs that have high homology but also a high difference in codon usage. For example, the gene pairs exhibiting differences in GC3 content of HRas/KRas, AKT1/AKT3, PI3KR1/PI3KR2, PRKAR1A/PRKAR1B, PRKACA/PRKACB and RPS6KB2/RPS6KB1, are signaling proteins in the insulin pathway (Figure 11B). Importantly, analysis of gene pairs with high homology but no GC3 difference, genes with low GC3 content, and genes with high homology did not identify any signaling pathways with high confidence. Thus, the combination of two seemingly unrelated criteria, high protein homology and high difference in codon usage, identified a unique set of pathways.

### 3.3.6 Discussion

In summary, we demonstrate that rare codons limit translation elongation and correspondingly protein levels of both ectopic and endogenous KRas, which has a functional consequence, namely curbing the tumorigenic potential of the oncogenic version of the protein. This result supports the suggestion that synonymous site nucleotides may have functional consequences at the protein level in mammals (Parmley and Huynen 2009). Indeed, the mRNA coding sequences for two similar actin isoforms direct their differential ubiquitination and arginylation in human cells (Zhang, Saha et al. 2010), and synonymous SNPs within the coding sequence of the MDR1 transporter alter protein folding and its subsequent transport functions (Kimchi-Sarfaty, Oh et al. 2007). However, this does not necessarily imply that natural selection is responsible for the rare codon bias observed in *KRAS* (Chamary, Parmley et al. 2006). In this regard, isochores are large domains of relatively homogenous GC content in mammalian genomes, and the GC content at synonymous sites (and thus codon usage) strongly correlates with the isochores in which the gene resides (Aota and Ikemura 1986; Sharp, Averof et al. 1995). Indeed, *KRAS* resides within an isochores with a relatively low GC content, while *HRAS* does not. Nevertheless, the bias of rare codons in *KRAS* may help explain why *KRAS* mutation-positive tumors sometimes exhibit amplification of the *KRAS* gene (Yamada, Sakamoto et al. 1986; Radinsky, Kraemer et al. 1987; Liu, Von Lintig et al. 1998; Heidenblad, Jonson et al. 2002; O'Hagan, Chang et al. 2002; Aguirre, Bardeesy et al. 2003; Mita, Toyota et al. 2009; Modrek, Ge et al. 2009; Wagner, Perner et al. 2009; Sasaki, Hikosaka et al. 2011), as gene amplification is conceivably one way overcome the multitude of rare codons throughout *KRAS* limiting protein expression and oncogenic activity. In this regard, it is worth pointing out that increasing tRNA levels can promote tumorigenesis (White 2004; Marshall, Kenneth et al. 2008). Our

identification of other homologous gene pairs that exhibit a strong bias in codon usage and their enrichment in multiple signaling networks suggests that codon bias may serve to fine tune the regulatory potential of these networks. Finally, the observation that the expression and tumorigenic potential of *KRAS* are limited by rare codons not only defines a novel mechanism regulating KRas function, but may reflect more expansive exploitation of codon usage in signaling pathways.

## 4. Targeting eNOS in Pancreatic Cancer

### 4.1 Introduction

Pancreatic ductal adenocarcinoma (PDAC) has among the worst prognosis for any solid tumor, as five year survival rates do not exceed 5% (Jemal, Siegel et al. 2009). The current frontline treatment for advanced PDAC, consisting of single agent gemcitabine, was introduced thirteen years ago (Burris, Moore et al. 1997). Since that time, the largest improvement in therapy has been the addition of the small molecule EGFR inhibitor erlotinib to the gemcitabine regimen, which extends median survival by 10 days (Bria, Milella et al. 2007; Moore, Goldstein et al. 2007). This indicates a pressing need to develop truly new therapeutic approaches for pancreatic cancer that can be rapidly introduced into the clinic.

One advantage in the effort to develop new therapeutics for PDAC is that 90% of these cancers possess oncogenic mutations within the same gene *KRAS* (Almoguera, Shibata et al. 1988; Hruban, van Mansfeld et al. 1993; Downward 2003), which renders the encoded small GTPase constitutively GTP-bound and active (Downward 2003; Karnoub and Weinberg 2008). These oncogenic mutations are detected in the earliest pancreatic intraepithelial neoplastic (PanIN) lesions in humans (Lohr, Kloppel et al. 2005). Expression of oncogenic KRas can convert normal human ductal pancreatic epithelial cells to a tumorigenic state (Qian, Niu et al. 2005). Similarly, expression of an endogenous oncogenic *KRAS* allele in the pancreas of mice leads to PanIN lesions that progress to PDAC (Hingorani, Petricoin et al. 2003). Conversely, silencing oncogenic Ras expression in fully developed mouse tumors (Chin, Tam et al. 1999) or in tumors established from human PDAC cell lines leads to spontaneous tumor regression (Brummelkamp, Bernards et al. 2002; Lim and Counter 2005). KRas is thus the initiating oncogene for pancreatic

cancer, and very much like CML is addicted to BCR-Abl (Huettnner, Zhang et al. 2000) and hence sensitive to imatinib (Quintas-Cardama, Kantarjian et al. 2007), pancreatic cancers are addicted to oncogenic KRas.

Despite the pivotal role of oncogenic KRas in PDAC, to date it has not been possible to develop small molecules to inhibit the picomolar affinity of Ras for guanosine nucleotides (John, Sohmen et al. 1990; Cox and Der 2002). Similarly, it has proven challenging to effectively inhibit lipidation of the protein as a means to interfere with Ras function, as exemplified by the inability of a farnesyltransferase inhibitor to provide an advantage over the frontline therapy of gemcitabine in a phase III clinical trial of PDAC (Van Cutsem, van de Velde et al. 2004). However, KRas exerts its tumorigenic functions by activating primarily three effector proteins, Raf kinases, phosphatidylinositol 3-kinases (PI3K), and Ral guanine nucleotide exchange factors, and pharmacological inhibitors of the first two pathways (Sebolt-Leopold and Herrera 2004; Engelman 2009; Liu, Cheng et al. 2009) reduce tumor growth in some cancers, with numerous clinical trials currently underway (Montagut and Settleman 2009; Wong 2009; Courtney, Corcoran et al. 2010). As such, targeting druggable components of oncogenic KRas signaling is a potential strategy to treat PDAC.

Of the three aforementioned KRas effectors, only active PI3K, or its principal target AKT kinases, are sufficient to maintain xenograft tumor growth upon silencing oncogenic Ras (Lim and Counter 2005). This suggests that pancreatic cancer cells become addicted to the PI3K-AKT signaling arm of oncogenic KRas, and hence components of this pathway represent attractive targets. While the families of PI3K and AKT proteins are druggable and hence offer great potential as therapeutic targets, they are comprised of highly related proteins involved in a large number of normal physiological processes, and consequently general inhibitors of these kinases

can be toxic (Engelman 2009; Liu, Cheng et al. 2009). However, the AKT substrate endothelial Nitric Oxide Synthase (eNOS or NOS III) (Dudzinski and Michel 2007) has been detected in the active phosphorylated state in human PDAC tissues (Lim, Ancrile et al. 2008). eNOS is a member of the NOS family of enzymes composed of eNOS, neuronal NOS (nNOS or NOS I), and inducible NOS (iNOS or NOS II) that generate nitric oxide (Alderton, Cooper et al. 2001). Unlike AKT, eNOS plays a limited role in normal physiology, mainly in vasorelaxation (Dudzinski, Igarashi et al. 2006), and *eNOS*<sup>-/-</sup> mice are viable (Huang, Huang et al. 1995; Shesely, Maeda et al. 1996). Moreover, mounting evidence suggests that inhibition of eNOS has anti-tumor effects. Specifically, *eNOS*<sup>-/-</sup> mice are resistant to DMBA/TPA chemical carcinogenesis (Lim, Ancrile et al. 2008) and PDGF-induced gliomagenesis (Charles, Ozawa et al. 2010), while peptide-mediated inhibition of eNOS decreases tumor vascular permeability and tumor growth in hepatocarcinoma and lung carcinoma xenograft models (Gratton, Lin et al. 2003). In regards to pancreatic cancer, shRNA knockdown of eNOS inhibited the tumorigenic growth of two human PDAC cell lines with highly phosphorylated eNOS (Lim, Ancrile et al. 2008). Thus, inhibiting eNOS may be a way to indirectly exploit the addiction of pancreatic cancer cells to oncogenic KRas. In this regard, the NOS inhibitor N<sup>G</sup>-nitro-L-arginine methyl ester (L-NAME), which is moderately selective for eNOS and nNOS over iNOS (Alderton, Cooper et al. 2001), was developed and clinically evaluated in phase I and II trials for cardiogenic (Cotter, Kaluski et al. 2003) and septic (Avontuur, Tutein Nolthenius et al. 1998) shock, and has been evaluated in numerous other clinical trials, including those involving normal healthy subjects (Morgan, Silke et al. 2003; Muldowney, Davis et al. 2004). This drug is relatively benign compared to conventional cytotoxic chemotherapy; the major side effect of chronic administration is

hypertension (Baylis, Mitruka et al. 1992). These findings support the exciting possibility that eNOS could be targeted by simply repurposing the drug L-NAME to treat PDAC.

Before eNOS inhibition could be considered as a clinical strategy for the treatment of PDAC, a number of issues needed to be addressed. First, there is evidence that nitric oxide can both inhibit and enhance tumorigenesis (Fukumura, Kashiwagi et al. 2006), including in different animal models of pancreatic cancer (Wang, Xiong et al. 2001; Wang, Wei et al. 2003; Takahashi, Kitahashi et al. 2008). However, the critical test of evaluating the effect of genetic ablation of *eNOS* in mouse models of spontaneously arising PDAC remained to be performed. Second, it was unknown whether the global loss of *eNOS* throughout the body, such as would occur upon systemic administration of a NOS inhibitor, would outweigh possible benefits afforded by the loss of *eNOS* in the cancer. Third, even if genetic ablation of eNOS inhibited PDAC, it was unknown whether this could be translated into a clinically relevant approach using a small molecule NOS inhibitor, whether side effects from NOS inhibition might limit the clinical utility of such a pharmacologic approach, or whether such small molecule inhibition would affect the tumorigenic growth of human PDAC cells. To address these critical issues we first evaluated whether genetic ablation of *eNOS*, and then inhibition of eNOS with the drug L-NAME, impacted the development of PanIN lesions in a genetically engineered mouse (GEM) model of early pancreatic cancer (Hingorani, Petricoin et al. 2003). Next we explored whether genetic and pharmacologic inhibition of eNOS could extend survival in a GEM model that develops fully invasive PDAC, which faithfully recapitulates the genetics, clinical syndrome, histopathology, metastatic profile, and refractoriness to treatment of human pancreatic cancer (Hingorani, Wang et al. 2005; Olive, Jacobetz et al. 2009). Lastly, we confirmed the murine findings in a

human setting, testing the effect of L-NAME on xenograft growth of human pancreatic cancer cell lines.

## 4.2 Results

### 4.2.1 eNOS Is Upregulated During PDAC

We capitalized on the ability to model different stages of pancreatic cancer in mice to evaluate if and when during the tumorigenic process eNOS becomes upregulated. Specifically, *LSL-Kras<sup>G12D/+</sup>;Pdx-1-Cre<sup>tg/+</sup>* (KC) mice conditionally express endogenous mutant *Kras<sup>G12D</sup>* in the pancreas, and hence develop pancreatic intraepithelial neoplastic lesions (PanINs), presumed precursors to invasive disease that at low frequency progress to PDAC (Hingorani, Petricoin et al. 2003; Feldmann, Beaty et al. 2007). *LSL-Kras<sup>G12D/+</sup>;LSL-Trp53<sup>R172H/+</sup>;Pdx-1-Cre<sup>tg/+</sup>* (KPC) mice conditionally express endogenous mutant *Kras<sup>G12D</sup>* and *p53<sup>R172H</sup>* in the pancreas, which leads to fully invasive, lethal PDAC that is strikingly similar to human PDAC (Hingorani, Wang et al. 2005; Olive, Jacobetz et al. 2009). Thus, KC and KPC mice can serve as models of early and late stage disease, respectively. Immunohistochemical analysis revealed, as previously reported (Worl, Wiesand et al. 1994), that eNOS was confined to endothelial cells in the normal pancreas. However, focal, weak eNOS reactivity was observed in PanIN lesions in KC mice, and robust eNOS reactivity was detected in adenocarcinomas of KPC mice, which was specific to eNOS, as there was an absence of reactivity in *eNOS<sup>-/-</sup>* KPC mice (Figure 12). These results were confirmed by RT-PCR (not shown). Thus, eNOS is gradually elevated throughout the development of spontaneously occurring PDAC in GEM models of this disease.

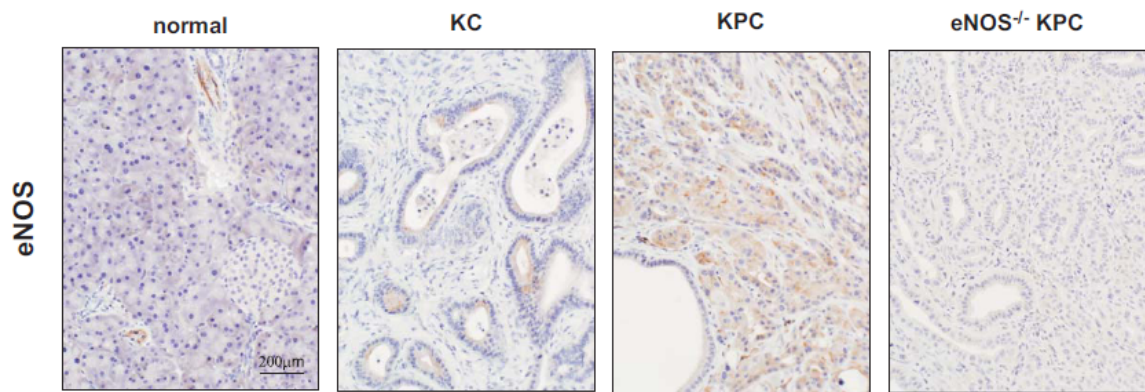


**Figure 12: eNOS is upregulated during pancreatic tumorigenesis.**

eNOS protein, as detected by immunohistochemical staining, in the pancreas of a normal control mouse, a KC mouse at the termination of the experiment (330 days of age), a KPC mouse at the mortality endpoint, or an *eNOS*<sup>-/-</sup> KPC mouse at the mortality endpoint.

#### 4.2.2 Genetic Ablation of eNOS Decreases PanIN Development

Given the increase in eNOS expression early in PDAC development, we tested whether ablation of the *eNOS* gene would disrupt the onset of pancreatic tumorigenesis. To this end, knockout alleles of *eNOS* were crossed into the aforementioned KC model of preinvasive pancreatic cancer, and both a cohort of *eNOS*<sup>-/-</sup> KC and a control cohort of *eNOS*<sup>+/+</sup> KC mice were aged to ~330 days to allow a spectrum of PanINs to develop (Hingorani, Petricoin et al. 2003). At this time point, the pancreata were removed and H&E stained to visualize overall tissue architecture and histopathology (Figure 13A). In each group, the area of remaining normal acinar tissue was quantified from five high power fields per pancreas from cohorts of sixteen mice, amounting to eighty random high power fields analyzed (Figure 13B). Additionally, since PanIN lesions can be histologically graded on a progressive scale (Hruban, Adsay et al. 2006), the tissues were examined blindly by two pathologists who quantified >2600 lobules per group – approximately 200 lobules per mouse – and then scored each lobule according to the highest grade ductal PanIN lesion present (Figure 13C).

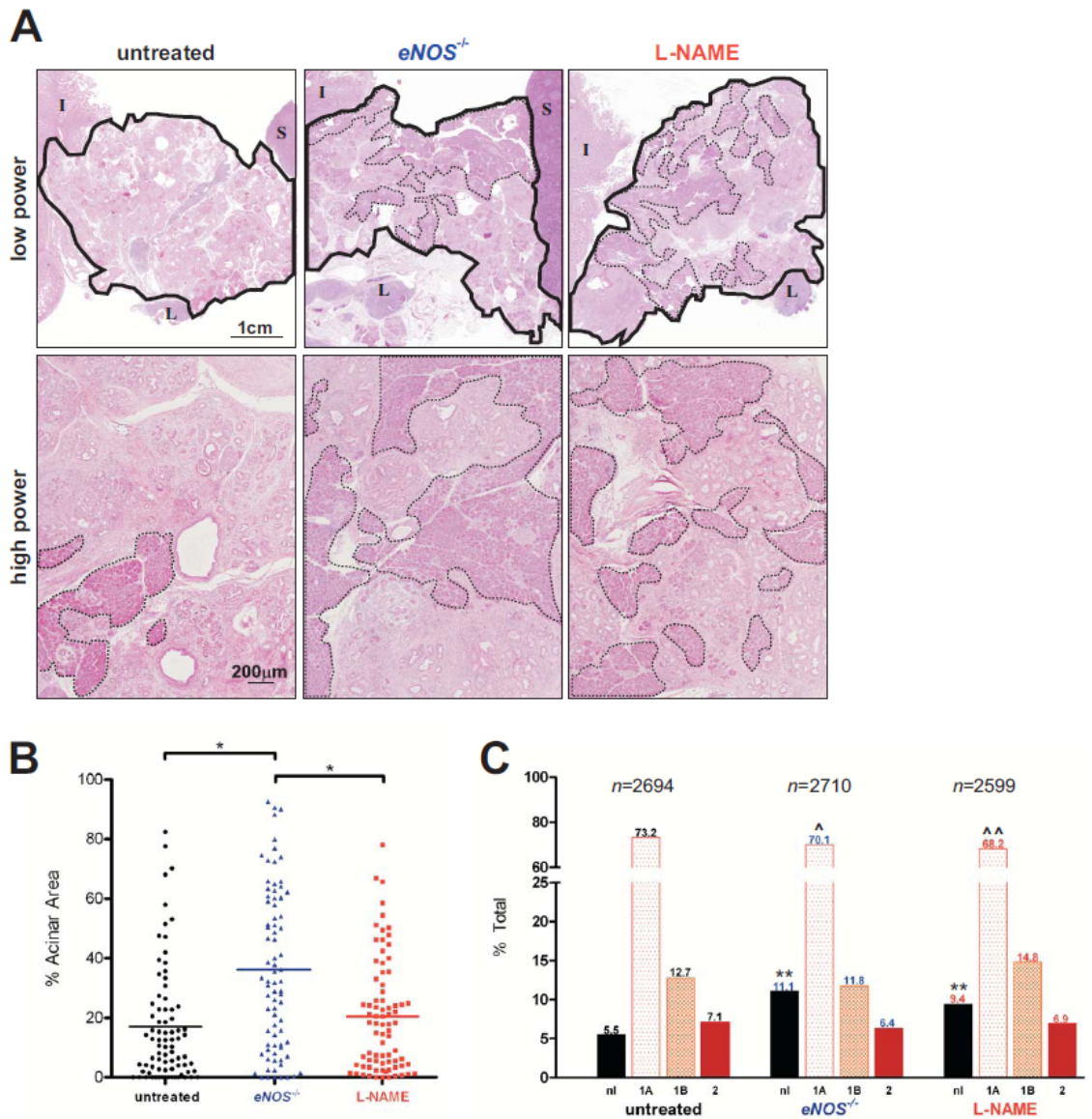


**Figure 13: Reduction in area and grade of pancreatic lesions in *eNOS*<sup>-/-</sup> and L-NAME treated mice**

(A) Whole mount (low power) and magnified (high power) H&E stained representative pancreata from KC mice either randomly assigned to be untreated ( $n=16$ ) or treated with L-NAME ( $n=16$ ), or from *eNOS*<sup>-/-</sup> KC mice ( $n=16$ ). (solid line: outline of pancreas, dashed line: normal acinar tissue, I: intestine, L: lymph node, S: spleen). (B) The area of normal pancreatic tissue was blindly assessed by outlining normal acini as in A. Five random high power fields from all the mice ( $n=16$ ) in each of the indicated cohorts were examined and are represented as data points. Bar, mean % normal acini.  $*P<0.001$ . (C) Percent of lobules with the highest grade lesion being normal duct (nl), PanIN-1A (1A), PanIN-1B (1B), or PanIN-2 (2) in the indicated cohorts.  $n$ , total number of lobules blindly graded from the mice in each cohort.  $**P<0.0001$  normal versus abnormal ducts compared to untreated.  $^{\wedge}P<0.05$  or  $^{\wedge\wedge}P<0.0001$  PanIN-1A versus all other ducts compared to untreated. Disease Kendall quantified the normal remaining acinar area depicted in (B), and Michael Shealy and Diana Cardona graded the ductal lesions quantified in (C).

As previously reported (Hingorani, Petricoin et al. 2003), most of the pancreas in untreated control KC animals was replaced with abnormal tissue. This consisted of varying grades of PanIN lesions with abundant surrounding fibrotic stroma and associated chronic inflammatory cells (Figure 13A). Quantification revealed that the average area of normal acinar tissue remaining in these mice was reduced to 17% (Figure 13B), with 94.5% of lobules having abnormal ducts, mainly consisting of low grade PanIN-1A and, to a lesser extent, higher grade PanIN lesions (Figure 13C). In comparison to these mice, *eNOS*<sup>-/-</sup> KC mice exhibited over twice as much normal pancreatic tissue area (Figure 13, A and B), a significant drop in lobules with PanIN lesions, and an accompanying doubling in the number of lobules with normal ducts (Figure 13C). This reduction in the transition from normal ducts to early lesions, coupled with the upregulation of eNOS in the PanIN lesions and not accompanying stroma (Figure 12), suggests an early, tumor cell autonomous role for eNOS. We conclude that the loss of eNOS not only was tolerated in diseased mice, but actually inhibited development of preinvasive pancreatic neoplasia.

#### **4.2.3 Genetic Ablation of eNOS Decreases Development of Other Oncogenic KRAS-Driven Tumors**

KC mice developed vulvar and facial papillomas (Figure 14A, B) with a high penetrance that occasionally progress into squamous cell carcinomas. These tumors possess a recombined oncogenic *Kras*<sup>G12D</sup> allele, as evidenced by the detection of the floxed allele by PCR in isolated tumors (Figure 14C), likely due Pdx-1 mediated Cre expression (Hingorani, Petricoin et al. 2003; Gades, Ohash et al. 2008; Mazur, Gruner et al. 2010). *eNOS*<sup>-/-</sup> KC mice exhibited a significant 50% decrease in the number of facial papillomas per mouse at the time of sacrifice (~330 days) compared to control *eNOS*<sup>+/+</sup> KC mice (Figure 14D). Grossly apparent vulvar papillomas were

also resected from the mice at necropsy and weighed. Again, *eNOS*<sup>-/-</sup> KC mice exhibited a significant 85% decrease in the weight of vulvar papillomas compared to the control *eNOS*<sup>+/+</sup> KC mice at the time of sacrifice (Figure 14D). These results in two more independent oncogenic KRAS-driven cancer models corroborate the aforementioned findings in preinvasive pancreatic cancer, and further suggest the intriguing possibility of a requirement of *eNOS* for the development of other malignancies.

#### **4.2.4 Genetic ablation of *eNOS* increases the lifespan of mice with lethal PDAC**

Encouraged by the fact that loss of *eNOS* inhibited early pancreatic disease, we investigated whether genetic ablation of *eNOS* would provide a survival benefit, the most clinically relevant endpoint, in the KPC mouse model of metastatic PDAC. Thus, *eNOS* null alleles were crossed into the KPC background, and littermates generated over the course of a year were used to populate cohorts of ultimately 35 *eNOS*<sup>+/+</sup> KPC control mice and 32 *eNOS*<sup>-/-</sup> KPC mice. These mice were monitored for moribundity endpoints known to immediately precede death, humanely defined as 20% weight loss, ascites, or extreme inactivity (Hingorani, Wang et al. 2005). Consistent with previous studies, the control cohort of *eNOS*<sup>+/+</sup> KPC mice had a median survival of 142 days (Hingorani, Wang et al. 2005). *eNOS*<sup>-/-</sup> KPC mice, on the other hand, exhibited a median survival of 176 days ( $P = 0.093$ , HR = 0.709, CI<sub>95</sub> = 0.431-1.167), a trend that corresponded to an increase of 34 days or nearly 25% of the control lifespan (Figure 15A). Thus, the loss of *eNOS* increased survival in a highly aggressive PDAC mouse model.

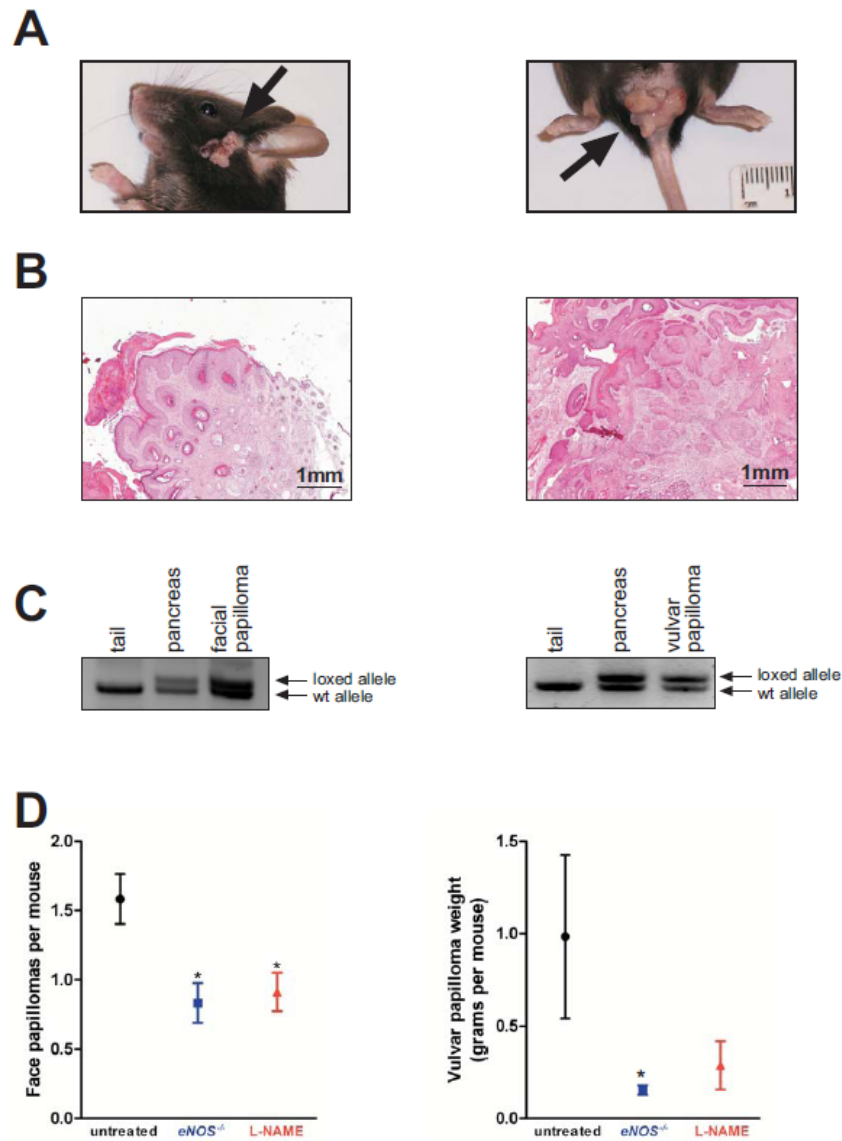


**Figure 14: *eNOS*<sup>-/-</sup> and L-NAME treated KC mice are resistant to spontaneously arising facial and vulvar tumors**

(A) Gross photograph and (B) H&E stained section of a representative facial squamous papilloma (left) and a vulvar papilloma (right) from KC mice. (C) PCR analysis with primers specific for either the wild type KRAS allele (wt allele) or the LSL-Kras<sup>G12D</sup> allele after Cre excision (loxped allele). Samples include DNA isolated from the tail (negative control), pancreas (positive control sample) and a facial (left) and a vulvar (right) tumor. (D) Mean ± SEM of the total number of new facial tumors (left) developing over the course of 330 days in cohorts ( $n=24$ ) of KC mice either untreated or treated with L-NAME, or *eNOS*<sup>-/-</sup> KC mice. Mean weight ± SEM of vulvar tumors (right) arising at 330 days of age in females in cohorts of KC mice either untreated ( $n=9$ ) or treated with L-NAME ( $n=7$ ) and in a cohort of *eNOS*<sup>-/-</sup> KC mice ( $n=11$ ). \* $P<0.05$  (compared to untreated).

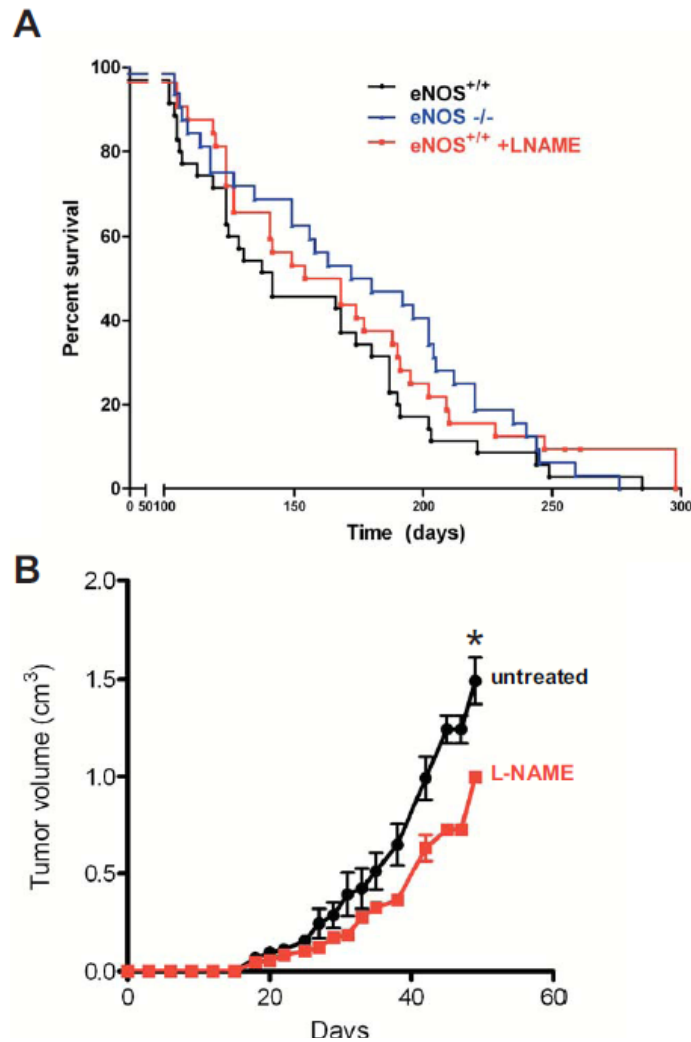


**Figure 15: NOS inhibition provides a survival advantage to KPC mice**

(A) Kaplan-Meier survival curve of cohorts of KPC mice untreated ( $n=35$ ) or treated with L-NAME ( $n=32$ ) and  $eNOS^{-/-}$  KPC mice ( $n=32$ ). (B) Mean size  $\pm$  SEM of subcutaneous xenograft tumors generated by a cell line derived from a KPC adenocarcinoma injected in isogenic immunocompetent cohorts of mice randomly assigned to either be untreated ( $n=4$ ) or treated with L-NAME ( $n=4$ ). \* $P < 0.05$ . Disease Kendall and Meghan Morrison performed the experiment depicted in (B).

#### 4.2.5 L-NAME treatments retard development of preinvasive pancreatic lesions

We next explored whether clinically relevant methods to inhibit the enzyme would similarly impact the early pancreatic cancer of KC mice. As no specific small molecule eNOS inhibitor exists, we employed the general NOS inhibitor L-NAME for this investigation. This drug was chosen because it does show some specificity for eNOS, namely a ten-fold preference for eNOS and nNOS over iNOS (Alderton, Cooper et al. 2001), and is one of only two NOS inhibitors to have been brought to a phase II clinical trial for the treatment of shock (Avontuur, Buijk et al. 1998; Avontuur, Tutein Nolthenius et al. 1998; Cotter, Kaluski et al. 2003; Morgan, Silke et al. 2003). L-NAME is a relatively benign drug, especially when compared to conventional cytotoxic chemotherapy. The major side effect of chronic administration is hypertension and resultant end organ damage, such as left ventricular hypertrophy and glomerulosclerosis (Baylis, Mitruka et al. 1992). Nevertheless, such organ damage can be prevented by co-administration of antihypertensives (Navarro-Cid, Maeso et al. 1996; Akuzawa, Nakamura et al. 1998). L-NAME can also be orally dosed, a quality that would facilitate administration in the clinic. For these reasons L-NAME is an attractive drug to evaluate in preclinical models of PDAC.

We therefore designed a preclinical mouse trial in which a cohort of 16 KC mice was provided L-NAME in the drinking water at a dose established to increase blood pressure, indicating effective eNOS inhibition (see below and refs. (Shesely, Maeda et al. 1996; Kurihara, Alfie et al. 1998)). Treatment began at weaning and ended when the mice were sacrificed at ~330 days of age. The pancreata were then analyzed as detailed above. KC mice treated with L-NAME demonstrated decreased tumor development compared to untreated controls, although not to the same degree as seen in *eNOS*<sup>-/-</sup> animals. Specifically, the L-NAME treated group

trended towards retaining more normal tissue architecture than untreated controls, with the mean percent of remaining normal acinar tissue increasing from 17.0% in KC mice to 20.5% in KC mice treated with L-NAME (Figure 13A,B). L-NAME treatments similarly led to a significant decrease in lobules with PanIN-1A lesions and a nearly two fold increase in lobules with normal ducts compared to the untreated counterparts (Figure 13C). Anecdotally, there was also a reduction in the number of mice progressing to invasive PDAC in this model, with three mice developing PDAC in the untreated control group, two mice in the *eNOS*<sup>-/-</sup> cohort, and one mouse in the L-NAME treated group. Thus, L-NAME treatments reduced tumor burden in a mouse model of preinvasive pancreatic cancer.

#### **4.2.6 L-NAME treatments inhibit other oncogenic KRas-driven tumors**

As was done with *eNOS*<sup>-/-</sup> KC mice, development of facial and vulvar papillomas was also monitored in KC mice treated with L-NAME. L-NAME treatment halved the number of facial papillomas and reduced the weight of vulvar papillomas by almost three quarters in KC mice (Figure 14D). These results suggest that pharmacologic targeting of eNOS is both feasible and potentially beneficial for other KRas-driven cancers.

#### **4.2.7 L-NAME treatments increase the lifespan of mice with lethal PDAC**

To address whether L-NAME could affect survival in the aggressive KPC mouse model of PDAC, we undertook a preclinical mouse trial in which 32 KPC mice orally treated as above with L-NAME were monitored for mortality endpoints. As was done previously for the *eNOS*<sup>-/-</sup> KPC mice, all-cause mortality was assessed to include any deaths that may be due to adverse effects from the drug itself. Median survival for the L-NAME treated mice was 161 days ( $P=0.208$ , HR=0.725, CI95=0.439-1.196), a trend that reflected a 19 day survival advantage over the cohort

of 35 untreated control KPC mice (Figure 15A). Thus, both genetic ablation of *eNOS* and pharmacologic inhibition with the drug L-NAME led to a clinically relevant endpoint of increased survival in KPC mice. While this effect could be ascribed to an initial decrease in PanIN lesions, as observed in KC mice treated with L-NAME (Figure 13), L-NAME could similarly inhibit the adenocarcinomas. To address this possibility, a PDAC cell line established from a KPC mouse was subcutaneously injected into isogenic immunocompetent mice that were either left untreated or treated with L-NAME. L-NAME reduced the tumorigenic growth of these xenografts (Figure 15B). Thus, pharmacologic inhibition with the drug L-NAME inhibits the development and moreover, the maintenance of PDAC, resulting in a clinically relevant outcome of increased survival.

#### **4.2.8 L-NAME decreases tumorigenic growth of human PDAC cell lines**

Since genetic and pharmacologic inhibition of eNOS reduced pancreatic tumorigenesis in the KC and KPC mouse models, we next explored the potential of targeting NOS in a human cell setting, an important consideration given that oncogenic RAS signaling can exhibit species differences (Hamad, Elconin et al. 2002; Rangarajan, Hong et al. 2004). Specifically, eight *KRAS* mutation-positive human PDAC cell lines were each injected subcutaneously into the flank of ten immunocompromised mice, of which half were left untreated and half were orally dosed with L-NAME. Seven out of eight tested cell lines demonstrated a significant response to the drug, with L-NAME typically halving the tumor size by the termination of the experiment (Figure 16A and Figure 17A-G). This is consistent with early studies demonstrating that N-nitro-L-arginine (L-NNA), an insoluble active metabolite of L-NAME (Griffith and Kilbourn 1996), halved both subcutaneous and orthotopic xenograft tumor growth of the human PDAC cell line L3.6pl

(Camp, Yang et al. 2006). Additionally, aminoguanidine, a broad NOS inhibitor with some specificity for iNOS (Misko, Moore et al. 1993), also decreased xenograft tumor growth when given at high doses; interestingly, it caused decreased eNOS expression in the treated xenografts (Mohamad, Cricco et al. 2009).

To evaluate the effect of treating established human tumors, immunocompromised mice were again injected with a human PDAC cell line, and once tumors reached a size of  $0.75\text{cm}^3$ , the animals were either left untreated or were dosed with L-NAME. Within days of beginning L-NAME treatments, tumor size was reduced compared to untreated controls, and at the termination of the experiment tumor size was again halved (Figure 16B). To address the impact of L-NAME in combination with the standard of care therapeutic gemcitabine (Ko and Tempero 2005), mice with established tumors were also treated with gemcitabine or a combination of gemcitabine and L-NAME. Mice treated with the combination therapy had smaller tumors than those treated with gemcitabine alone (Figure 16B), a promising sign because most agents tested in combination with gemcitabine show little survival benefit in clinical trials (Bria, Milella et al. 2007). Thus, L-NAME broadly inhibited human PDAC xenograft growth, could be combined with gemcitabine, and caused regression of established tumors.

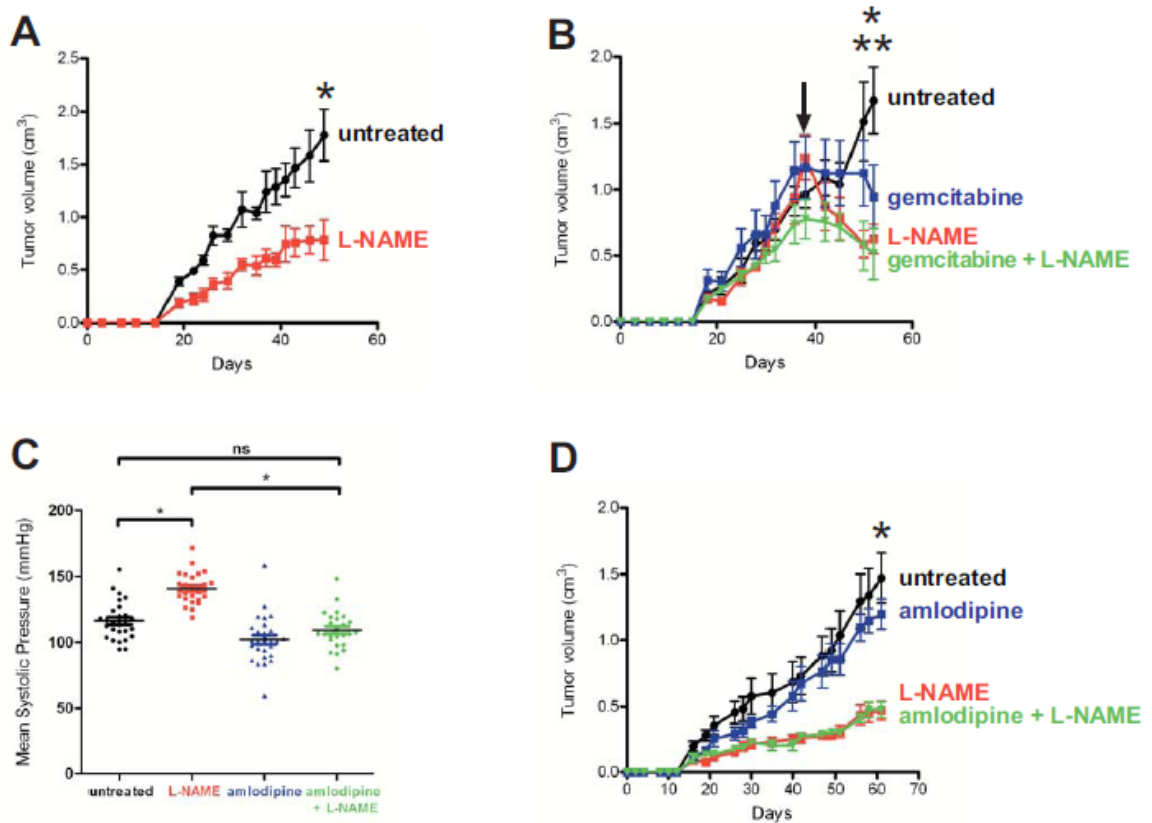


**Figure 16: L-NAME decreases the tumorigenic growth of human pancreatic cancer cells, even when its antihypertensive effect is abrogated**

(A) Mean size  $\pm$  SEM of subcutaneous tumors derived from CFPac-1 cells in cohorts ( $n=5$ ) of mice untreated or treated with L-NAME.  $*P<0.05$ . (B) Mean size  $\pm$  SEM of subcutaneous CFPac-1 tumors in cohorts of mice ( $n=5$ ) that, upon reaching an established size of  $0.75\text{cm}^3$  (arrow), were untreated or treated with L-NAME, gemcitabine, or L-NAME + gemcitabine.  $P<0.05$ ,  $*$ each treatment compared to untreated,  $**$  gemcitabine versus gemcitabine + L-NAME. (C) The daily mean systolic pressure taken over 8 weeks in cohorts of mice ( $n=5$ ) with subcutaneous CFPac-1 tumors that were either untreated or treated with L-NAME, amlodipine, or L-NAME + amlodipine.  $*P<0.05$ . ns, non-significant. (D) Mean size  $\pm$  SEM of CFPac-1 xenografts in animals corresponding to treatment groups described in C.  $*P<0.05$ , L-NAME  $\pm$  amlodipine compared to untreated. All data in this figure were generated by Disean Kendall and Meghan Morrison.

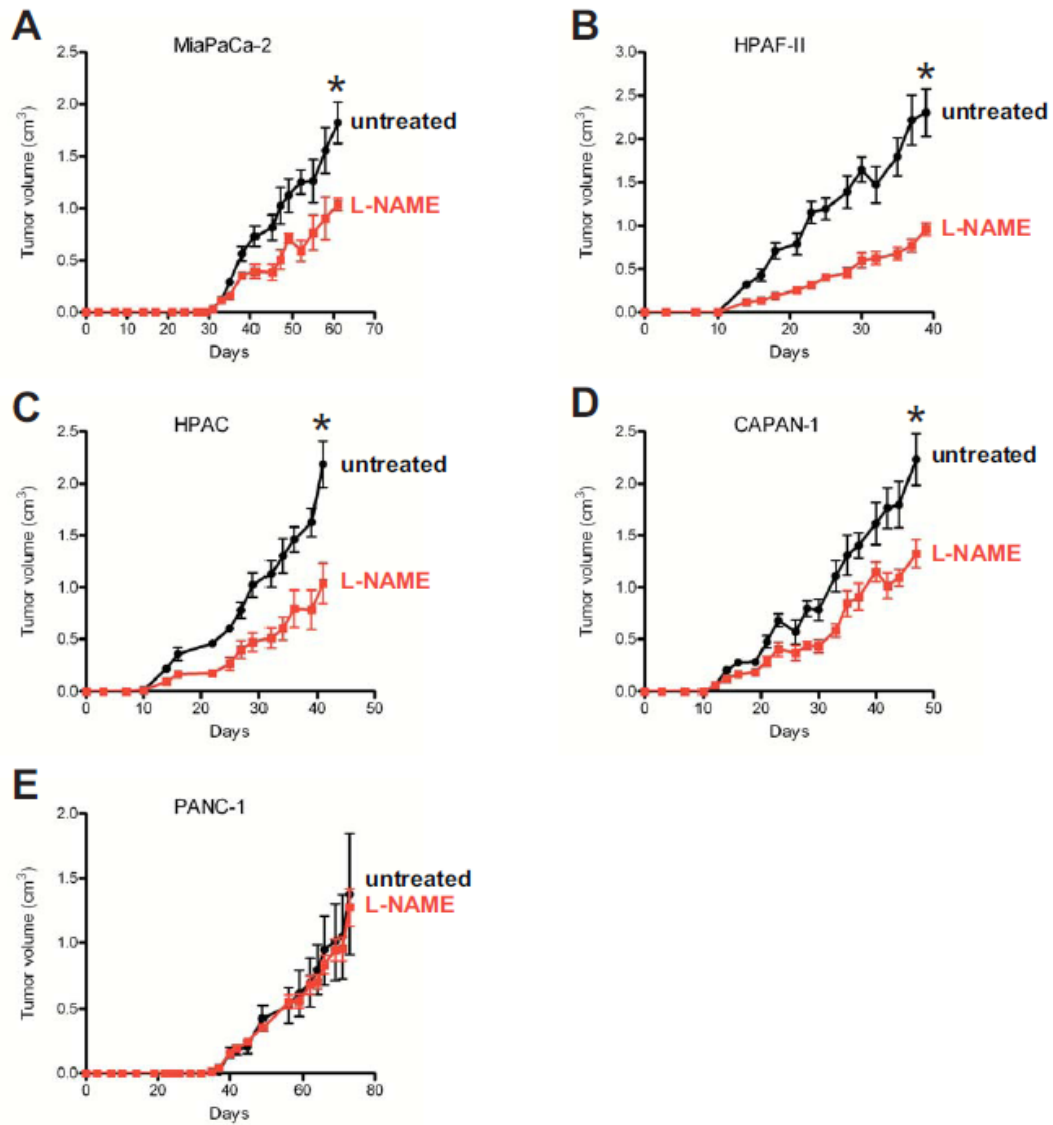


**Figure 17: L-NAME broadly decreases the tumorigenic growth of many human pancreatic cancer cell lines**

Mean size  $\pm$  SEM of tumors derived from (A) MiaPaCa-2; (B) HPAF-II; (C) HPAC; (D) CAPAN-1 and (E) PANC-1 human pancreatic cancer cells in cohorts ( $n=5$ ) of mice untreated or treated with L-NAME. \* $P<0.05$ . All data in this figure were generated by Disean Kendall and Meghan Morrison.

#### **4.2.9 L-NAME reduced PDAC tumor growth in mice treated with an anti-hypertensive**

The primary effect of L-NAME is an elevation in blood pressure (Figure 16C and (Baylis, Mitruka et al. 1992)). Specifically, acute dosing of L-NAME variably causes transient hypertension in some, but not all healthy human subjects (Lepori, Sartori et al. 1998; Ritchie, Alexander et al. 2002; Morgan, Silke et al. 2003). Chronic daily dosing of L-NAME over the course of six weeks also caused hypertension in rats (Ribeiro, Antunes et al. 1992; Navarro-Cid, Maeso et al. 1996; Akuzawa, Nakamura et al. 1998). However, this hypertension and resultant end-organ consequences were prevented by a wide spectrum of antihypertensives (Erley, Rebmann et al. 1995; Navarro-Cid, Maeso et al. 1996; Akuzawa, Nakamura et al. 1998). We therefore evaluated whether concurrent therapy with the widely used antihypertensive amlodipine influenced the anti-tumor effects of L-NAME. Specifically, cohorts of five mice injected with human PDAC cells were left untreated or were treated with amlodipine, L-NAME, or both drugs; all cohorts were then monitored for blood pressure and tumor growth. Five times weekly, ten blood pressure measurements were taken and tumor volume was measured in each mouse. This analysis revealed that amlodipine consistently reduced systolic blood pressure of L-NAME treated animals, as previously reported (Akuzawa, Nakamura et al. 1998), from  $141 \pm 2.2$  mmHg to the normal level of  $109 \pm 2.7$  mmHg (Figure 16C). Importantly, amlodipine had no effect on the anti-tumor activity of L-NAME, as the size of tumors at the termination of the experiment in the L-NAME and L-NAME+amlodipine cohorts were identical in size, but nevertheless were significantly smaller compared to the untreated or amlodipine

treated mice (Figure 16D). Thus, as the primary side effect of repeated L-NAME dosing was managed with an antihypertensive, L-NAME may be well tolerated in a therapeutic setting.

### 4.3 Discussion

We demonstrate that genetic ablation of *eNOS* and/or pharmacologic inhibition with L-NAME reduced the development of pancreatic lesions, facial papillomas, and vulvar papillomas in the KC mouse model of preinvasive pancreatic cancer and broadly inhibited the tumorigenic growth of human PDAC cell lines. *eNOS* ablation and L-NAME treatment also trended towards a 34 and 19 day increase in survival in KPC mice, corresponding to a 25% and 13% increase in lifespan compared to that of control KPC mice, respectively. It is worth noting that treating late stage pancreatic cancer in KPC mice with standard of care therapy gemcitabine provides no survival benefit (Olive, Jacobetz et al. 2009), highlighting just how difficult it is to impact the survival of KPC mice. Collectively, these data argue that *eNOS* is a therapeutic target that could be inhibited with the available drug L-NAME for the treatment of PDAC.

Not only is targeting *eNOS* a potentially novel strategy to treat PDAC, but the drug used to inhibit the enzyme, L-NAME, appears to be relatively non-toxic. Specifically, KC mice treated daily with L-NAME for roughly ten months had no overt adverse effects, and analysis of all-cause mortality in KPC mice, which would take into account deaths due to adverse drug events, was actually decreased in the L-NAME treatment group compared to untreated controls. In fact, the undesirable effects of L-NAME on blood pressure were ameliorated with a commonly used antihypertensive with no change to the anti-tumor activity of the drug. Indeed, L-NAME has been used in many clinical trials, including those involving normal human subjects, suggesting that this drug may have low toxicities in a cancer setting. Presumably since *eNOS* knockout and

L-NAME treatments exhibited similar effects on tumorigenesis in KC and KPC mice, and since L-NAME inhibits eNOS *in vivo*, as measured by an increase in blood pressure, the anti-tumor effects of L-NAME can be attributed, at least in part, to eNOS inhibition. However, L-NAME also reduced tumor burden in *eNOS*<sup>-/-</sup> KC mice, and extended the survival of *eNOS*<sup>-/-</sup> KPC mice (see 5.4.3 Identify and Inhibit the Other Targets of L-NAME). Whether this is a result of iNOS and nNOS compensating for the loss of eNOS during tumorigenesis or because these enzymes also play a role in tumorigenesis remains to be determined. Nevertheless, L-NAME clearly reduced tumor burden in KC mice and xenograft models of PDAC, as well as extended the lifespan of KPC mice, suggesting value in exploring this drug for the treatment of PDAC.

The precise cell type that is sensitive to eNOS inhibition during the development of pancreatic cancer remains to be determined. NO can be produced both by stromal cells and the tumor cells (Fukumura, Kashiwagi et al. 2006). eNOS is upregulated within the tumor cells (Figure 12), is activated downstream of the driving oncogene KRas, and knockdown of eNOS in two pancreatic cancer cell lines reduces their tumorigenic potential (Lim, Ancrile et al. 2008). On the other hand, eNOS is also expressed in the vasculature of pancreatic tumors (Figure 12) and *eNOS*<sup>-/-</sup> animals are deficient, for example, in endothelial progenitor cell mobilization and neovascularization (Aicher, Heeschen et al. 2003), which may be necessary for tumor angiogenesis. Nevertheless, regardless of the source of eNOS, global genetic ablation of the *eNOS* clearly reduces pancreatic tumorigenesis. Moreover, while inhibiting NO production has been reported to have both pro- and anti-tumor effects, the net result of genetic ablation and/or pharmacologic inhibition of eNOS in all of the tested pancreatic cancer models was a reduction in tumorigenesis.

The inhibition of eNOS may have therapeutic utility in malignancies beyond pancreatic cancer. Indeed, two types of spontaneously arising oncogenic KRas-driven epithelial neoplasias, vulvar and facial papillomas, both responded to L-NAME treatment and exhibited reduced tumor growth in an *eNOS*<sup>-/-</sup> background. This effect may extend even beyond *KRAS* mutation-positive cancers. Specifically, *eNOS*<sup>-/-</sup> mice are also resistant to DMBA/TPA chemical carcinogenesis (Lim, Ancrile et al. 2008) and were recently reported to have prolonged survival in a PDGF-induced glioma mouse model (Charles, Ozawa et al. 2010). Similarly, peptide-mediated inhibition of eNOS decreases tumor vascular permeability and tumor growth in hepatocarcinoma and lung carcinoma xenograft models (Gratton, Lin et al. 2003). Finally, eNOS generated nitric oxide has been shown to regulate the recruitment of pericytes and stabilization of angiogenic vessels in a xenograft model of murine melanoma (Kashiwagi, Izumi et al. 2005). In sum, these data suggest exploring eNOS inhibition as a potential therapeutic option in other cancers.

eNOS inhibition is a novel therapeutic strategy that could be explored clinically for the treatment of PDAC. The advantages of this strategy are that eNOS inhibition i) reduces tumorigenesis in multiple mouse and human models of pancreatic cancer, ii) causes regression of established human tumors, iii) works well with existing frontline therapy for pancreatic cancer based on xenograft studies, iv) is relatively nontoxic, with one primary side effect in terms of cancer treatment, namely elevated blood pressure, that can be managed with an antihypertensive without abrogating the antitumor effect, and v) can be achieved using pre-existing, orally dosed inhibitors that have already been tested in humans, potentially curtailing the 12 to 15 years and 0.5 to 2 billion dollars of investment (DiMasi, Hansen et al. 2003; Adams and Brantner 2006) typically needed for drug development. Collectively, these data suggest that

eNOS is a viable target that can be inhibited with the available drug L-NAME for the treatment of the incurable cancer PDAC.

## 5. Conclusion and Future Directions

### 5.1 Summary of Studies on the Role of Codon Usage in the Control of KRAS Expression

KRAS has a reduced expression level when compared to HRAS in side-by-side transfection experiments where equivalent amounts of DNA are introduced. This is paradoxical because the two proteins are 82% similar (leaving little room for unique regulatory information) and they are considered essentially identical in most cellular assays. Multiple hypotheses could explain this fact, including (1) an artifact of the system, (2) a property of the KRAS protein, or (3) a property of the KRAS mRNA. To rule out the first possibility, I showed the following: the difference existed in many different cell types, the difference existed no matter the method used to introduce the DNA into the cell (stable versus transient transfection), the difference was consistent despite the expression vectors used (with varying promoters, with and without introns, and with varying polyA signal sequences), the difference was independent of the RAS protein activity, and the difference existed no matter what tag was used to detect the protein. This all suggests a true intrinsic defect of KRAS, and not an artifact of the system. To distinguish if the KRAS protein or mRNA was responsible, I created a KRAS protein encoded by an altered cDNA, KRAS\*; this construct still could be expressed. Hypotheses to explain how mRNA sequence can regulate protein expression include RNA binding proteins, miRNA target sequences, mRNA secondary structure, and codon usage. The first two of these hypotheses have previously been demonstrated to play a role in the expression of *endogenously expressed* mammalian genes; the last two, however, have not. Studies with chimeric proteins indicated that no single part of the *KRAS* message was responsible for the low expression; rather, all parts of *KRAS* seemed to partially contribute to lowering its expression. This rules out the first three of

the above hypotheses, as regulation imparted by RNA binding proteins (Elliott and Ladomery 2010), miRNAs (Lewis, Shih et al. 2003), or mRNA secondary structure (Svoboda and Di Cara 2006) would be due to a discrete, defined set of nucleotides within the protein; e.g. a stem-loop or a 6 base pair seed sequence. Only regulation by codon usage would be expected to gradually disappear as more and more of the *KRAS* sequence was replaced. This accepted-by-default codon usage hypothesis was experimentally confirmed by sequentially optimizing particular codons within the *KRAS* message; this did result in a gradual elevation of the protein. Other work done established that rare codon usage causes low expression of the protein through a block in translation elongation.

The possibility still remained that the limited expression of *KRAS* was an effect of plasmid based, ectopic gene overexpression studies. To test whether codon usage controls expression of the endogenous *KRAS* gene required optimizing the codons of *KRAS* in the endogenous cellular genome. To achieve this, I used homologous recombination to knock a *KRAS* cDNA into exon 1 of the endogenous *KRAS* sequence. This cDNA contained 142 synonymous mutations (changing around 25% of the total 567 base pair sequence of *KRAS*) that were selected to make every codon within *KRAS* be the most commonly chosen codon according to Table 1. Analysis of clones that had undergone successful homologous recombination indicated that they did indeed express more *KRAS* protein than either the parental cell line, clones that had undergone non-homologous integration of the neomycin resistance gene, or clones that had a regular *KRAS* cDNA knocked into the locus. (They also had slightly higher levels of *KRAS* mRNA, which may be due to the effect that increasing GC3 content has on mRNA stability, see 1.3.3 Codon Choice as a Possible Mechanism for Control of Translation Elongation?.) As with the exogenous expression studies, at least part of the mechanism of

control is at the level of translation elongation, as *KRAS* mRNAs exhibit reduced ribosomal transit when compared to *HRAS* mRNAs or *KRAS* mRNAs with optimized codons.

After discovering the mechanism of inhibition of *KRAS* expression and showing that it is relevant to studies of both ectopic and endogenous genes, I tested whether codon manipulation of *KRAS* has any biological effect. *KRAS* is important for tumorigenesis, and elevated levels of *HRAS* and *KRAS* are known to increase tumorigenicity in xenograft assays (see 1.1.5.2 Increased RAS Protein Levels in Cancer), so I studied the effects of *KRAS* codon usage on xenograft tumor growth. First, using an immortalized cell line that depends on ectopic expression of a *RAS*<sup>G12V</sup> mutant for tumorigenesis, I showed that a codon optimized *KRAS*\*<sup>G12V</sup> caused tumors that reached endpoint size in 11 days, while *KRAS*<sup>G12V</sup> caused tumors with a three month latency period. The earlier studies of the effect of codon optimization on endogenous *KRAS* expression were done on a colon cancer cell line with a *KRAS*<sup>G13D</sup> mutation; this line depends on *KRAS* expression for tumorigenesis. I used clones of this cell line to compare the effects that a codon optimized knock in of *KRAS*<sup>G13D</sup> has compared to a codon wild type knock in of *KRAS*<sup>G13D</sup>. Again, increased levels of *KRAS* resulted in increased tumorigenesis.

The difference in codon usage between *HRAS* and *KRAS* does result in a difference in *KRAS* expression and function. Could other gene pairs exist that show this same dichotomy in codon usage? With Joey Prinz and David MacAlpine, I was able to identify 37 additional gene pairs that exhibit high homology and at the same time high differences in codon usage. Out of these, twelve gene pairs were tested in transient transfection cellular expression assays; all gene pairs had one member with higher expression and one member with lower expression, exactly as would be predicted by their codon usage. Furthermore, analysis of the gene pairs that exhibit this dichotomy showed that a proportion of them lie within the insulin signaling pathway, more

than would be expected by random chance. This pathway has previously been linked to regulation of translation, including regulation of translation elongation (see 1.3.2 Regulation of Translation Elongation as a Method of Controlling Protein Expression in Mammals). These studies broaden the scope of the finding with RAS and suggest that there may be ways the cell regulates expression of genes with rare codons.

## **5.2 Future Areas of Study Concerning the Role of Codon Usage in the Control of Gene Expression**

Future studies can be divided into two general categories: studies of the effects that KRAS codon usage may have at an organismal level, and studies of pathways that may regulate the translation of rare codon containing genes.

### **5.2.1 Studies of KRAS Codon Usage on an Organismal Level**

As discussed in section 1.1.3.3 Organismal Differences Between the Three RAS Family Members, *KRAS* is important in both development and tumorigenesis. Future studies of mice with a knocked in, optimized *Kras* gene could allow determination of the role that *Kras* codon usage plays in development and tumorigenesis. It is also in these two areas that *KRAS* is different from the other *RAS* isoforms; it is the only *RAS* gene that is embryonic lethal when deleted or when present in a strongly activated form, and it is the most commonly mutated member of the *RAS* family. Studies of knock in mice expressing codon optimized variants of *Kras* can determine if this difference in codon usage may be responsible for some of the differences seen between the *RAS* isoforms at the organismal level.

We have created a knock in mouse with optimization of exon 3 of *Kras*. At the time the targeting strategy was planned, the cell culture studies in HCT116 cells were being initiated and there were no results from these studies to inform design of the mouse. Studies with ectopically

expressed *KRAS* genes indicated that optimizing individual portions of the *KRAS* gene corresponding to exons 1, 2, and 3 did increase KRAS protein (although not to the level seen with KRAS\*); of these exon replacement constructs, for an unknown reason optimization of exon 3 gave the largest increase in protein (Figure 18A). Thus, we designed a mouse in which only exon 3 had been optimized and replaced, an allele designated *Kras<sup>op3</sup>* (Figure 18B). *Kras* is a gene encoded by 188 codons and 564 base pairs. With this mouse, instead of replacing 130 codons and 142 nucleotides as was done with the cDNA knockin constructs, only 27 codons and 33 nucleotides were changed. Successful targeting was verified and sequencing of the full length *Kras* mRNA in these cells indicated the presence of the knockin mutations (Figure 18C). The earliest data to be generated from this knockin mouse are with animals that still have the neomycin resistance cassette in the intron between exons 3 and 4 (designated *Kras<sup>op3neo</sup>*). Thus, this data is confounded by the fact that two items have been changed about the *Kras* locus – the codons used for exon 3 and a neomycin cassette in an intron. However, the data will be presented here with this caveat kept in mind. Studies with a version of the mouse with the neomycin cassette removed are still ongoing.

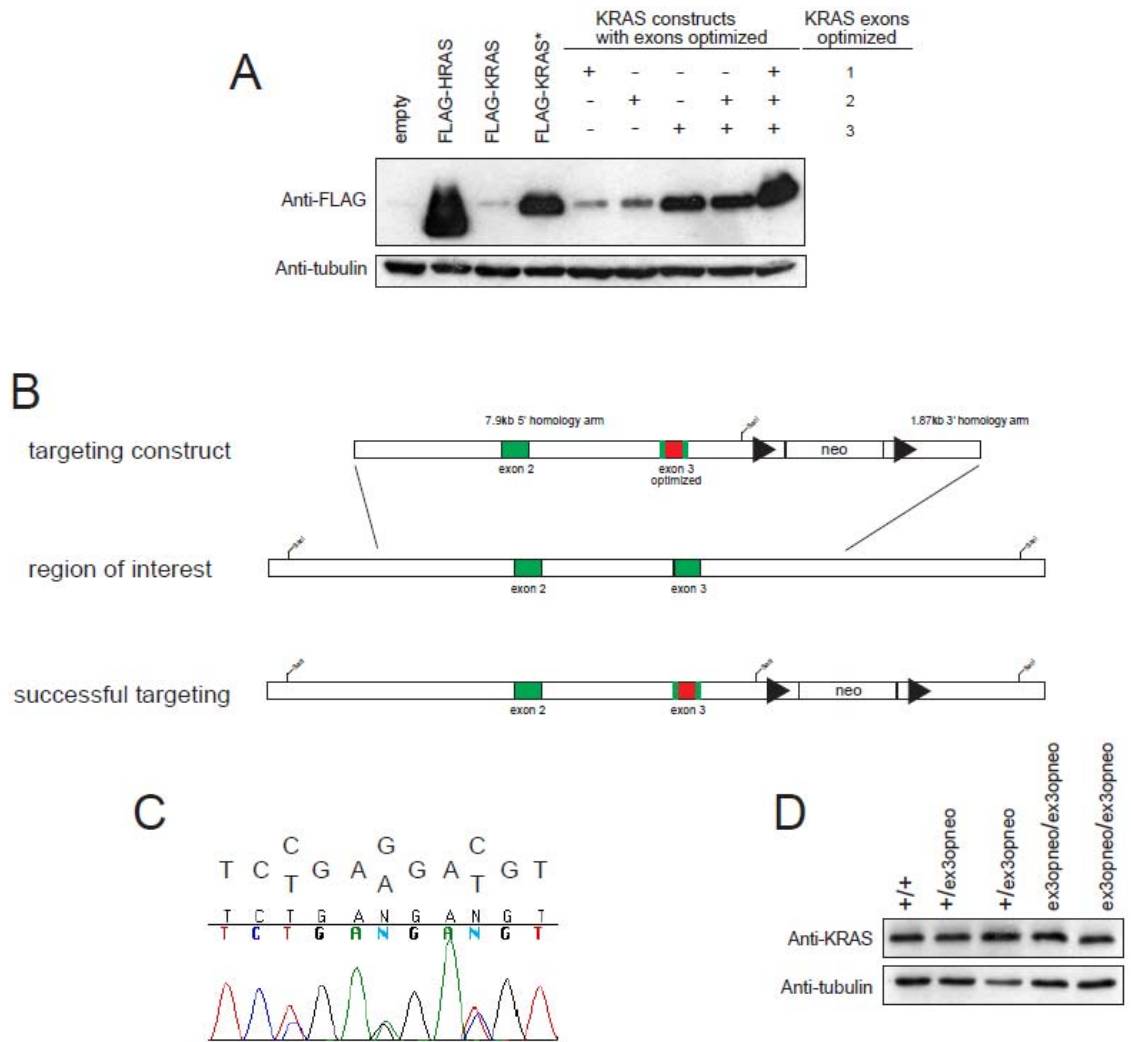


**Figure 18: Exon 3 optimization in the mouse**

(A) Immunoblot of HEK TtH cells expressing KRAS constructs that have the indicated exons optimized. (B) Targeting strategy for creation of the exon 3 optimized mouse. neo, neomycin resistance cassette driven by a PGK promoter with a BGH poly A signal sequence, in the same orientation as the gene. (C) Sequencing analysis of full length KRAS cDNA from a mouse heterozygous for the exon 3 optimized allele, indicating successful targeting. (D) Immunoblot of KRAS in MEFs isolated from mice with the indicated genotypes.

Studies on protein expression in MEFs from the *Kras*<sup>op3neo</sup> mice showed no alteration in KRAS protein levels (Figure 18D). This may be because not enough codons were changed, given that an optimized whole cDNA knockin did elevate KRAS protein levels. Thus, for future studies of *Kras* in tumorigenesis and development, the “next generation” mouse model that should be made is a model that follows the same targeting strategy as the cell-based *KRAS* cDNA knockin approach. Four possible knockin mice include: *Kras* codon optimized cDNA knocked into the *Kras* locus (*Kras*<sup>opcDNA</sup>), *Kras* codon wild-type knocked into the *Kras* locus as a control (*Kras*<sup>wtcDNA</sup>), mutant *Kras*<sup>G12D</sup> codon optimized cDNA knocked into the *Kras* locus behind a lox-stop-lox cassette (*LSL-Kras*<sup>opG12DcDNA</sup>), and mutant *Kras*<sup>G12D</sup> codon wild-type knocked into the *Kras* locus as a control (*LSL-Kras*<sup>wcG12DcDNA</sup>). The first pair will be used for developmental studies, and the second pair for tumorigenesis studies, as described below.

#### 5.2.1.1 The Effects of KRAS Codon Optimization on Murine Development

While humans have been identified with weakly activating oncogenic mutations in *KRAS*, no human has been identified with a strongly activating germline mutation in *KRAS* (Schubbert, Shannon et al. 2007). Patients with weakly activating mutations in *KRAS* exhibit the features of Noonan syndrome, including cardiac abnormalities, craniofacial defects, short stature, and developmental delay (Schubbert, Zenker et al. 2006). Endogenous expression of *Kras*<sup>G12D</sup> in the mouse results in embryonic lethality (E9.5-E11.5); this early lethality is due to dysfunction of the extraembryonic tissue and can be avoided by driving oncogenic *KRAS* expression only in the embryo proper (Shaw, Meissner et al. 2007). This still results in embryonic lethality at a slightly later time point (E14.5), with evidence of cardiac structural defects, fetal liver apoptosis, and blocks in erythroid progenitor cell differentiation (Shaw, Meissner et al. 2007). No experiment

has yet been reported that tests the phenotype of a knock in of a weakly activating *Kras* mutation in mice. However, from the codon usage point of view, a mouse with an *Hras* cDNA knocked into the *Kras* locus has been made (Potenza, Vecchione et al. 2005). While this is knocking a different protein into the locus, it is also similar to knocking a codon optimized *Kras* cDNA into the locus. These *HrasKI* mice display no overt developmental phenotype. Adult (3 month old) mice have hypertension and a dilated cardiomyopathy compared to controls, indicating that *Kras* may play a particularly important role in the cardiovascular system (Potenza, Vecchione et al. 2005).

Given that elevated KRAS activity affects development, *Kras*<sup>opcDNA/+</sup> and *Kras*<sup>opcDNA/opcDNA</sup> mice could have developmental phenotypes if KRAS protein expression is elevated. Embryonic lethality is unlikely because the elevation in KRAS signaling, if there is any, will likely not reach the level of a lethal germline *Kras*<sup>G12D</sup> mutation. Given the phenotypes seen in humans and mice with elevated KRAS activity, the *Kras*<sup>opcDNA</sup> mice could have defects in the following areas: craniofacial features, blood cell counts and morphology, liver structure and function, and cardiovascular structure and function. Molecular characterization of KRAS signaling in fibroblasts from these mice (e.g. elevated responses to stimuli of the RAS pathway) would be useful support for studies that find any developmental difference. As a final note, studies with the *Kras*<sup>op3neo/+</sup> and *Kras*<sup>op3neo/op3neo</sup> mice indicate that they are born at expected Mendelian ratios and exhibit no gross defects, although detailed analysis has not been done.

#### **5.2.1.2 The Effects of KRAS Codon Optimization on Murine Tumorigenesis**

As detailed earlier (see 1.1.5.2 Increased RAS Protein Levels in Cancer), once a cell is fully transformed, elevated RAS protein expression results in more aggressive tumorigenesis.

However, in the early development of cancer, this is not the case. Elevated RAS signaling in a normal cell promotes oncogene induced senescence via hyperactivation of the MAPK pathway, which causes ARF-mediated accumulation of p53 (Serrano, Lin et al. 1997; Lin and Lowe 2001). This has been demonstrated in a model of murine cancer where the levels of an MMTV-driven *Hras*<sup>G12V</sup> transgene could be titrated with varying doses of doxycycline (Sarkisian, Keister et al. 2007). High levels of HRAS<sup>G12V</sup> induced senescence, while low levels did not. This senescence could be bypassed by deleting *Arf*. Interestingly, the tumors that did eventually form in the animals on low dose doxycycline had very high levels of HRAS expression and had inactivated p53. This suggests a multi-step process for RAS dependent tumors: first, gene mutation, then *TP53* mutation, followed by increased gene expression.

The *LSL-Kras*<sup>opG12DcDNA</sup> gene is inactive until specifically turned on in tissues where Cre is expressed, thus avoiding the embryonic lethality associated with strongly activating *Kras* mutations. Cancer studies with this mouse could be done either with the *Pdx-1* promoter driving pancreatic-specific expression or nasally administered adenoviral Cre driving lung expression. Assuming that elevated expression of the optimized transgene can be demonstrated compared to normal controls, it is unknown if the cancer burden in a *LSL-KRAS*<sup>opG13DcDNA</sup> mouse would be larger or smaller. On one hand, higher levels of KRAS typically promote tumorigenesis. On the other hand, higher levels of KRAS expression may cause many potentially tumorigenic cells to enter senescence, and overall cancer burden would be lower. (In the second case, studies to confirm the role of senescence could be completed by crossing the mice into an *Arf*-null background.)

Two experiments have been done that could inform future studies of tumorigenesis in *LSL-Kras*<sup>opG13DcDNA</sup> mice; however, they each offer contradicting results. As mentioned, mice have been created with *Hras* knocked into the *Kras* locus. Mice that were heterozygote at the *Kras*

allele, with one copy of regular *Kras* and one copy of the *HrasKI* gene, were subjected to a urethane chemical carcinogenesis protocol. Urethane causes lung tumors with KRAS Q61L activating mutations. In these animals, there is a “choice;” the RAS mutation can occur in either the *Kras* or the *HrasKI* gene. Ninety two percent of the time, the mutation occurred in the *HrasKI* gene (To, Wong et al. 2008). If knocking *Hras* into the *Kras* locus is interpreted as knocking a codon optimized version of *Kras* into the locus, then the cell “prefers” mutations in the “codon optimized” gene. Alternatively, similar preliminary studies have been done with the *Kras<sup>op3neo</sup>* mice. In this case, the urethane-induced mutation can occur on either the wild type allele or the exon 3 optimized *Kras* allele. One hundred percent of tested tumors (7/7) with a detectable *Kras* mutation had the mutation on the wild type allele. Three possible interpretations include: (1) there is preference for the wild-type allele / avoidance of the optimized allele because of differences in the level of expression (perhaps because of oncogene-induced senescence), (2) there is a preference for the wild-type allele because of the intronic neomycin cassette on the other allele, or (3) there is a preference for the wild-type allele because the synonymous mutations in the optimized exon interfere with its proper splicing. Studies with the *LSL-Kras<sup>opG13DcDNA</sup>* mice can address these shortcomings by directly introducing a mutation into the allele and then assessing the effect on tumor development.

### **5.2.2 Studies of Pathways That May Regulate Expression of Rare Codon Containing Genes**

Rare codons can limit the expression of a gene, but there may be situations where this limitation is eased and the genes containing rare codons are easier to translate. Regulation of an entire class of mRNAs at the step of translation has been described in eukaryotic cells; this is the case for 5' TOP mRNAs (reviewed in Sonenberg, Hershey et al. 2000). Many protein components

of the cellular translation machinery, including ribosomal proteins, eEF1A, poly-A binding protein, and eEF2, are regulated at the level of translation. A common hallmark of these mRNAs is a 5' terminal oligopyrimidine (5' TOP) tract -- a string of 6-15 cytosines and thymidines in the 5' UTR of the message, at or very near the 5' terminus. Through an unknown mechanism, these messages are selectively recruited to polysomes in response to mitogenic stimuli (and also mTOR activation); they are also translationally repressed in cells undergoing growth arrest (Livingstone, Atas et al. 2010). In sum, it is conceivable that the cell would spend resources and energy to maintain a pool of mRNAs defined by sequence motifs whose translational capacity rapidly increases in response to extracellular stimuli. The key is discovering what such a stimulus might be for rare codon containing mRNAs. Here, I discuss ways such a stimulus might be discovered and also the process that might be used to investigate the as-yet-undetermined stimulus.

#### **5.2.2.1 Comparative Quantitative Analysis of mRNA Shifts Upon Polysome Treatment**

One way to identify a stimulus that may regulate expression of rare codon containing genes is to determine if the rare codon containing genes lie in any particular pathway. Then, a stimulus which alters signaling flux through that pathway may also alter rare codon gene expression. This approach reinterprets the task of finding a stimulus as the task of finding signaling pathways. Joey Prinz and David MacAlpine combined two independent variables to reach a concise list of genes; from this list they identified the insulin signaling pathway, among others, as over-represented (discussed in 5.2.2.3 Insulin Control of KRAS Expression). The two independent variables used to create a pathway list were homologous gene pairs and rare codon containing genes. I now propose creating a second list using a different set of

independent variables; following the lead of MacAlpine and Prinz, this list can also be computationally probed to identify statistically over-represented signaling pathways.

The first variable used to create the list will again be rare codon containing genes. The second variable used to create the list will be genes whose mRNAs show only small shifts upon pactamycin treatment of cells. This variable could be determined by SAGE examination of mRNAs contained with each fraction, for example, or any other large scale, unbiased, quantitative method of determining mRNA levels. It will require a computational method of calculating how much the polysome profile of an mRNA skews upon pactamycin treatment. Not all genes with rare codons may be translated poorly. For example, not all mRNAs that contain 5' TOP sequences exhibit the characteristic regulatory control;  $\beta$ 1- and  $\beta$ 2-tubulin exhibit all the characteristics of a 5' TOP mRNA, but yet these messages are constitutively translated, regardless of the external stimuli (Avni, Biberman et al. 1997). Thus, the second biochemical assay can be considered as a purifier on the list of all rare codon containing genes, identifying only those which have rare codons and are translated slowly. The intersection of the lists of rare codon containing genes and the list of genes that do not shift upon pactamycin treatment will create a new catalog of genes. This catalog can then be analyzed for over-representation of particular signaling pathways. Thus, this method can complement the original approach used by MacAlpine and Prinz to functionally identify even more pathways for study; it would be interesting to see if there is overlap between the pathways identified by these independent methodologies.

### 5.2.2.2 Analysis of Ratio of KRAS Protein to KRAS mRNA Ratio in Various Tissues

While there is no data in this thesis to suggest how rare codons work to slow translation of a gene, it may be helpful to consider the example of prokaryotes and lower eukaryotes, where rare codons correspond to tRNAs with low abundance and the process of translation is slowed as ribosomes wait for the proper tRNA to attach to the A site. Mammals are more complex in that they are not single celled organisms and tRNA content may vary from organ to organ. Studies of tRNAs and their relative abundance in mammalian tissues have been difficult because of the high amount of post-transcriptional nucleotide modifications, their strong secondary structures, and the high sequence similarity between tRNAs that nevertheless recognize different codons. A recent study using a fluorescence-based microarray approach was the first to compare the relative tRNA levels in different tissues (Dittmar, Goodenbour et al. 2006). They found that both total tRNA levels and the levels of individual isoacceptors varied broadly from tissue to tissue. For one example, the ovary had relatively high levels of the tRNA that recognizes the two AGC/T serine codons, while the thymus instead had high levels of the tRNA that recognizes the TCG serine codons. The brain had the highest overall levels of tRNAs (Dittmar, Goodenbour et al. 2006). This raises the possibility that certain tissues may be better at translating rare codon mRNAs than other tissues. A block in translation decreases the protein yield per RNA. Finding tissues where the KRAS protein to mRNA ratio is abnormally high – or abnormally low – will serve two purposes. First, it may provide a further indication of what pathways may be important for expression of rare codon containing genes. For example, if the KRAS protein to mRNA ratio is extremely low in the liver, this would be interesting in light of the role of liver in energy metabolism and the identification of the insulin signaling pathway by Prinz and MacAlpine. It would be interesting to see if this ratio then changed upon stimuli that

changed the metabolic state of the animal. The second reason why this analysis is important is that it may identify organs which should be carefully examined for abnormalities in *Kras*<sup>opcDNA</sup> mice. Organs where the protein to mRNA ratio is very low may be particularly sensitive to codon optimization of the *KRAS*.

### 5.2.2.3 Insulin Control of KRAS Expression

The study of homologous gene pairs with codon usage differences identified insulin signaling as a pathway that contains an over-representation of these gene pairs. Other work has previously linked insulin signaling and its downstream effector mTOR to regulation of cellular translation (see 1.3.2 Regulation of Translation Elongation as a Method of Controlling Protein Expression in Mammals). The idea that a nutrient sensing pathway may control translation elongation, a process which can consume large amounts of energy and metabolites (Sonenberg, Hershey et al. 2000), makes teleological sense. Based on the fact that insulin signaling stimulates translation in the other areas of translation that it is known to control (see 1.3.2 Regulation of Translation Elongation as a Method of Controlling Protein Expression in Mammals), one hypothesis is that insulin signaling (which would only happen in nutrient replete conditions) through some unknown process promotes translation particularly of rare codon mRNAs. Since many of these genes lie in the insulin signaling pathway itself, enhanced translation of rare codon containing genes would act as a feed-forward mechanism, creating more signaling molecules to amplify the insulin signal (Figure 19A). This feedback loop is analogous to the increased translation of 5' TOP mRNAs leading to greater synthesis of translational apparatus components. The identification of these genes as members of closely related gene pairs is also

interesting, suggesting that the cell could have duplicate pathways – one for basal level signaling and one to be activated only in times of nutrient abundance (Figure 19B).

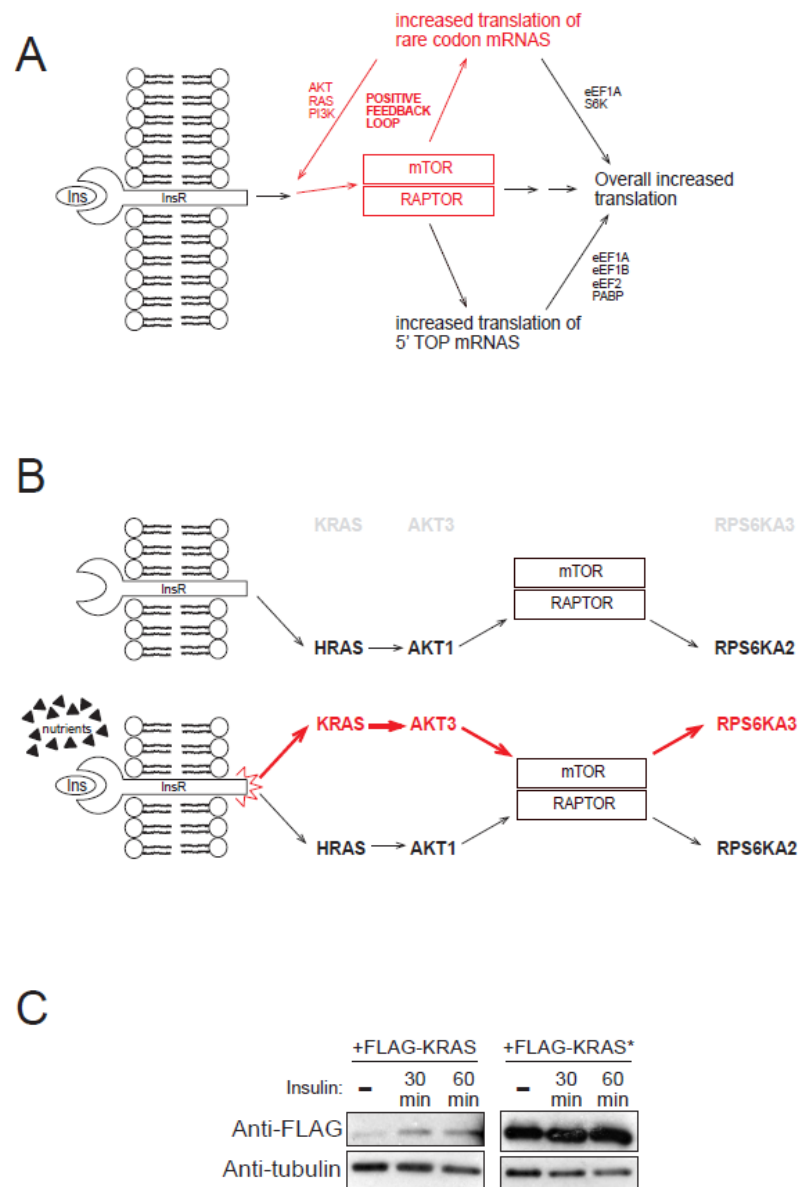


**Figure 19: Possible interactions between insulin signaling pathway and rare codon containing genes**

(A) Diagram of a possible feed-forward loop between rare codon containing genes and the insulin signaling pathway. Some rare codon containing genes also lie downstream of mTOR and promote translation. Note the similarity to 5' TOP mRNAs. (B) Greatly simplified representation of hypothetical dual insulin signaling pathways that may exist within the cell, one pathway involving genes with common codons (lower) and one involving genes with rare codons (upper), which are only synthesized in the presence of insulin and nutrients that can support translation. (C) Immunoblot of ectopic KRAS and KRAS\* expression in HEK TtH cells upon 24 hour serum starvation followed by addition of insulin to the media for the indicated length of time.

The hypothesis that insulin increases translation specifically of rare codon containing genes can be tested. Cells that ectopically express either KRAS or KRAS\* can be serum-starved and then stimulated with insulin; the protein levels of KRAS and KRAS\* before and after insulin stimulation can be compared. Early results of experiments like this are promising (Figure 19C), but more controls are needed. For example, the increase seen in KRAS expression, if due to an increased ability to translate rare codon containing mRNAs, should be actinomycin-independent but cycloheximide-dependent. In other words, the increase should not depend on RNA polymerase II transcription but should depend on the process of translation. Furthermore, if these results are true for *KRAS* because it has rare codons, then they should also be true for other genes that contain rare codons, but not their counterparts that contain common codons. Finally, it would be necessary to see if insulin can specifically impact the translation of endogenous rare codon containing mRNAs. For this experiment, the HCT116 KRas<sup>G13D</sup>wt knock in cell line described above can be exposed to insulin and total KRAS levels assessed as compared to the KRas<sup>G13D</sup>op knock in cell line that has undergone the same treatment. To take these studies even farther, it would then be interesting to assess the biological impact of insulin regulated translation of *KRAS*. Since *KRAS*, but not *KRAS*<sup>G13D</sup>op, may particularly depend on insulin signaling to ensure its translation, cancer cells lines driven by *KRAS* -- but not those driven by *KRAS*<sup>G13D</sup>op -- may be particularly sensitive to inhibitors of insulin signaling (e.g. mTOR inhibitors).

#### **5.2.2.4 Empirical Testing of Other Stimuli That Are Known to Affect Elongation**

If the signaling pathways identified by the methods above do not specifically affect translation elongation of messages containing rare codons, other pathways known to regulate

translation elongation can be empirically explored. Below are two examples of stimuli that regulate the process of translation.

Phorbol esters are known to increase the rate of translation elongation (Traugh 2001). Protein kinase C phosphorylates eEF1A; this stimulates its GDP/GTP exchange activity and thus increases the speed with which it can bind another charged aa-tRNA (Venema, Peters et al. 1991). As a first pass experiment, as described with the insulin studies, cells expressing both KRAS and KRAS\* could be stimulated with phorbol esters and the relative impact on expression levels of the rare codon containing KRAS could be assessed. Since these chemicals activate protein kinase C which affects both transcription and translation (Newton 1995), proper controls must be done to ensure any elevations seen are via modulation of protein synthesis rate.

RNA polymerase III is responsible for transcribing the tRNAs on which protein synthesis depends; it also transcribes the 5S rRNA and other small nuclear RNAs (White 2004). This RNA polymerase depends on two multi-protein complexes for its function. First, TFIIC2 recognizes promoter sequences in RNA polymerase III transcribed genes; second, TFIIB serves as a bridge between TFIIC2 and RNA polymerase III (White 2004). Increased output from the RNA polymerase III machinery is common in cancers, and one way that this is done is through overexpression of the TFIIC2 and TFIIB complexes (White 2004). Overexpression of just a single part of TFIIB, the protein BRF1, has been shown to increase RNA polymerase III activity (particularly its output of tRNAs) and to be sufficient for transformation (see 1.3.2 Regulation of Translation Elongation as a Method of Controlling Protein Expression in Mammals) (Marshall, Kenneth et al. 2008). Overactivity of the RNA polymerase III machinery may specifically facilitate translation of rare codon containing mRNAs, because only for these mRNAs might translation

elongation be rate-limiting. A simple experiment would be to express BRF1 in cells and assess respective effects on KRAS and KRASop levels.

### 5.2.3 Studies of Other Rare-Codon Containing Gene Pairs

Codon usage may regulate many other genes besides *KRAS*. We have identified many other interesting homologous gene pairs that contain one member with rare codons and one without. Some of these genes may be explored in future studies that essentially follow the format used in the *RAS* studies.

*PRL1* and *PRL3* are two lipidated protein tyrosine phosphatases that are 79% identical. *PRL1* has many rare codons while *PRL3* does not; the GC3 log ratio for these genes is 1.39 (compared to the *RAS* gene pair where the GC3 log ratio is 1.28). These genes are 522 base pairs in size, smaller than *RAS*. I have demonstrated that expression of these genes is different, as expected by their codon usage differences, and the low level of *PRL1* can be rescued by codon optimization (Figure 20). Furthermore, the protein levels of these genes are important in cancer. A study of 18 colorectal cancer liver metastases demonstrated that *PRL3* was the only gene overexpressed in 100% of the metastatic samples but not normal tissue or the primary cancers; in three of the cases, this was due to gene amplification (Saha, Bardelli et al. 2001). Overexpression of both *PRL1* and *PRL3* in chinese hamster ovary cells gave the cells metastatic potential in nude mice as assessed by tail vein injections, with more lung metastases forming in *PRL3* expressing cells than their *PRL1* counterparts (Zeng, Dong et al. 2003). Since codon usage controls relative expression levels of *PRL1* and *PRL3*, and overexpression of the *PRL* genes promotes a metastatic phenotype, codon usage may have an effect on the biological readout of metastasis.

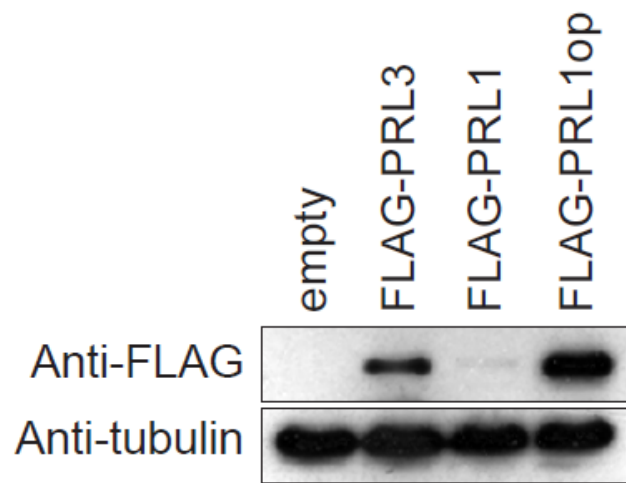


**Figure 20: Relative expression of PRL genes**

Immunoblot demonstrating relative levels of PRL3, PRL1, and a codon optimized PRL1 gene in 293 cells transiently transfected with pBabe vectors containing these constructs.

Another gene pair identified contains calmodulin 3 and calmodulin 2. These 450 base pair genes are 100% identical with a GC3 log ratio of 1.23. They exhibit almost the maximum theoretical possible difference in codon usage given the constraint that they still encode for the same protein (Toutenhoofd and Strehler 2000); furthermore, they also have completely divergent 5' and 3' UTRs (Toutenhoofd and Strehler 2000). Cells with artificially elevated levels of calmodulin proliferate faster, due to faster progression through G1 and mitosis (Means and Rasmussen 1988; Rasmussen and Means 1989). This indicates that if a difference in protein level could be demonstrated, a biological phenotype will be likely. Study of these genes, however, may be hindered by technical difficulties. Immunoblotting for calmodulin – a highly charged, small protein – is difficult, and endogenous cellular calmodulin levels are already quite high, so it may be difficult to detect an increase.

Finally, instead of trying to increase the expression of a rare codon containing gene, it may be informative to deoptimize a gene which contains mostly optimal codons, e.g. one of the histone genes. Many histone genes exhibit very high usage of optimal codons. A phenotype is possible if codon deoptimization can decrease levels of one of these critically important genes.

### **5.3 Summary of Studies on the Role of eNOS in a Spontaneous Murine Model of Tumorigenesis**

Genetically engineered mouse models of pancreatic cancer have recently been developed that faithfully recapitulate the genetics, clinical syndrome, histopathology, metastatic profile, and refractoriness to treatment of the human disease. Furthermore, the response to chemotherapy in these models is similar to responses seen in human clinical trials (Singh, Lima et al. 2010), suggesting that testing of novel drugs in these models could be a valuable preclinical step. Previous work identified eNOS as a necessary target of KRAS in xenograft

models of cancer (Lim, Ancrile et al. 2008). Studies within this thesis attempt to bring this work closer to the clinic in two ways: first, by testing the requirement for eNOS in a spontaneously arising model of KRAS-driven pancreatic cancer, and second, by testing whether a small molecule inhibitor of NOS enzymes has any anti-cancer effect.

Two models of genetically engineered pancreatic cancer were examined. The KC model is driven by the expression of oncogenic KRAS<sup>G12D</sup> solely in the pancreas, under its endogenous promoter; early preinvasive PanIN lesions result. The KPC model adds a pancreatic-specific dominant negative mutation in p53; advanced ductal adenocarcinoma and lethality results. eNOS expression increases during the development of disease, consistent with earlier studies that found phosphorylated eNOS was elevated in pancreatic cancer specimens but not matched normal tissue (Lim, Ancrile et al. 2008). eNOS in the normal pancreas is limited to the endothelial cells. Early stage PanIN-1 lesions and late stage adenocarcinomas stain positive for eNOS; corroborating this data, cultured adenocarcinoma cells are positive for eNOS by RT-PCR.

We then crossed *eNOS* knockout alleles into the KC and KPC mouse model to assess the effect that *eNOS* gene ablation had on pancreatic cancer development and mortality. We found that ablation of the *eNOS* gene did indeed retard development of early pancreatic lesions, roughly doubling the amount of total normal pancreatic tissue and also the number of normal pancreatic ducts that remained in these mice at 11 months of age. This was also accompanied by a reduction in the off-target facial and vulvar papillomas in these mice, indicating that *eNOS* ablation may have effectiveness in a wide variety of spontaneously arising KRAS-driven tumors. These results were extended to the KPC model of lethal pancreatic adenocarcinoma; *eNOS* ablation extended lifespan by about 25% in these mice, although the effect did not reach significance ( $P = 0.093$ ), partly due the wide variation in life span of KPC mice.

To see if pharmacologic inhibition of eNOS could also have a beneficial effect in the treatment of pancreatic cancer, we then repeated the previous studies in both mouse models using a small molecule inhibitor of eNOS, L-NAME. This drug is relatively non-toxic (mice were treated with L-NAME for up to eleven months), orally dosed, and has been used in phase II clinical trials in humans. However, it is a general NOS inhibitor and does inhibit iNOS and nNOS in addition to eNOS. In general, the drug had a positive effect on all pancreatic cancer readouts tested, but these effects were less than that of complete *eNOS* knockout and did not always reach significance. In the KC mice, there was a 3% increase in normal pancreatic tissue and a 1.7-fold increase in normal pancreatic ducts remaining at the fixed time point of 11 months. In the KPC mice, there was a 13% increase in median survival with L-NAME treatment ( $P = 0.208$ ). Experiments done by Disean Kendall and Meghan Morrison show that these effects may extend to human cancers, as an anti-tumor effect of L-NAME was also seen in human cancer xenografts, typically cutting the tumor burden in half. Treatment with an anti-hypertensive, as might be done in the clinic, did not abrogate L-NAME's anti-tumor effect in this setting.

These studies confirm that eNOS is a novel target in treating pancreatic cancer, but also show that more efficacious eNOS inhibitors are needed to achieve the maximum benefit of this therapeutic strategy. Furthermore, while these studies use a clinically relevant compound in a cancer model that recapitulates the human disease, they do not use a dosing strategy that would be used in the clinic. Mice in these studies were dosed with L-NAME from the age of weaning until the endpoint of the experiment; humans would start dosing at a much later point in the disease. The future directions below address these deficiencies.

## **5.4 Future Areas of Study on the Role of eNOS in KRAS-Driven Tumorigenesis**

The ultimate goal of these studies is to introduce into the clinic an efficacious new therapeutic option for pancreatic cancer. Here, I discuss some future experiments that, if completed, can inform the design of a clinical trial testing the effects of NOS inhibition on human disease, potentially increasing the chances that such a clinical trial would be successful.

### **5.4.1 Testing of L-NAME in Combination with Front-Line Therapy**

The results of xenograft studies, both those in Lim et al. (Lim, Ancrile et al. 2008) and those presented here, support a chemotherapeutic role for eNOS and L-NAME. The studies in the murine pancreatic cancer models, however, do not distinguish the chemotherapeutic versus chemopreventative roles that *eNOS* knockout and L-NAME might have. Animals are missing eNOS from birth, or are administered L-NAME from weaning. Thus, the studies in the spontaneous cancer models do not recapitulate treatment in the clinic.

Additionally, in human patients, L-NAME will not be tested as a monotherapy in the treatment of pancreatic cancer. The current frontline standard of care for non-resectable pancreatic cancer is gemcitabine (Burriss, Moore et al. 1997); therefore, an initial clinical trial in humans would likely test gemcitabine versus L-NAME plus gemcitabine in subjects presenting with a new diagnosis of pancreatic cancer. These two arms are currently being tested in the KPC mice.

At 100 days of age, approximately 50% of the KPC mice will be dead within one month from pancreatic cancer. Therefore, this time point was chosen as the time to initiate treatment, as mice at this age likely have a spectrum of disease ranging from nearly lethal cancer to newly developing cancer. (It may be helpful to perform a necropsy on a cohort of animals at this time

point to determine what the spectrum of disease burden actually is.) At the 100 day time point, mice undergo a single two week cycle of gemcitabine treatment, a commonly used regimen that corresponds to what is used in humans (Singh, Lima et al. 2010). After these two weeks, L-NAME is started to avoid any drug-drug pharmacokinetic interactions that may confound interpretation of the results. Cohort sizes in this study are increased from the initial survival studies in KPC mice to enhance statistical power. This study testing L-NAME versus placebo in combination with front-line therapy in mice with adenocarcinoma attempts to emulate the predicted design of such a trial in humans.

#### **5.4.2 Development of a Specific eNOS Inhibitor**

In all of the models tested here, and in many different cancer models tested elsewhere (see 1.2.4 Role of eNOS in Cancer), specific inhibition of eNOS has consistently been shown to reduce tumorigenesis. This suggests that a specific eNOS inhibitor with greater efficacy than L-NAME may be a useful anti-cancer drug in a variety of different settings.

While specific eNOS inhibitors do not currently exist, this likely reflects lack of a reason to develop them as opposed to technical impediments to their development. Crystal structure studies indicate that the binding pocket of eNOS and iNOS are nearly identical, but that inhibitors with side chains that extend out of the binding pocket may be able to distinguish between the two (Fischmann, Hruza et al. 1999). In fact, a compound with >4000-fold selectivity for iNOS over eNOS, and ~30-fold selectivity for iNOS over nNOS, has been developed (Garvey, Oplinger et al. 1997; Alderton, Cooper et al. 2001), suggesting that potent, efficacious inhibitors that target only a single NOS enzyme can be designed.

### 5.4.3 Identify and Inhibit the Other Targets of L-NAME

In addition to the studies of L-NAME in wild-type mice, the effect of L-NAME in *eNOS*<sup>-/-</sup> mice was also assessed. This addresses concerns that any effects seen with L-NAME may be due to inhibition of the other NOS isoforms, since L-NAME is a non-specific inhibitor. Surprisingly, in all tested tumor assays, L-NAME combined with *eNOS* knockout to give a greater anti-tumor effect than either *eNOS* knockout or L-NAME treatment alone. Some data shown earlier in the thesis will be repeated here to facilitate comparison of the L-NAME treated, *eNOS*<sup>-/-</sup> mice with the other treatment groups.

*eNOS*<sup>-/-</sup> KPC mice treated with L-NAME are the only group to show a statistically significant increase in survival compared to the control group (Figure 21A). This group had a survival increase of 42 days over untreated controls ( $P = 0.011$ , HR = 0.575, CI<sub>95</sub> = 0.341-0.968), more than either the *eNOS*<sup>-/-</sup> KPC or L-NAME treated KPC mice. Furthermore, in the KC model, the genetic loss of *eNOS* combined with L-NAME treatment resulted in 52.9% of the normal tissue remaining in the pancreas, a significant fourfold increase in normal ducts, and a significant decrease in PanIN lesions per lobule (Figure 21B). Specifically, the percent normal tissue remaining *above control* was 3.5% in L-NAME treated KC mice and 19.2% in *eNOS*<sup>-/-</sup> KC mice, but 35.9% in *eNOS*<sup>-/-</sup> + L-NAME-treated mice. Similarly, the percent normal ducts remaining *above control* was 3.9% in L-NAME treated KC mice and 5.6% in *eNOS*<sup>-/-</sup> KC mice, but 14.4% in *eNOS*<sup>-/-</sup> + L-NAME-treated mice (Figure 21C).

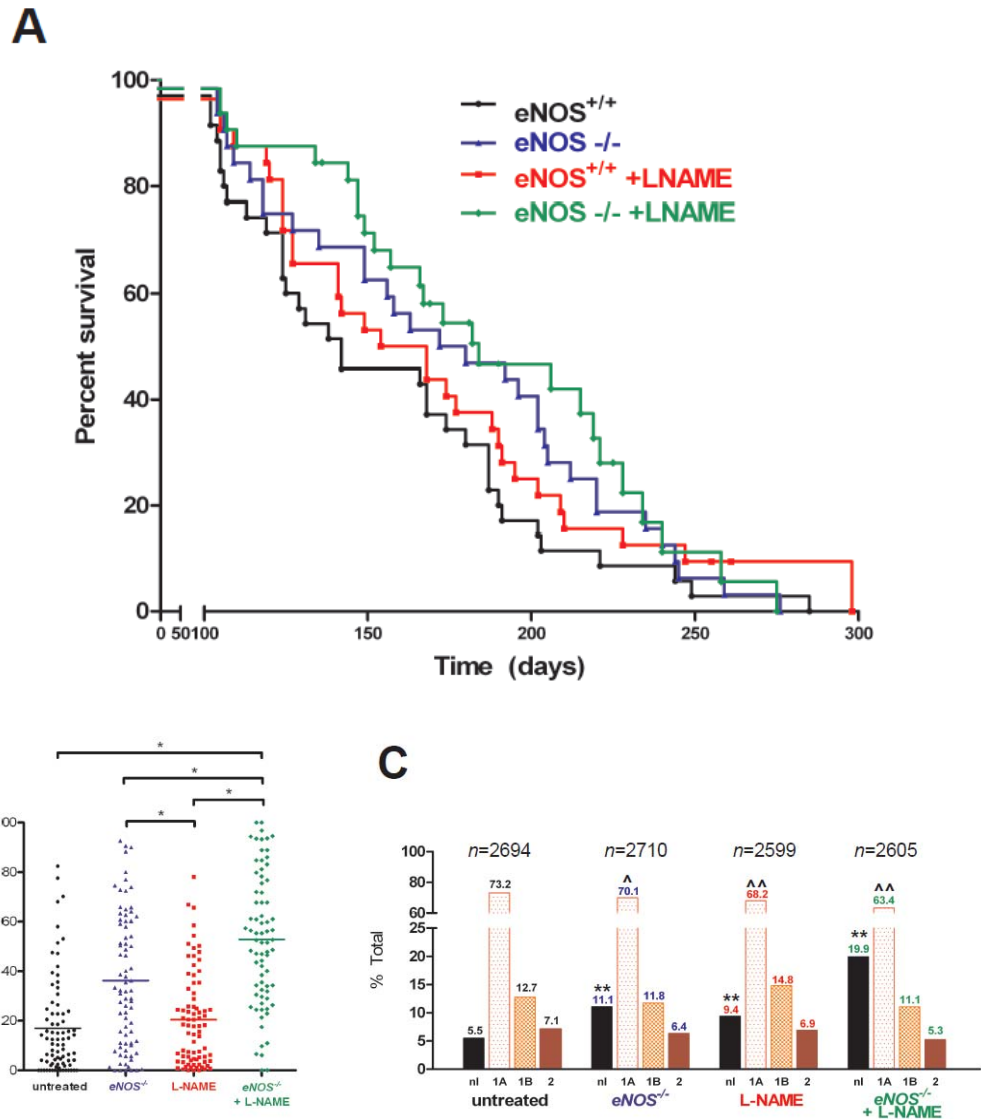


**Figure 21: Effects of L-NAME Treatment in *eNOS*<sup>-/-</sup> Mice**

(A) Kaplan-Meier survival curve of cohorts of KPC *eNOS*<sup>-/-</sup> mice (green) compared to previously shown survival curves of wild type, *eNOS*<sup>-/-</sup>, and L-NAME treated wild type mice. (B) Blind assessment of normal remaining pancreatic tissue on five random high power fields from sixteen mice. Bar, mean % normal acini. \**P*<0.001. (C) Percent of lobules with the highest grade lesion being normal duct (nl), PanIN-1A (1A), PanIN-1B (1B), or PanIN-2 (2) in wild-type, L-NAME treated, *eNOS*<sup>-/-</sup> or *eNOS*<sup>-/-</sup> treated with L-NAME mice. *n*, total number of lobules graded from the 13 mice in each group. \*\**P*<0.0001 normal versus abnormal ducts compared to untreated. ^*P*<0.05 or ^^*P*<0.0001 PanIN-1A versus all other ducts compared to untreated. Disease Kendall quantified the normal remaining acinar area depicted in (B), and Michael Shealy and Diana Cardona graded the ductal lesions quantified in (C).

This finding indicates that L-NAME has other targets which may be exploited to augment the anti-tumor effects of eNOS inhibition. The two other NOS isoforms that L-NAME inhibits, nNOS and iNOS, are the leading candidates in this regard. Of note, iNOS is important for tumor immune surveillance and high levels of iNOS can be directly toxic to tumor cells (Crowell, Steele et al. 2003; Fukumura, Kashiwagi et al. 2006), but conversely iNOS inhibitors also decrease tumor growth in a hamster model of chemically induced pancreatic carcinogenesis (Takahashi, Kitahashi et al. 2008), and *iNOS*<sup>-/-</sup> mice are resistant to chemically induced lung carcinogenesis characterized by *Kras* mutations (Kisley, Barrett et al. 2002).

Tumor development in the following groups of mice (in either the KC or KPC model) could be compared to determine if inhibition of iNOS or nNOS can phenocopy the beneficial combination effect of L-NAME seen in *eNOS*<sup>-/-</sup> mice: *eNOS*<sup>-/-</sup> plus L-NAME treatment, *eNOS*<sup>-/-</sup> *iNOS*<sup>-/-</sup> combination, *eNOS*<sup>-/-</sup> *iNOS*<sup>-/-</sup> plus L-NAME, *eNOS*<sup>-/-</sup> *nNOS*<sup>-/-</sup>, and *eNOS*<sup>-/-</sup> *nNOS*<sup>-/-</sup> plus L-NAME. Such a study would be lengthy and require extensive breeding; we are currently looking for other models of KRAS-driven pancreatic cancer that can recapitulate the combination effect. In cell culture models neither eNOS knockdown nor L-NAME treatment has an effect on cellular proliferation, thus this approach is not useful for investigation of the combination effect. We have isolated tumor cells lines from the KPC *eNOS*<sup>-/-</sup> mice and demonstrated that these lines form subcutaneous tumors in wild type or *eNOS*<sup>-/-</sup> hosts, resulting in a subcutaneous xenograft model of *eNOS*<sup>-/-</sup> pancreatic cancer cells in an *eNOS*<sup>-/-</sup> host. It remains to be seen if L-NAME will have an effect in this model and thus make it a path for investigation of the combination effect. We are currently in the process of developing shRNAs to target the other NOS isoforms in these cells, but even without these reagents, specific pharmacologic inhibition of each of the other NOS enzymes (which is possible for iNOS and nNOS) could be used. In sum, we are actively

looking for simpler models which recapitulate the finding that L-NAME still has an effect on cancer growth when eNOS is absent. If such a model cannot be found, then another experiment with the genetically engineered mice can be done, with either genetic or pharmacologic inhibition of the other NOS isoforms. Once the other target of L-NAME is identified, drugs that block it can be combined with a potent, specific eNOS inhibitor to hopefully have a large therapeutic effect when treating pancreatic cancer.

#### **5.4.4 Identify the Mechanism by which eNOS Inhibits Tumor Growth**

Given the previous studies of eNOS in cancer (see 1.2.4 Role of eNOS in Cancer), we can put forth at least three putative, non-exclusive mechanisms that may explain why eNOS inhibition slows cancer growth: (1) eNOS may have pro-proliferative, anti-apoptotic effects, possibly by amplifying RAS pathway signaling, (2) eNOS knockout may negatively impact tumor angiogenesis, (3) eNOS knockout may be toxic to a subpopulation of Notch-expressing tumor stem cells. The third possibility is less likely, given that it was discovered in gliomas, and the literature on pancreatic cancer stem-like cells suggests that these cells depend on the hedgehog pathway (Li, Heidt et al. 2007).

The identification of mechanism of action has been difficult because the phenotype is only seen *in vivo*; L-NAME treatment has no effect on cellular proliferation in culture. Ki67 and TUNEL staining of tumors from wild type, *eNOS*<sup>-/-</sup>, and L-NAME treated KC and KPC mice are being examined to see if they exhibit any differences in proliferation or apoptosis. To determine if tumors in KC and KPC *eNOS*<sup>-/-</sup> or L-NAME treated animals have reduced vasculature, CD31 staining will also be quantified. However, even this approach may not yield answers. Tumors are isolated from KPC mice that have reached a mortality endpoint; at this late stage, any effect that

eNOS may have had early in tumor development could be masked. As such, it may also help to examine CD31, Ki67, and TUNEL staining in xenograft tumors expressing a doxycycline-inducible form of eNOS shRNA, comparing these three markers before and after eNOS knockdown.

The hypothesis that eNOS has pro-proliferative or anti-apoptotic effects may imply that eNOS plays a cell intrinsic role in tumor development (see 1.2.4.1 eNOS Mediates RAS Signaling); the hypothesis that eNOS has antiangiogenic effects may imply that eNOS plays a cell extrinsic role in tumor development (see 1.2.4.2 eNOS Mediates Angiogenesis). To distinguish between these two hypotheses, mice with tissue-specific eNOS knockout will be informative; these are currently being constructed.

## 5.5 Concluding Remarks

These studies on oncogenic KRas expression and signaling arrive at two conclusions. First, the translation of *KRAS* mRNA is slow due to the usage of rare codons within the transcript. This phenomenon is seen on both exogenously and endogenously expressed *KRAS* genes and limits tumorigenesis driven by oncogenic KRAS. Second, eNOS inhibition, both genetically and pharmacologically, is anti-tumorigenic in multiple models of pancreatic cancer.

The ultimate goal of these studies is to alleviate human disease caused by KRAS. Identification of methods by which KRAS protein is synthesized brings this goal closer, as this could identify pathways that control KRAS protein synthesis and thus elucidate novel, unique targets to block KRAS signaling. Confirmation of eNOS as a therapeutic target also brings this goal closer, as such studies support the development of eNOS inhibitors as novel signal transduction inhibitors to be used for the treatment of pancreatic cancer.

## References

- Adams, C. P. and V. V. Brantner (2006). "Estimating the cost of new drug development: is it really 802 million dollars?" Health Aff (Millwood) **25**(2): 420-428.
- Agrawal, A. G. and R. R. Somani (2009). "Farnesyltransferase inhibitor as anticancer agent." Mini Rev Med Chem **9**(6): 638-652.
- Aguirre, A. J., N. Bardeesy, et al. (2003). "Activated Kras and Ink4a/Arf deficiency cooperate to produce metastatic pancreatic ductal adenocarcinoma." Genes Dev **17**(24): 3112-3126.
- Aguirre, A. J., C. Brennan, et al. (2004). "High-resolution characterization of the pancreatic adenocarcinoma genome." Proc Natl Acad Sci U S A **101**(24): 9067-9072.
- Aicher, A., C. Heeschen, et al. (2003). "Essential role of endothelial nitric oxide synthase for mobilization of stem and progenitor cells." Nat Med **9**(11): 1370-1376.
- Akashi, H. (2003). "Translational selection and yeast proteome evolution." Genetics **164**(4): 1291-1303.
- Akhand, A. A., M. Pu, et al. (1999). "Nitric oxide controls src kinase activity through a sulfhydryl group modification-mediated Tyr-527-independent and Tyr-416-linked mechanism." J Biol Chem **274**(36): 25821-25826.
- Akuzawa, N., T. Nakamura, et al. (1998). "Antihypertensive agents prevent nephrosclerosis and left ventricular hypertrophy induced in rats by prolonged inhibition of nitric oxide synthesis." Am J Hypertens **11**(6 Pt 1): 697-707.
- Alberts, B., J. H. Wilson, et al. (2008). Molecular biology of the cell. New York, Garland Science.
- Alderton, W. K., C. E. Cooper, et al. (2001). "Nitric oxide synthases: structure, function and inhibition." Biochem J **357**(Pt 3): 593-615.
- Alexander, J. H., H. R. Reynolds, et al. (2007). "Effect of tilarginine acetate in patients with acute myocardial infarction and cardiogenic shock: the TRIUMPH randomized controlled trial." JAMA **297**(15): 1657-1666.

- Almoguera, C., D. Shibata, et al. (1988). "Most human carcinomas of the exocrine pancreas contain mutant c-K-ras genes." Cell **53**(4): 549-554.
- Andrews, S., D. R. Snowflack, et al. (2011). "Multiple mechanisms collaborate to repress nanos translation in the Drosophila ovary and embryo." RNA **17**(5): 967-977.
- Aoki, Y., T. Niihori, et al. (2005). "Germline mutations in HRAS proto-oncogene cause Costello syndrome." Nat Genet **37**(10): 1038-1040.
- Aota, S. and T. Ikemura (1986). "Diversity in G + C content at the third position of codons in vertebrate genes and its cause." Nucleic Acids Res **14**(16): 6345-6355.
- Arena, S., C. Isella, et al. (2007). "Knock-in of oncogenic Kras does not transform mouse somatic cells but triggers a transcriptional response that classifies human cancers." Cancer Res **67**(18): 8468-8476.
- Armbruster, B. N., S. S. Banik, et al. (2001). "N-terminal domains of the human telomerase catalytic subunit required for enzyme activity in vivo." Mol Cell Biol **21**(22): 7775-7786.
- Avni, D., Y. Biberman, et al. (1997). "The 5' terminal oligopyrimidine tract confers translational control on TOP mRNAs in a cell type- and sequence context-dependent manner." Nucleic Acids Res **25**(5): 995-1001.
- Avontuur, J. A., S. L. Buijk, et al. (1998). "Distribution and metabolism of N(G)-nitro-L-arginine methyl ester in patients with septic shock." Eur J Clin Pharmacol **54**(8): 627-631.
- Avontuur, J. A., R. P. Tutein Nolthenius, et al. (1998). "Prolonged inhibition of nitric oxide synthesis in severe septic shock: a clinical study." Crit Care Med **26**(4): 660-667.
- Bachmann, S., H. M. Bosse, et al. (1995). "Topography of nitric oxide synthesis by localizing constitutive NO synthases in mammalian kidney." Am J Physiol **268**(5 Pt 2): F885-898.
- Barbacid, M. (1987). "ras genes." Annu Rev Biochem **56**: 779-827.

- Bashyam, M. D., R. Bair, et al. (2005). "Array-based comparative genomic hybridization identifies localized DNA amplifications and homozygous deletions in pancreatic cancer." Neoplasia **7**(6): 556-562.
- Baylis, C., B. Mitruka, et al. (1992). "Chronic blockade of nitric oxide synthesis in the rat produces systemic hypertension and glomerular damage." J Clin Invest **90**(1): 278-281.
- Bellacosa, A., D. de Feo, et al. (1995). "Molecular alterations of the AKT2 oncogene in ovarian and breast carcinomas." Int J Cancer **64**(4): 280-285.
- Benencia, F., M. C. Courreges, et al. (2001). "Effect of aminoguanidine, a nitric oxide synthase inhibitor, on ocular infection with herpes simplex virus in Balb/c mice." Invest Ophthalmol Vis Sci **42**(6): 1277-1284.
- Benhar, M., M. T. Forrester, et al. (2009). "Protein denitrosylation: enzymatic mechanisms and cellular functions." Nat Rev Mol Cell Biol **10**(10): 721-732.
- Bivona, T. G., S. E. Quatela, et al. (2006). "PKC regulates a farnesyl-electrostatic switch on K-Ras that promotes its association with Bcl-XL on mitochondria and induces apoptosis." Mol Cell **21**(4): 481-493.
- Blundell, T. L., B. L. Sibanda, et al. (2006). "Structural biology and bioinformatics in drug design: opportunities and challenges for target identification and lead discovery." Philos Trans R Soc Lond B Biol Sci **361**(1467): 413-423.
- Bos, J. L. (1989). "ras oncogenes in human cancer: a review." Cancer Res **49**(17): 4682-4689.
- Bria, E., M. Milella, et al. (2007). "Gemcitabine-based combinations for inoperable pancreatic cancer: have we made real progress? A meta-analysis of 20 phase 3 trials." Cancer **110**(3): 525-533.
- Browne, G. J. and C. G. Proud (2002). "Regulation of peptide-chain elongation in mammalian cells." Eur J Biochem **269**(22): 5360-5368.
- Brummelkamp, T. R., R. Bernards, et al. (2002). "Stable suppression of tumorigenicity by virus-mediated RNA interference." Cancer Cell **2**(3): 243-247.

- Bucci, M., J. P. Gratton, et al. (2000). "In vivo delivery of the caveolin-1 scaffolding domain inhibits nitric oxide synthesis and reduces inflammation." Nat Med **6**(12): 1362-1367.
- Burgess-Brown, N. A., S. Sharma, et al. (2008). "Codon optimization can improve expression of human genes in Escherichia coli: A multi-gene study." Protein Expr Purif **59**(1): 94-102.
- Burns, C. C., J. Shaw, et al. (2006). "Modulation of poliovirus replicative fitness in HeLa cells by deoptimization of synonymous codon usage in the capsid region." J Virol **80**(7): 3259-3272.
- Burris, H. A., 3rd, M. J. Moore, et al. (1997). "Improvements in survival and clinical benefit with gemcitabine as first-line therapy for patients with advanced pancreas cancer: a randomized trial." J Clin Oncol **15**(6): 2403-2413.
- Camp, E. R., A. Yang, et al. (2006). "Roles of nitric oxide synthase inhibition and vascular endothelial growth factor receptor-2 inhibition on vascular morphology and function in an in vivo model of pancreatic cancer." Clin Cancer Res **12**(8): 2628-2633.
- Campbell, L. E., X. Wang, et al. (1999). "Nutrients differentially regulate multiple translation factors and their control by insulin." Biochem J **344 Pt 2**: 433-441.
- Cannarozzi, G., N. N. Schraudolph, et al. (2010). "A role for codon order in translation dynamics." Cell **141**(2): 355-367.
- Carlberg, U., A. Nilsson, et al. (1990). "Functional properties of phosphorylated elongation factor 2." Eur J Biochem **191**(3): 639-645.
- Carlini, D. B. (2004). "Experimental reduction of codon bias in the Drosophila alcohol dehydrogenase gene results in decreased ethanol tolerance of adult flies." J Evol Biol **17**(4): 779-785.
- Carlini, D. B. and W. Stephan (2003). "In vivo introduction of unpreferred synonymous codons into the Drosophila Adh gene results in reduced levels of ADH protein." Genetics **163**(1): 239-243.

- Carr-Schmid, A., N. Durko, et al. (1999). "Mutations in a GTP-binding motif of eukaryotic elongation factor 1A reduce both translational fidelity and the requirement for nucleotide exchange." J Biol Chem **274**(42): 30297-30302.
- Carr-Schmid, A., L. Valente, et al. (1999). "Mutations in elongation factor 1beta, a guanine nucleotide exchange factor, enhance translational fidelity." Mol Cell Biol **19**(8): 5257-5266.
- Cartegni, L., S. L. Chew, et al. (2002). "Listening to silence and understanding nonsense: exonic mutations that affect splicing." Nat Rev Genet **3**(4): 285-298.
- Cattan, N., T. Saison-Behmoaras, et al. (2000). "Screening of human bladder carcinomas for the presence of Ha-ras codon 12 mutation." Oncol Rep **7**(3): 497-500.
- Cepero, V., J. R. Sierra, et al. (2010). "MET and KRAS gene amplification mediates acquired resistance to MET tyrosine kinase inhibitors." Cancer Res **70**(19): 7580-7590.
- Chamary, J. V. and L. D. Hurst (2005). "Evidence for selection on synonymous mutations affecting stability of mRNA secondary structure in mammals." Genome Biol **6**(9): R75.
- Chamary, J. V., J. L. Parmley, et al. (2006). "Hearing silence: non-neutral evolution at synonymous sites in mammals." Nat Rev Genet **7**(2): 98-108.
- Charles, N., T. Ozawa, et al. (2010). "Perivascular nitric oxide activates notch signaling and promotes stem-like character in PDGF-induced glioma cells." Cell Stem Cell **6**(2): 141-152.
- Chen, X., N. Mitsutake, et al. (2009). "Endogenous expression of Hras(G12V) induces developmental defects and neoplasms with copy number imbalances of the oncogene." Proc Natl Acad Sci U S A **106**(19): 7979-7984.
- Cheng, J. Q., A. K. Godwin, et al. (1992). "AKT2, a putative oncogene encoding a member of a subfamily of protein-serine/threonine kinases, is amplified in human ovarian carcinomas." Proc Natl Acad Sci U S A **89**(19): 9267-9271.

- Cheung, B. H., F. Arellano-Carbajal, et al. (2004). "Soluble guanylate cyclases act in neurons exposed to the body fluid to promote *C. elegans* aggregation behavior." Curr Biol **14**(12): 1105-1111.
- Chevallier, A. and J. P. Garel (1979). "Studies on tRNA adaptation, tRNA turnover, precursor tRNA and tRNA gene distribution in *Bombyx mori* by using two-dimensional polyacrylamide gel electrophoresis." Biochimie **61**(2): 245-262.
- Chin, L., A. Tam, et al. (1999). "Essential role for oncogenic Ras in tumour maintenance." Nature **400**(6743): 468-472.
- Cho, D. H., T. Nakamura, et al. (2009). "S-nitrosylation of Drp1 mediates beta-amyloid-related mitochondrial fission and neuronal injury." Science **324**(5923): 102-105.
- Cho, K. R. and B. Vogelstein (1992). "Suppressor gene alterations in the colorectal adenoma-carcinoma sequence." J Cell Biochem Suppl **16G**: 137-141.
- Cobbs, C. S., J. E. Brenman, et al. (1995). "Expression of nitric oxide synthase in human central nervous system tumors." Cancer Res **55**(4): 727-730.
- Cohen, S. J., L. Ho, et al. (2003). "Phase II and pharmacodynamic study of the farnesyltransferase inhibitor R115777 as initial therapy in patients with metastatic pancreatic adenocarcinoma." J Clin Oncol **21**(7): 1301-1306.
- Coleman, J. R., D. Papamichail, et al. (2008). "Virus attenuation by genome-scale changes in codon pair bias." Science **320**(5884): 1784-1787.
- Cooper, C. E. (1999). "Nitric oxide and iron proteins." Biochim Biophys Acta **1411**(2-3): 290-309.
- Cotter, G., E. Kaluski, et al. (2003). "LINCS: L-NAME (a NO synthase inhibitor) in the treatment of refractory cardiogenic shock: a prospective randomized study." Eur Heart J **24**(14): 1287-1295.
- Courtney, K. D., R. B. Corcoran, et al. (2010). "The PI3K pathway as drug target in human cancer." J Clin Oncol **28**(6): 1075-1083.

- Cox, A. D. and C. J. Der (2002). "Ras family signaling: therapeutic targeting." Cancer Biol Ther **1**(6): 599-606.
- Crouthamel, M. C., J. A. Kahana, et al. (2009). "Mechanism and management of AKT inhibitor-induced hyperglycemia." Clin Cancer Res **15**(1): 217-225.
- Crowell, J. A., V. E. Steele, et al. (2003). "Is inducible nitric oxide synthase a target for chemoprevention?" Mol Cancer Ther **2**(8): 815-823.
- Dahanukar, A. and R. P. Wharton (1996). "The Nanos gradient in Drosophila embryos is generated by translational regulation." Genes Dev **10**(20): 2610-2620.
- Datta, S. R., A. Brunet, et al. (1999). "Cellular survival: a play in three Akts." Genes Dev **13**(22): 2905-2927.
- Diez, D., F. Sanchez-Jimenez, et al. (2011). "Evolutionary expansion of the Ras switch regulatory module in eukaryotes." Nucleic Acids Res.
- Diggle, T. A., N. T. Redpath, et al. (1998). "Regulation of protein-synthesis elongation-factor-2 kinase by cAMP in adipocytes." Biochem J **336** ( Pt 3): 525-529.
- DiMasi, J. A., R. W. Hansen, et al. (2003). "The price of innovation: new estimates of drug development costs." J Health Econ **22**(2): 151-185.
- Dimmeler, S., I. Fleming, et al. (1999). "Activation of nitric oxide synthase in endothelial cells by Akt-dependent phosphorylation." Nature **399**(6736): 601-605.
- Dittmar, K. A., J. M. Goodenbour, et al. (2006). "Tissue-specific differences in human transfer RNA expression." PLoS Genet **2**(12): e221.
- Donovan, S., K. M. Shannon, et al. (2002). "GTPase activating proteins: critical regulators of intracellular signaling." Biochim Biophys Acta **1602**(1): 23-45.
- Downward, J. (2003). "Targeting RAS signalling pathways in cancer therapy." Nat Rev Cancer **3**(1): 11-22.

- Duan, J. and M. A. Antezana (2003). "Mammalian mutation pressure, synonymous codon choice, and mRNA degradation." J Mol Evol **57**(6): 694-701.
- Dudzinski, D. M., J. Igarashi, et al. (2006). "The regulation and pharmacology of endothelial nitric oxide synthase." Annu Rev Pharmacol Toxicol **46**: 235-276.
- Dudzinski, D. M. and T. Michel (2007). "Life history of eNOS: partners and pathways." Cardiovasc Res **75**(2): 247-260.
- Duplain, H., R. Burcelin, et al. (2001). "Insulin resistance, hyperlipidemia, and hypertension in mice lacking endothelial nitric oxide synthase." Circulation **104**(3): 342-345.
- Elenbaas, B., L. Spirio, et al. (2001). "Human breast cancer cells generated by oncogenic transformation of primary mammary epithelial cells." Genes Dev **15**(1): 50-65.
- Elliott, D. and M. Lodomery (2010). Molecular Biology of RNA. Oxford, UK, Oxford University Press.
- Ellis, C. A. and G. Clark (2000). "The importance of being K-Ras." Cell Signal **12**(7): 425-434.
- Engelman, J. A. (2009). "Targeting PI3K signalling in cancer: opportunities, challenges and limitations." Nat Rev Cancer **9**(8): 550-562.
- Erley, C. M., S. Rebmann, et al. (1995). "Effects of antihypertensive therapy on blood pressure and renal function in rats with hypertension due to chronic blockade of nitric oxide synthesis." Exp Nephrol **3**(5): 293-299.
- Esquela-Kerscher, A., P. Trang, et al. (2008). "The let-7 microRNA reduces tumor growth in mouse models of lung cancer." Cell Cycle **7**(6): 759-764.
- Esteban, L. M., C. Vicario-Abejon, et al. (2001). "Targeted genomic disruption of H-ras and N-ras, individually or in combination, reveals the dispensability of both loci for mouse growth and development." Mol Cell Biol **21**(5): 1444-1452.

- Fath, S., A. P. Bauer, et al. (2011). "Multiparameter RNA and codon optimization: a standardized tool to assess and enhance autologous mammalian gene expression." PLoS One **6**(3): e17596.
- Fayard, E., L. A. Tintignac, et al. (2005). "Protein kinase B/Akt at a glance." J Cell Sci **118**(Pt 24): 5675-5678.
- Feig, L. A. (2003). "Ral-GTPases: approaching their 15 minutes of fame." Trends Cell Biol **13**(8): 419-425.
- Feldmann, G., R. Beaty, et al. (2007). "Molecular genetics of pancreatic intraepithelial neoplasia." J Hepatobiliary Pancreat Surg **14**(3): 224-232.
- Feldser, D. M., K. K. Kostova, et al. (2010). "Stage-specific sensitivity to p53 restoration during lung cancer progression." Nature **468**(7323): 572-575.
- Ferro, E. and L. Trabalzini (2010). "RalGDS family members couple Ras to Ral signalling and that's not all." Cell Signal **22**(12): 1804-1810.
- Fiordalisi, J. J., R. L. Johnson, 2nd, et al. (2001). "Mammalian expression vectors for Ras family proteins: generation and use of expression constructs to analyze Ras family function." Methods Enzymol **332**: 3-36.
- Fischmann, T. O., A. Hruza, et al. (1999). "Structural characterization of nitric oxide synthase isoforms reveals striking active-site conservation." Nat Struct Biol **6**(3): 233-242.
- Forbes, M. S., B. A. Thornhill, et al. (2007). "Lack of endothelial nitric-oxide synthase leads to progressive focal renal injury." Am J Pathol **170**(1): 87-99.
- Fukumura, D., S. Kashiwagi, et al. (2006). "The role of nitric oxide in tumour progression." Nat Rev Cancer **6**(7): 521-534.
- Fulton, D., J. P. Gratton, et al. (1999). "Regulation of endothelium-derived nitric oxide production by the protein kinase Akt." Nature **399**(6736): 597-601.

- Furchgott, R. F. (1999). "Endothelium-derived relaxing factor: discovery, early studies, and identification as nitric oxide." Biosci Rep **19**(4): 235-251.
- Gades, N. M., A. Ohashi, et al. (2008). "Spontaneous vulvar papillomas in a colony of mice used for pancreatic cancer research." Comp Med **58**(3): 271-275.
- Garnett, M. J. and R. Marais (2004). "Guilty as charged: B-RAF is a human oncogene." Cancer Cell **6**(4): 313-319.
- Garvey, E. P., J. A. Oplinger, et al. (1997). "1400W is a slow, tight binding, and highly selective inhibitor of inducible nitric-oxide synthase in vitro and in vivo." J Biol Chem **272**(8): 4959-4963.
- Geller, D. A. and T. R. Billiar (1998). "Molecular biology of nitric oxide synthases." Cancer Metastasis Rev **17**(1): 7-23.
- Gomez, F. P., J. A. Barbera, et al. (1998). "Effect of nitric oxide synthesis inhibition with nebulized L-NAME on ventilation-perfusion distributions in bronchial asthma." Eur Respir J **12**(4): 865-871.
- Gratton, J. P., M. I. Lin, et al. (2003). "Selective inhibition of tumor microvascular permeability by cavtratin blocks tumor progression in mice." Cancer Cell **4**(1): 31-39.
- Griffith, O. W. and R. G. Kilbourn (1996). "Nitric oxide synthase inhibitors: amino acids." Methods Enzymol **268**: 375-392.
- Grover, R., D. Zaccardelli, et al. (1999). "An open-label dose escalation study of the nitric oxide synthase inhibitor, N(G)-methyl-L-arginine hydrochloride (546C88), in patients with septic shock. Glaxo Wellcome International Septic Shock Study Group." Crit Care Med **27**(5): 913-922.
- Gupta, S., A. R. Ramjaun, et al. (2007). "Binding of ras to phosphoinositide 3-kinase p110alpha is required for ras-driven tumorigenesis in mice." Cell **129**(5): 957-968.
- Gyurko, R., S. Leupen, et al. (2002). "Deletion of exon 6 of the neuronal nitric oxide synthase gene in mice results in hypogonadism and infertility." Endocrinology **143**(7): 2767-2774.

- Hahn, W. C., C. M. Counter, et al. (1999). "Creation of human tumour cells with defined genetic elements." Nature **400**(6743): 464-468.
- Hamad, N. M., J. H. Elconin, et al. (2002). "Distinct requirements for Ras oncogenesis in human versus mouse cells." Genes Dev **16**(16): 2045-2057.
- Hamilton, T. L., M. Stoneley, et al. (2006). "TOPs and their regulation." Biochem Soc Trans **34**(Pt 1): 12-16.
- Han, R. N., S. Babaei, et al. (2004). "Defective lung vascular development and fatal respiratory distress in endothelial NO synthase-deficient mice: a model of alveolar capillary dysplasia?" Circ Res **94**(8): 1115-1123.
- Hanahan, D. and R. A. Weinberg (2000). "The hallmarks of cancer." Cell **100**(1): 57-70.
- Hanahan, D. and R. A. Weinberg (2011). "Hallmarks of cancer: the next generation." Cell **144**(5): 646-674.
- Hancock, J. F. (2003). "Ras proteins: different signals from different locations." Nat Rev Mol Cell Biol **4**(5): 373-384.
- Hara, K., Y. Maruki, et al. (2002). "Raptor, a binding partner of target of rapamycin (TOR), mediates TOR action." Cell **110**(2): 177-189.
- Heidenblad, M., T. Jonson, et al. (2002). "Detailed genomic mapping and expression analyses of 12p amplifications in pancreatic carcinomas reveal a 3.5-Mb target region for amplification." Genes Chromosomes Cancer **34**(2): 211-223.
- Hense, W., N. Anderson, et al. (2010). "Experimentally increased codon bias in the Drosophila Adh gene leads to an increase in larval, but not adult, alcohol dehydrogenase activity." Genetics **184**(2): 547-555.
- Hingorani, S. R., E. F. Petricoin, et al. (2003). "Preinvasive and invasive ductal pancreatic cancer and its early detection in the mouse." Cancer Cell **4**(6): 437-450.

- Hingorani, S. R., L. Wang, et al. (2005). "Trp53R172H and KrasG12D cooperate to promote chromosomal instability and widely metastatic pancreatic ductal adenocarcinoma in mice." Cancer Cell **7**(5): 469-483.
- Hollestelle, A., F. Elstrodt, et al. (2007). "Phosphatidylinositol-3-OH kinase or RAS pathway mutations in human breast cancer cell lines." Mol Cancer Res **5**(2): 195-201.
- Hruban, R. H., N. V. Adsay, et al. (2006). "Pathology of genetically engineered mouse models of pancreatic exocrine cancer: consensus report and recommendations." Cancer Res **66**(1): 95-106.
- Hruban, R. H., A. D. van Mansfeld, et al. (1993). "K-ras oncogene activation in adenocarcinoma of the human pancreas. A study of 82 carcinomas using a combination of mutant-enriched polymerase chain reaction analysis and allele-specific oligonucleotide hybridization." Am J Pathol **143**(2): 545-554.
- Huang, P. L., Z. Huang, et al. (1995). "Hypertension in mice lacking the gene for endothelial nitric oxide synthase." Nature **377**(6546): 239-242.
- Huettner, C. S., P. Zhang, et al. (2000). "Reversibility of acute B-cell leukaemia induced by BCR-ABL1." Nat Genet **24**(1): 57-60.
- Hussey, G. S., A. Chaudhury, et al. (2011). "Identification of an mRNP complex regulating tumorigenesis at the translational elongation step." Mol Cell **41**(4): 419-431.
- Ibiza, S., A. Perez-Rodriguez, et al. (2008). "Endothelial nitric oxide synthase regulates N-Ras activation on the Golgi complex of antigen-stimulated T cells." Proc Natl Acad Sci U S A **105**(30): 10507-10512.
- Ignarro, L. J., G. M. Buga, et al. (1987). "Endothelium-derived relaxing factor produced and released from artery and vein is nitric oxide." Proc Natl Acad Sci U S A **84**(24): 9265-9269.
- Ikemura, T. (1985). "Codon usage and tRNA content in unicellular and multicellular organisms." Mol Biol Evol **2**(1): 13-34.

- Ise, K., K. Nakamura, et al. (2000). "Targeted deletion of the H-ras gene decreases tumor formation in mouse skin carcinogenesis." Oncogene **19**(26): 2951-2956.
- Iwakiri, Y., A. Satoh, et al. (2006). "Nitric oxide synthase generates nitric oxide locally to regulate compartmentalized protein S-nitrosylation and protein trafficking." Proc Natl Acad Sci U S A **103**(52): 19777-19782.
- Jackson, E. L., N. Willis, et al. (2001). "Analysis of lung tumor initiation and progression using conditional expression of oncogenic K-ras." Genes Dev **15**(24): 3243-3248.
- Jackson, R. J. and N. Standart (2007). "How do microRNAs regulate gene expression?" Sci STKE **2007**(367): re1.
- James, G. L., J. L. Goldstein, et al. (1995). "Polylysine and CVIM sequences of K-RasB dictate specificity of prenylation and confer resistance to benzodiazepine peptidomimetic in vitro." J Biol Chem **270**(11): 6221-6226.
- Jemal, A., R. Siegel, et al. (2009). "Cancer statistics, 2009." CA Cancer J Clin **59**(4): 225-249.
- John, J., R. Sohmen, et al. (1990). "Kinetics of interaction of nucleotides with nucleotide-free H-ras p21." Biochemistry **29**(25): 6058-6065.
- Johnson, L., D. Greenbaum, et al. (1997). "K-ras is an essential gene in the mouse with partial functional overlap with N-ras." Genes Dev **11**(19): 2468-2481.
- Johnson, S. M., H. Grosshans, et al. (2005). "RAS is regulated by the let-7 microRNA family." Cell **120**(5): 635-647.
- Josse, J., A. D. Kaiser, et al. (1961). "Enzymatic synthesis of deoxyribonucleic acid. VIII. Frequencies of nearest neighbor base sequences in deoxyribonucleic acid." J Biol Chem **236**: 864-875.
- Junttila, M. R., A. N. Karnezis, et al. (2010). "Selective activation of p53-mediated tumour suppression in high-grade tumours." Nature **468**(7323): 567-571.

- Jura, N., E. Scotto-Lavino, et al. (2006). "Differential modification of Ras proteins by ubiquitination." Mol Cell **21**(5): 679-687.
- Karnoub, A. E. and R. A. Weinberg (2008). "Ras oncogenes: split personalities." Nat Rev Mol Cell Biol **9**(7): 517-531.
- Kashiwagi, S., Y. Izumi, et al. (2005). "NO mediates mural cell recruitment and vessel morphogenesis in murine melanomas and tissue-engineered blood vessels." J Clin Invest **115**(7): 1816-1827.
- Katz, M. E. and F. McCormick (1997). "Signal transduction from multiple Ras effectors." Curr Opin Genet Dev **7**(1): 75-79.
- Keller, J. W., J. L. Franklin, et al. (2007). "Oncogenic KRAS provides a uniquely powerful and variable oncogenic contribution among RAS family members in the colonic epithelium." J Cell Physiol **210**(3): 740-749.
- Kim, K., M. J. Lindstrom, et al. (2002). "Regions of H- and K-ras that provide organ specificity/potency in mammary cancer induction." Cancer Res **62**(5): 1241-1245.
- Kimchi-Sarfaty, C., J. M. Oh, et al. (2007). "A "silent" polymorphism in the MDR1 gene changes substrate specificity." Science **315**(5811): 525-528.
- Kisley, L. R., B. S. Barrett, et al. (2002). "Genetic ablation of inducible nitric oxide synthase decreases mouse lung tumorigenesis." Cancer Res **62**(23): 6850-6856.
- Kleinert, H., A. Pautz, et al. (2004). "Regulation of the expression of inducible nitric oxide synthase." Eur J Pharmacol **500**(1-3): 255-266.
- Kloog, Y. and A. D. Cox (2000). "RAS inhibitors: potential for cancer therapeutics." Mol Med Today **6**(10): 398-402.
- Knowles, R. G. and S. Moncada (1994). "Nitric oxide synthases in mammals." Biochem J **298** ( Pt **2**): 249-258.

- Ko, A. H. and M. A. Tempero (2005). "Treatment of metastatic pancreatic cancer." J Natl Compr Canc Netw **3**(5): 627-636.
- Kohl, N. E., C. A. Omer, et al. (1995). "Inhibition of farnesyltransferase induces regression of mammary and salivary carcinomas in ras transgenic mice." Nat Med **1**(8): 792-797.
- Kohli, M., C. Rago, et al. (2004). "Facile methods for generating human somatic cell gene knockouts using recombinant adeno-associated viruses." Nucleic Acids Res **32**(1): e3.
- Kojda, G., J. B. Laursen, et al. (1999). "Protein expression, vascular reactivity and soluble guanylate cyclase activity in mice lacking the endothelial cell nitric oxide synthase: contributions of NOS isoforms to blood pressure and heart rate control." Cardiovasc Res **42**(1): 206-213.
- Konishi, H., B. Karakas, et al. (2007). "Knock-in of mutant K-ras in nontumorigenic human epithelial cells as a new model for studying K-ras mediated transformation." Cancer Res **67**(18): 8460-8467.
- Kozak, M. (1999). "Initiation of translation in prokaryotes and eukaryotes." Gene **234**(2): 187-208.
- Krege, J. H., J. B. Hodgin, et al. (1995). "A noninvasive computerized tail-cuff system for measuring blood pressure in mice." Hypertension **25**(5): 1111-1115.
- Krengel, U., I. Schlichting, et al. (1990). "Three-dimensional structures of H-ras p21 mutants: molecular basis for their inability to function as signal switch molecules." Cell **62**(3): 539-548.
- Kristof, A. S., P. Goldberg, et al. (1998). "Role of inducible nitric oxide synthase in endotoxin-induced acute lung injury." Am J Respir Crit Care Med **158**(6): 1883-1889.
- Kubota, Y., P. O'Grady, et al. (2011). "Oncogenic Ras abrogates MEK SUMOylation that suppresses the ERK pathway and cell transformation." Nat Cell Biol **13**(3): 282-291.
- Kudla, G., A. W. Murray, et al. (2009). "Coding-sequence determinants of gene expression in Escherichia coli." Science **324**(5924): 255-258.

- Kumar, M. S., S. J. Erkeland, et al. (2008). "Suppression of non-small cell lung tumor development by the let-7 microRNA family." Proc Natl Acad Sci U S A **105**(10): 3903-3908.
- Kurihara, N., M. E. Alfie, et al. (1998). "Role of nNOS in blood pressure regulation in eNOS null mutant mice." Hypertension **32**(5): 856-861.
- Lamas, S., P. A. Marsden, et al. (1992). "Endothelial nitric oxide synthase: molecular cloning and characterization of a distinct constitutive enzyme isoform." Proc Natl Acad Sci U S A **89**(14): 6348-6352.
- Lander, H. M., A. J. Milbank, et al. (1996). "Redox regulation of cell signalling." Nature **381**(6581): 380-381.
- Lane, P., G. Hao, et al. (2001). "S-nitrosylation is emerging as a specific and fundamental posttranslational protein modification: head-to-head comparison with O-phosphorylation." Sci STKE **2001**(86): re1.
- Lau, K. S. and K. M. Haigis (2009). "Non-redundancy within the RAS oncogene family: insights into mutational disparities in cancer." Mol Cells **28**(4): 315-320.
- Laubach, V. E., E. G. Shesely, et al. (1995). "Mice lacking inducible nitric oxide synthase are not resistant to lipopolysaccharide-induced death." Proc Natl Acad Sci U S A **92**(23): 10688-10692.
- Lee, P. C., A. N. Salyapongse, et al. (1999). "Impaired wound healing and angiogenesis in eNOS-deficient mice." Am J Physiol **277**(4 Pt 2): H1600-1608.
- Lepori, M., C. Sartori, et al. (1998). "Haemodynamic and sympathetic effects of inhibition of nitric oxide synthase by systemic infusion of N(G)-monomethyl-L-arginine into humans are dose dependent." J Hypertens **16**(4): 519-523.
- Lewis, B. P., I. H. Shih, et al. (2003). "Prediction of mammalian microRNA targets." Cell **115**(7): 787-798.
- Li, C., D. G. Heidt, et al. (2007). "Identification of pancreatic cancer stem cells." Cancer Res **67**(3): 1030-1037.

- Lim, K. H., B. B. Ancrile, et al. (2008). "Tumour maintenance is mediated by eNOS." Nature **452**(7187): 646-649.
- Lim, K. H. and C. M. Counter (2005). "Reduction in the requirement of oncogenic Ras signaling to activation of PI3K/AKT pathway during tumor maintenance." Cancer Cell **8**(5): 381-392.
- Lin, A. W. and S. W. Lowe (2001). "Oncogenic ras activates the ARF-p53 pathway to suppress epithelial cell transformation." Proc Natl Acad Sci U S A **98**(9): 5025-5030.
- Linardic, C. M., D. L. Downie, et al. (2005). "Genetic modeling of human rhabdomyosarcoma." Cancer Res **65**(11): 4490-4495.
- Little, A. S., K. Balmanno, et al. (2011). "Amplification of the Driving Oncogene, KRAS or BRAF, Underpins Acquired Resistance to MEK1/2 Inhibitors in Colorectal Cancer Cells." Sci Signal **4**(166): ra17.
- Liu, M. L., F. C. Von Lintig, et al. (1998). "Amplification of Ki-ras and elevation of MAP kinase activity during mammary tumor progression in C3(1)/SV40 Tag transgenic mice." Oncogene **17**(18): 2403-2411.
- Liu, P., H. Cheng, et al. (2009). "Targeting the phosphoinositide 3-kinase pathway in cancer." Nat Rev Drug Discov **8**(8): 627-644.
- Livingstone, M., E. Atas, et al. (2010). "Mechanisms governing the control of mRNA translation." Phys Biol **7**(2): 021001.
- Lohr, M., G. Kloppel, et al. (2005). "Frequency of K-ras mutations in pancreatic intraductal neoplasias associated with pancreatic ductal adenocarcinoma and chronic pancreatitis: a meta-analysis." Neoplasia **7**(1): 17-23.
- Lopez, A., J. A. Lorente, et al. (2004). "Multiple-center, randomized, placebo-controlled, double-blind study of the nitric oxide synthase inhibitor 546C88: effect on survival in patients with septic shock." Crit Care Med **32**(1): 21-30.
- Lowy, D. R. and B. M. Willumsen (1993). "Function and regulation of ras." Annu Rev Biochem **62**: 851-891.

- Ma, W. W. and A. A. Adjei (2009). "Novel agents on the horizon for cancer therapy." CA Cancer J Clin **59**(2): 111-137.
- MacMicking, J. D., R. J. North, et al. (1997). "Identification of nitric oxide synthase as a protective locus against tuberculosis." Proc Natl Acad Sci U S A **94**(10): 5243-5248.
- Majewski, J. and J. Ott (2002). "Distribution and characterization of regulatory elements in the human genome." Genome Res **12**(12): 1827-1836.
- Malumbres, M. and M. Barbacid (2003). "RAS oncogenes: the first 30 years." Nat Rev Cancer **3**(6): 459-465.
- Mannick, J. B., C. Schonhoff, et al. (2001). "S-Nitrosylation of mitochondrial caspases." J Cell Biol **154**(6): 1111-1116.
- Mao, J. H., M. D. To, et al. (2004). "Mutually exclusive mutations of the Pten and ras pathways in skin tumor progression." Genes Dev **18**(15): 1800-1805.
- Marin, P., K. L. Nastiuk, et al. (1997). "Glutamate-dependent phosphorylation of elongation factor-2 and inhibition of protein synthesis in neurons." J Neurosci **17**(10): 3445-3454.
- Maroney, P. A., Y. Yu, et al. (2006). "Evidence that microRNAs are associated with translating messenger RNAs in human cells." Nat Struct Mol Biol **13**(12): 1102-1107.
- Marshall, L., N. S. Kenneth, et al. (2008). "Elevated tRNA(iMet) synthesis can drive cell proliferation and oncogenic transformation." Cell **133**(1): 78-89.
- Martinez, A. (1995). "Nitric oxide synthase in invertebrates." Histochem J **27**(10): 770-776.
- Matallanas, D., I. Arozarena, et al. (2003). "Differences on the inhibitory specificities of H-Ras, K-Ras, and N-Ras (N17) dominant negative mutants are related to their membrane microlocalization." J Biol Chem **278**(7): 4572-4581.
- Mazur, P. K., B. M. Gruner, et al. (2010). "Identification of epidermal Pdx1 expression discloses different roles of Notch1 and Notch2 in murine Kras(G12D)-induced skin carcinogenesis in vivo." PLoS One **5**(10): e13578.

- McCabe, T. J., D. Fulton, et al. (2000). "Enhanced electron flux and reduced calmodulin dissociation may explain "calcium-independent" eNOS activation by phosphorylation." J Biol Chem **275**(9): 6123-6128.
- McCormick, F. (1999). "Signalling networks that cause cancer." Trends Cell Biol **9**(12): M53-56.
- Means, A. R. and C. D. Rasmussen (1988). "Calcium, calmodulin and cell proliferation." Cell Calcium **9**(5-6): 313-319.
- Michel, J. B., O. Feron, et al. (1997). "Caveolin versus calmodulin. Counterbalancing allosteric modulators of endothelial nitric oxide synthase." J Biol Chem **272**(41): 25907-25912.
- Michell, B. J., J. E. Griffiths, et al. (1999). "The Akt kinase signals directly to endothelial nitric oxide synthase." Curr Biol **9**(15): 845-848.
- Misko, T. P., W. M. Moore, et al. (1993). "Selective inhibition of the inducible nitric oxide synthase by aminoguanidine." Eur J Pharmacol **233**(1): 119-125.
- Mita, H., M. Toyota, et al. (2009). "A novel method, digital genome scanning detects KRAS gene amplification in gastric cancers: involvement of overexpressed wild-type KRAS in downstream signaling and cancer cell growth." BMC Cancer **9**: 198.
- Mita, K., S. Ichimura, et al. (1994). "Highly repetitive structure and its organization of the silk fibroin gene." J Mol Evol **38**(6): 583-592.
- Mocellin, S., V. Bronte, et al. (2007). "Nitric oxide, a double edged sword in cancer biology: searching for therapeutic opportunities." Med Res Rev **27**(3): 317-352.
- Modrek, B., L. Ge, et al. (2009). "Oncogenic activating mutations are associated with local copy gain." Mol Cancer Res **7**(8): 1244-1252.
- Mohamad, N. A., G. P. Cricco, et al. (2009). "Aminoguanidine impedes human pancreatic tumor growth and metastasis development in nude mice." World J Gastroenterol **15**(9): 1065-1071.

- Moncada, S. and A. Higgs (1993). "The L-arginine-nitric oxide pathway." N Engl J Med **329**(27): 2002-2012.
- Montagut, C. and J. Settleman (2009). "Targeting the RAF-MEK-ERK pathway in cancer therapy." Cancer Lett **283**(2): 125-134.
- Moore, M. J., D. Goldstein, et al. (2007). "Erlotinib plus gemcitabine compared with gemcitabine alone in patients with advanced pancreatic cancer: a phase III trial of the National Cancer Institute of Canada Clinical Trials Group." J Clin Oncol **25**(15): 1960-1966.
- Morgan, D. R., B. Silke, et al. (2003). "Central and peripheral haemodynamic effects of L-NAME infusion in healthy volunteers." Eur J Clin Pharmacol **59**(3): 195-199.
- Morishita, T., M. Tsutsui, et al. (2005). "Nephrogenic diabetes insipidus in mice lacking all nitric oxide synthase isoforms." Proc Natl Acad Sci U S A **102**(30): 10616-10621.
- Morley, S. J. and J. A. Traugh (1993). "Stimulation of translation in 3T3-L1 cells in response to insulin and phorbol ester is directly correlated with increased phosphate labelling of initiation factor (eIF-) 4F and ribosomal protein S6." Biochimie **75**(11): 985-989.
- Morton, D. B., M. L. Hudson, et al. (1999). "Soluble guanylyl cyclases in *Caenorhabditis elegans*: NO is not the answer." Curr Biol **9**(15): R546-547.
- Mount, P. F. and D. A. Power (2006). "Nitric oxide in the kidney: functions and regulation of synthesis." Acta Physiol (Oxf) **187**(4): 433-446.
- Muldowney, J. A., 3rd, S. N. Davis, et al. (2004). "NO synthase inhibition increases aldosterone in humans." Hypertension **44**(5): 739-745.
- Nakamura, K., H. Ichise, et al. (2008). "Partial functional overlap of the three ras genes in mouse embryonic development." Oncogene **27**(21): 2961-2968.
- Nakamura, Y., T. Gojobori, et al. (2000). "Codon usage tabulated from international DNA sequence databases: status for the year 2000." Nucleic Acids Res **28**(1): 292.

- Nakamura, Y., K. Ito, et al. (1996). "Emerging understanding of translation termination." Cell **87**(2): 147-150.
- Nathan, C. (1997). "Inducible nitric oxide synthase: what difference does it make?" J Clin Invest **100**(10): 2417-2423.
- Navarro-Cid, J., R. Maeso, et al. (1996). "Renal and vascular consequences of the chronic nitric oxide synthase inhibition. Effects of antihypertensive drugs." Am J Hypertens **9**(11): 1077-1083.
- Nelson, R. J., G. E. Demas, et al. (1995). "Behavioural abnormalities in male mice lacking neuronal nitric oxide synthase." Nature **378**(6555): 383-386.
- Neri, A., D. M. Knowles, et al. (1988). "Analysis of RAS oncogene mutations in human lymphoid malignancies." Proc Natl Acad Sci U S A **85**(23): 9268-9272.
- Newton, A. C. (1995). "Protein kinase C: structure, function, and regulation." J Biol Chem **270**(48): 28495-28498.
- Nowell, P. C. (1976). "The clonal evolution of tumor cell populations." Science **194**(4260): 23-28.
- O'Hagan, R. C., S. Chang, et al. (2002). "Telomere dysfunction provokes regional amplification and deletion in cancer genomes." Cancer Cell **2**(2): 149-155.
- O'Hayer, K. M. and C. M. Counter (2006). "A genetically defined normal human somatic cell system to study ras oncogenesis in vivo and in vitro." Methods Enzymol **407**: 637-647.
- Olive, K. P., M. A. Jacobetz, et al. (2009). "Inhibition of Hedgehog signaling enhances delivery of chemotherapy in a mouse model of pancreatic cancer." Science **324**(5933): 1457-1461.
- Olive, K. P., D. A. Tuveson, et al. (2004). "Mutant p53 gain of function in two mouse models of Li-Fraumeni syndrome." Cell **119**(6): 847-860.
- Oliveira, J. B., N. Bidere, et al. (2007). "NRAS mutation causes a human autoimmune lymphoproliferative syndrome." Proc Natl Acad Sci U S A **104**(21): 8953-8958.

- Omerovic, J., A. J. Laude, et al. (2007). "Ras proteins: paradigms for compartmentalised and isoform-specific signalling." Cell Mol Life Sci **64**(19-20): 2575-2589.
- Omholt, K., S. Karsberg, et al. (2002). "Screening of N-ras codon 61 mutations in paired primary and metastatic cutaneous melanomas: mutations occur early and persist throughout tumor progression." Clin Cancer Res **8**(11): 3468-3474.
- Pallares, P., R. A. Garcia-Fernandez, et al. (2008). "Disruption of the endothelial nitric oxide synthase gene affects ovulation, fertilization and early embryo survival in a knockout mouse model." Reproduction **136**(5): 573-579.
- Palmer, R. M., A. G. Ferrige, et al. (1987). "Nitric oxide release accounts for the biological activity of endothelium-derived relaxing factor." Nature **327**(6122): 524-526.
- Parikh, C., R. Subrahmanyam, et al. (2007). "Oncogenic NRAS, KRAS, and HRAS exhibit different leukemogenic potentials in mice." Cancer Res **67**(15): 7139-7146.
- Parmley, J. L. and M. A. Huynen (2009). "Clustering of codons with rare cognate tRNAs in human genes suggests an extra level of expression regulation." PLoS Genet **5**(7): e1000548.
- Plotkin, J. B. and G. Kudla (2011). "Synonymous but not the same: the causes and consequences of codon bias." Nat Rev Genet **12**(1): 32-42.
- Plowman, S. J., D. J. Williamson, et al. (2003). "While K-ras is essential for mouse development, expression of the K-ras 4A splice variant is dispensable." Mol Cell Biol **23**(24): 9245-9250.
- Poliseno, L., L. Salmena, et al. (2010). "A coding-independent function of gene and pseudogene mRNAs regulates tumour biology." Nature **465**(7301): 1033-1038.
- Potenza, N., C. Vecchione, et al. (2005). "Replacement of K-Ras with H-Ras supports normal embryonic development despite inducing cardiovascular pathology in adult mice." EMBO Rep **6**(5): 432-437.
- Prior, I. A., A. Harding, et al. (2001). "GTP-dependent segregation of H-ras from lipid rafts is required for biological activity." Nat Cell Biol **3**(4): 368-375.

- Protzel, A. and A. J. Morris (1974). "Gel chromatographic analysis of nascent globin chains. Evidence of nonuniform size distribution." J Biol Chem **249**(14): 4594-4600.
- Qian, J., J. Niu, et al. (2005). "In vitro modeling of human pancreatic duct epithelial cell transformation defines gene expression changes induced by K-ras oncogenic activation in pancreatic carcinogenesis." Cancer Res **65**(12): 5045-5053.
- Quilliam, L. A., J. F. Rebhun, et al. (2002). "A growing family of guanine nucleotide exchange factors is responsible for activation of Ras-family GTPases." Prog Nucleic Acid Res Mol Biol **71**: 391-444.
- Quinlan, M. P., S. E. Quatela, et al. (2008). "Activated Kras, but not Hras or Nras, may initiate tumors of endodermal origin via stem cell expansion." Mol Cell Biol **28**(8): 2659-2674.
- Quinlan, M. P. and J. Settleman (2009). "Isoform-specific ras functions in development and cancer." Future Oncol **5**(1): 105-116.
- Quintanilla, M., K. Brown, et al. (1986). "Carcinogen-specific mutation and amplification of H-ras during mouse skin carcinogenesis." Nature **322**(6074): 78-80.
- Quintas-Cardama, A., H. Kantarjian, et al. (2007). "Flying under the radar: the new wave of BCR-ABL inhibitors." Nat Rev Drug Discov **6**(10): 834-848.
- Radinsky, R., P. M. Kraemer, et al. (1987). "Amplification and rearrangement of the Kirsten ras oncogene in virus-transformed BALB/c 3T3 cells during malignant tumor progression." Proc Natl Acad Sci U S A **84**(15): 5143-5147.
- Rago, C., B. Vogelstein, et al. (2007). "Genetic knockouts and knockins in human somatic cells." Nat Protoc **2**(11): 2734-2746.
- Rajagopalan, H., A. Bardelli, et al. (2002). "Tumorigenesis: RAF/RAS oncogenes and mismatch-repair status." Nature **418**(6901): 934.
- Rangarajan, A., S. J. Hong, et al. (2004). "Species- and cell type-specific requirements for cellular transformation." Cancer Cell **6**(2): 171-183.

- Rasmussen, C. D. and A. R. Means (1989). "Calmodulin is required for cell-cycle progression during G1 and mitosis." EMBO J **8**(1): 73-82.
- Redpath, N. T. and C. G. Proud (1993). "Cyclic AMP-dependent protein kinase phosphorylates rabbit reticulocyte elongation factor-2 kinase and induces calcium-independent activity." Biochem J **293 ( Pt 1)**: 31-34.
- Regulski, M. and T. Tully (1995). "Molecular and biochemical characterization of dNOS: a *Drosophila* Ca<sup>2+</sup>/calmodulin-dependent nitric oxide synthase." Proc Natl Acad Sci U S A **92**(20): 9072-9076.
- Reuther, G. W. and C. J. Der (2000). "The Ras branch of small GTPases: Ras family members don't fall far from the tree." Curr Opin Cell Biol **12**(2): 157-165.
- Rhodes, N., D. A. Heerding, et al. (2008). "Characterization of an Akt kinase inhibitor with potent pharmacodynamic and antitumor activity." Cancer Res **68**(7): 2366-2374.
- Ribeiro, M. O., E. Antunes, et al. (1992). "Chronic inhibition of nitric oxide synthesis. A new model of arterial hypertension." Hypertension **20**(3): 298-303.
- Ritchie, J. L., H. D. Alexander, et al. (2002). "Effect of nitric oxide modulation on systemic haemodynamics and platelet activation determined by P-selectin expression." Br J Haematol **116**(4): 892-898.
- Robinson, F., R. J. Jackson, et al. (2008). "Expression of human nPTB is limited by extreme suboptimal codon content." PLoS One **3**(3): e1801.
- Rodriguez-Viciano, P., C. Sabatier, et al. (2004). "Signaling specificity by Ras family GTPases is determined by the full spectrum of effectors they regulate." Mol Cell Biol **24**(11): 4943-4954.
- Rotchell, J. M., J. S. Lee, et al. (2001). "Structure, expression and activation of fish ras genes." Aquat Toxicol **55**(1-2): 1-21.
- Ryazanov, A. G. (1987). "Ca<sup>2+</sup>/calmodulin-dependent phosphorylation of elongation factor 2." FEBS Lett **214**(2): 331-334.

- Ryazanov, A. G. and E. K. Davydova (1989). "Mechanism of elongation factor 2 (EF-2) inactivation upon phosphorylation. Phosphorylated EF-2 is unable to catalyze translocation." FEBS Lett **251**(1-2): 187-190.
- Saha, S., A. Bardelli, et al. (2001). "A phosphatase associated with metastasis of colorectal cancer." Science **294**(5545): 1343-1346.
- Sankaranarayanan, R. and D. Moras (2001). "The fidelity of the translation of the genetic code." Acta Biochim Pol **48**(2): 323-335.
- Sarkisian, C. J., B. A. Keister, et al. (2007). "Dose-dependent oncogene-induced senescence in vivo and its evasion during mammary tumorigenesis." Nat Cell Biol **9**(5): 493-505.
- Sasaki, H., Y. Hikosaka, et al. (2011). "Evaluation of Kras gene mutation and copy number gain in non-small cell lung cancer." J Thorac Oncol **6**(1): 15-20.
- Scheffzek, K., M. R. Ahmadian, et al. (1997). "The Ras-RasGAP complex: structural basis for GTPase activation and its loss in oncogenic Ras mutants." Science **277**(5324): 333-338.
- Schleger, C., N. Arens, et al. (2000). "Identification of frequent chromosomal aberrations in ductal adenocarcinoma of the pancreas by comparative genomic hybridization (CGH)." J Pathol **191**(1): 27-32.
- Schluter, D., M. Deckert-Schluter, et al. (1999). "Inhibition of inducible nitric oxide synthase exacerbates chronic cerebral toxoplasmosis in Toxoplasma gondii-susceptible C57BL/6 mice but does not reactivate the latent disease in T. gondii-resistant BALB/c mice." J Immunol **162**(6): 3512-3518.
- Schmidt, H. H., G. D. Gagne, et al. (1992). "Mapping of neural nitric oxide synthase in the rat suggests frequent co-localization with NADPH diaphorase but not with soluble guanylyl cyclase, and novel paraneural functions for nitrinergic signal transduction." J Histochem Cytochem **40**(10): 1439-1456.
- Schubbert, S., K. Shannon, et al. (2007). "Hyperactive Ras in developmental disorders and cancer." Nat Rev Cancer **7**(4): 295-308.

- Schubbert, S., M. Zenker, et al. (2006). "Germline KRAS mutations cause Noonan syndrome." Nat Genet **38**(3): 331-336.
- Schuhmacher, A. J., C. Guerra, et al. (2008). "A mouse model for Costello syndrome reveals an Ang II-mediated hypertensive condition." J Clin Invest **118**(6): 2169-2179.
- Sebolt-Leopold, J. S. and R. Herrera (2004). "Targeting the mitogen-activated protein kinase cascade to treat cancer." Nat Rev Cancer **4**(12): 937-947.
- Seligsohn, E. E. and A. Bill (1993). "Effects of NG-nitro-L-arginine methyl ester on the cardiovascular system of the anaesthetized rabbit and on the cardiovascular response to thyrotropin-releasing hormone." Br J Pharmacol **109**(4): 1219-1225.
- Serrano, M., A. W. Lin, et al. (1997). "Oncogenic ras provokes premature cell senescence associated with accumulation of p53 and p16INK4a." Cell **88**(5): 593-602.
- Seth, D. and J. S. Stamler (2011). "The SNO-proteome: causation and classifications." Curr Opin Chem Biol **15**(1): 129-136.
- Shapiro, P. (2002). "Ras-MAP kinase signaling pathways and control of cell proliferation: relevance to cancer therapy." Crit Rev Clin Lab Sci **39**(4-5): 285-330.
- Sharma, S. V., D. W. Bell, et al. (2007). "Epidermal growth factor receptor mutations in lung cancer." Nat Rev Cancer **7**(3): 169-181.
- Sharp, P. M., M. Averof, et al. (1995). "DNA sequence evolution: the sounds of silence." Philos Trans R Soc Lond B Biol Sci **349**(1329): 241-247.
- Sharp, P. M. and E. Cowe (1991). "Synonymous codon usage in *Saccharomyces cerevisiae*." Yeast **7**(7): 657-678.
- Sharp, P. M., T. M. Tuohy, et al. (1986). "Codon usage in yeast: cluster analysis clearly differentiates highly and lowly expressed genes." Nucleic Acids Res **14**(13): 5125-5143.
- Shaul, P. W., E. J. Smart, et al. (1996). "Acylation targets endothelial nitric-oxide synthase to plasmalemmal caveolae." J Biol Chem **271**(11): 6518-6522.

- Shaul, Y. D. and R. Seger (2007). "The MEK/ERK cascade: from signaling specificity to diverse functions." Biochim Biophys Acta **1773**(8): 1213-1226.
- Shaw, A. T., A. Meissner, et al. (2007). "Sprouty-2 regulates oncogenic K-ras in lung development and tumorigenesis." Genes Dev **21**(6): 694-707.
- Shesely, E. G., N. Maeda, et al. (1996). "Elevated blood pressures in mice lacking endothelial nitric oxide synthase." Proc Natl Acad Sci U S A **93**(23): 13176-13181.
- Shields, J. M., K. Pruitt, et al. (2000). "Understanding Ras: 'it ain't over 'til it's over'." Trends Cell Biol **10**(4): 147-154.
- Simpson, L. and R. Parsons (2001). "PTEN: life as a tumor suppressor." Exp Cell Res **264**(1): 29-41.
- Singh, M., A. Lima, et al. (2010). "Assessing therapeutic responses in Kras mutant cancers using genetically engineered mouse models." Nat Biotechnol **28**(6): 585-593.
- Smit, V. T., A. J. Boot, et al. (1988). "KRAS codon 12 mutations occur very frequently in pancreatic adenocarcinomas." Nucleic Acids Res **16**(16): 7773-7782.
- Snyder, S. H. (1992). "Nitric oxide: first in a new class of neurotransmitters." Science **257**(5069): 494-496.
- Sokolnicki, L. A., S. K. Roberts, et al. (2007). "Contribution of nitric oxide to cutaneous microvascular dilation in individuals with type 2 diabetes mellitus." Am J Physiol Endocrinol Metab **292**(1): E314-318.
- Sonenberg, N., J. W. B. Hershey, et al. (2000). Translational control of gene expression. Cold Spring Harbor, NY, Cold Spring Harbor Laboratory Press.
- Sousa, S. F., P. A. Fernandes, et al. (2008). "Farnesyltransferase inhibitors: a detailed chemical view on an elusive biological problem." Curr Med Chem **15**(15): 1478-1492.
- Stamler, J. S., S. Lamas, et al. (2001). "Nitrosylation. the prototypic redox-based signaling mechanism." Cell **106**(6): 675-683.

- Stamler, J. S., D. J. Singel, et al. (1992). "Biochemistry of nitric oxide and its redox-activated forms." Science **258**(5090): 1898-1902.
- Stansfield, I., K. M. Jones, et al. (1995). "The end in sight: terminating translation in eukaryotes." Trends Biochem Sci **20**(12): 489-491.
- Stanton, V. P., Jr., D. W. Nichols, et al. (1989). "Definition of the human raf amino-terminal regulatory region by deletion mutagenesis." Mol Cell Biol **9**(2): 639-647.
- Stone, J. R. and M. A. Marletta (1994). "Soluble guanylate cyclase from bovine lung: activation with nitric oxide and carbon monoxide and spectral characterization of the ferrous and ferric states." Biochemistry **33**(18): 5636-5640.
- Stuehr, D. J. (1999). "Mammalian nitric oxide synthases." Biochim Biophys Acta **1411**(2-3): 217-230.
- Svoboda, P. and A. Di Cara (2006). "Hairpin RNA: a secondary structure of primary importance." Cell Mol Life Sci **63**(7-8): 901-908.
- Takahashi, M., T. Kitahashi, et al. (2008). "Increased expression of inducible nitric oxide synthase (iNOS) in N-nitrosobis(2-oxopropyl)amine-induced hamster pancreatic carcinogenesis and prevention of cancer development by ONO-1714, an iNOS inhibitor." Carcinogenesis **29**(8): 1608-1613.
- Takai, Y., T. Sasaki, et al. (2001). "Small GTP-binding proteins." Physiol Rev **81**(1): 153-208.
- Takamizawa, J., H. Konishi, et al. (2004). "Reduced expression of the let-7 microRNAs in human lung cancers in association with shortened postoperative survival." Cancer Res **64**(11): 3753-3756.
- Teichert, A. M., T. L. Miller, et al. (2000). "In vivo expression profile of an endothelial nitric oxide synthase promoter-reporter transgene." Am J Physiol Heart Circ Physiol **278**(4): H1352-1361.
- To, M. D., C. E. Wong, et al. (2008). "Kras regulatory elements and exon 4A determine mutation specificity in lung cancer." Nat Genet **40**(10): 1240-1244.

- Toutenhoofd, S. L. and E. E. Strehler (2000). "The calmodulin multigene family as a unique case of genetic redundancy: multiple levels of regulation to provide spatial and temporal control of calmodulin pools?" Cell Calcium **28**(2): 83-96.
- Traugh, J. A. (2001). "Insulin, phorbol ester and serum regulate the elongation phase of protein synthesis." Prog Mol Subcell Biol **26**: 33-48.
- Trifilieff, A., Y. Fujitani, et al. (2000). "Inducible nitric oxide synthase inhibitors suppress airway inflammation in mice through down-regulation of chemokine expression." J Immunol **165**(3): 1526-1533.
- Tuller, T., A. Carmi, et al. (2010). "An evolutionarily conserved mechanism for controlling the efficiency of protein translation." Cell **141**(2): 344-354.
- Tuller, T., Y. Y. Waldman, et al. (2010). "Translation efficiency is determined by both codon bias and folding energy." Proc Natl Acad Sci U S A **107**(8): 3645-3650.
- Tuveson, D. A., A. T. Shaw, et al. (2004). "Endogenous oncogenic K-ras(G12D) stimulates proliferation and widespread neoplastic and developmental defects." Cancer Cell **5**(4): 375-387.
- Umanoff, H., W. Edelmann, et al. (1995). "The murine N-ras gene is not essential for growth and development." Proc Natl Acad Sci U S A **92**(5): 1709-1713.
- Urrutia, A. O. and L. D. Hurst (2003). "The signature of selection mediated by expression on human genes." Genome Res **13**(10): 2260-2264.
- Vallance, P. and J. Leiper (2002). "Blocking NO synthesis: how, where and why?" Nat Rev Drug Discov **1**(12): 939-950.
- Van Cutsem, E., H. van de Velde, et al. (2004). "Phase III trial of gemcitabine plus tipifarnib compared with gemcitabine plus placebo in advanced pancreatic cancer." J Clin Oncol **22**(8): 1430-1438.
- Velasco, A., E. Bussaglia, et al. (2006). "PIK3CA gene mutations in endometrial carcinoma: correlation with PTEN and K-RAS alterations." Hum Pathol **37**(11): 1465-1472.

- Venema, R. C., H. I. Peters, et al. (1991). "Phosphorylation of elongation factor 1 (EF-1) and valyl-tRNA synthetase by protein kinase C and stimulation of EF-1 activity." J Biol Chem **266**(19): 12574-12580.
- Vigil, D., J. Cherfils, et al. (2010). "Ras superfamily GEFs and GAPs: validated and tractable targets for cancer therapy?" Nat Rev Cancer **10**(12): 842-857.
- Vivanco, I. and C. L. Sawyers (2002). "The phosphatidylinositol 3-Kinase AKT pathway in human cancer." Nat Rev Cancer **2**(7): 489-501.
- Vogelstein, B., E. R. Fearon, et al. (1988). "Genetic alterations during colorectal-tumor development." N Engl J Med **319**(9): 525-532.
- Wagner, P. L., S. Perner, et al. (2009). "In situ evidence of KRAS amplification and association with increased p21 levels in non-small cell lung carcinoma." Am J Clin Pathol **132**(4): 500-505.
- Wang, B., D. Wei, et al. (2003). "A novel model system for studying the double-edged roles of nitric oxide production in pancreatic cancer growth and metastasis." Oncogene **22**(12): 1771-1782.
- Wang, B., Q. Xiong, et al. (2001). "Intact nitric oxide synthase II gene is required for interferon-beta-mediated suppression of growth and metastasis of pancreatic adenocarcinoma." Cancer Res **61**(1): 71-75.
- Wang, R. Y., K. C. Kuo, et al. (1982). "Heat- and alkali-induced deamination of 5-methylcytosine and cytosine residues in DNA." Biochim Biophys Acta **697**(3): 371-377.
- Wang, X., W. Li, et al. (2001). "Regulation of elongation factor 2 kinase by p90(RSK1) and p70 S6 kinase." EMBO J **20**(16): 4370-4379.
- Wang, Y. and M. You (2001). "Alternative splicing of the K-ras gene in mouse tissues and cell lines." Exp Lung Res **27**(3): 255-267.
- Wecht, J. M., J. P. Weir, et al. (2008). "Direct and reflexive effects of nitric oxide synthase inhibition on blood pressure." Am J Physiol Heart Circ Physiol **294**(1): H190-197.

- Wecht, J. M., J. P. Weir, et al. (2007). "Normalization of supine blood pressure after nitric oxide synthase inhibition in persons with tetraplegia." J Spinal Cord Med **30**(1): 5-9.
- Wei, X. Q., I. G. Charles, et al. (1995). "Altered immune responses in mice lacking inducible nitric oxide synthase." Nature **375**(6530): 408-411.
- Weinstein, I. B. and A. Joe (2008). "Oncogene addiction." Cancer Res **68**(9): 3077-3080; discussion 3080.
- Wellbrock, C., M. Karasarides, et al. (2004). "The RAF proteins take centre stage." Nat Rev Mol Cell Biol **5**(11): 875-885.
- Wennerberg, K., K. L. Rossman, et al. (2005). "The Ras superfamily at a glance." J Cell Sci **118**(Pt 5): 843-846.
- White, M. A., C. Nicolette, et al. (1995). "Multiple Ras functions can contribute to mammalian cell transformation." Cell **80**(4): 533-541.
- White, R. J. (2004). "RNA polymerase III transcription and cancer." Oncogene **23**(18): 3208-3216.
- White, R. J. (2005). "RNA polymerases I and III, growth control and cancer." Nat Rev Mol Cell Biol **6**(1): 69-78.
- White, R. J. (2011). "Transcription by RNA polymerase III: more complex than we thought." Nat Rev Genet.
- White, R. J., D. Trouche, et al. (1996). "Repression of RNA polymerase III transcription by the retinoblastoma protein." Nature **382**(6586): 88-90.
- Whitwam, T., M. W. Vanbrocklin, et al. (2007). "Differential oncogenic potential of activated RAS isoforms in melanocytes." Oncogene **26**(31): 4563-4570.
- Whyte, D. B., P. Kirschmeier, et al. (1997). "K- and N-Ras are geranylgeranylated in cells treated with farnesyl protein transferase inhibitors." J Biol Chem **272**(22): 14459-14464.

- Willumsen, B. M., A. Christensen, et al. (1984). "The p21 ras C-terminus is required for transformation and membrane association." Nature **310**(5978): 583-586.
- Winter, A. G., G. Sourvinos, et al. (2000). "RNA polymerase III transcription factor TFIIIC2 is overexpressed in ovarian tumors." Proc Natl Acad Sci U S A **97**(23): 12619-12624.
- Wolin, S. L. and P. Walter (1988). "Ribosome pausing and stacking during translation of a eukaryotic mRNA." EMBO J **7**(11): 3559-3569.
- Wong, K. K. (2009). "Recent developments in anti-cancer agents targeting the Ras/Raf/ MEK/ERK pathway." Recent Pat Anticancer Drug Discov **4**(1): 28-35.
- Worl, J., M. Wiesand, et al. (1994). "Neuronal and endothelial nitric oxide synthase immunoreactivity and NADPH-diaphorase staining in rat and human pancreas: influence of fixation." Histochemistry **102**(5): 353-364.
- Yamada, H., H. Sakamoto, et al. (1986). "Amplifications of both c-Ki-ras with a point mutation and c-myc in a primary pancreatic cancer and its metastatic tumors in lymph nodes." Jpn J Cancer Res **77**(4): 370-375.
- Yamashita, T., S. Kawashima, et al. (2000). "Mechanisms of reduced nitric oxide/cGMP-mediated vasorelaxation in transgenic mice overexpressing endothelial nitric oxide synthase." Hypertension **36**(1): 97-102.
- Yan, J., S. Roy, et al. (1998). "Ras isoforms vary in their ability to activate Raf-1 and phosphoinositide 3-kinase." J Biol Chem **273**(37): 24052-24056.
- Young, C. N., J. P. Fisher, et al. (2009). "Inhibition of nitric oxide synthase evokes central sympatho-excitation in healthy humans." J Physiol **587**(Pt 20): 4977-4986.
- Yu, C. X., S. Li, et al. (2005). "Redox regulation of PTEN by S-nitrosothiols." Mol Pharmacol **68**(3): 847-854.
- Yu, G., X. Liang, et al. (2001). "Diverse effects of chronic treatment with losartan, fosinopril, and amlodipine on apoptosis, angiotensin II in the left ventricle of hypertensive rats." Int J Cardiol **81**(2-3): 123-129; discussion 129-130.

- Zachos, G. and D. A. Spandidos (1997). "Expression of ras proto-oncogenes: regulation and implications in the development of human tumors." Crit Rev Oncol Hematol **26**(2): 65-75.
- Zemojtel, T., R. C. Wade, et al. (2003). "In search of the prototype of nitric oxide synthase." FEBS Lett **554**(1-2): 1-5.
- Zeng, Q., J. M. Dong, et al. (2003). "PRL-3 and PRL-1 promote cell migration, invasion, and metastasis." Cancer Res **63**(11): 2716-2722.
- Zhang, F., S. Saha, et al. (2010). "Differential arginylation of actin isoforms is regulated by coding sequence-dependent degradation." Science **329**(5998): 1534-1537.
- Zhang, F. L., P. Kirschmeier, et al. (1997). "Characterization of Ha-ras, N-ras, Ki-Ras4A, and Ki-Ras4B as in vitro substrates for farnesyl protein transferase and geranylgeranyl protein transferase type I." J Biol Chem **272**(15): 10232-10239.
- Zhang, H., A. Berezov, et al. (2007). "ErbB receptors: from oncogenes to targeted cancer therapies." J Clin Invest **117**(8): 2051-2058.
- Ziche, M., L. Morbidelli, et al. (1994). "Nitric oxide mediates angiogenesis in vivo and endothelial cell growth and migration in vitro promoted by substance P." J Clin Invest **94**(5): 2036-2044.
- Zolotukhin, S., M. Potter, et al. (1996). "A "humanized" green fluorescent protein cDNA adapted for high-level expression in mammalian cells." J Virol **70**(7): 4646-4654.

## Biography

### **BENJAMIN LOGAN LAMPSON**

Born: July 10, 1982 in Miami, Florida

#### **GRADUATE EDUCATION**

**Duke University**, Durham, North Carolina

Combined MD/PhD Medical Scientist Training Program. Start August 2004.

#### **UNDERGRADUATE EDUCATION**

**Duke University**, Durham, North Carolina

BS in both Biomedical and Electrical Engineering, May 2004.

#### **HONORS**

**Alpha Omega Alpha**. Medical honor society. Inducted Spring 2007.

**GlaxoSmithKline – American Foundation for Aging Research Award**. 2009.

**Best Oral Presentation**. GSK/AFAR Symposium on the Biology of Aging. 2010.

**Second Place**. Arnold P. Gold Humanism in Medicine Essay Contest. 2006.

#### **PAPERS**

**Lampson B**. Gold Foundation Essay: Untitled. *Acad Med* 82(11):1112-3.

Byrd JC, Gribben JG, Peterson BL, Grever MR, Lozanski G, Lucas DM, **Lampson B**, Larson RA, Caligiuri MA, Heerema NA. Select high-risk genetic features predict earlier progression following chemoimmunotherapy with fludarabine and rituximab in chronic lymphocytic leukemia: justification for risk-adapted therapy. *J Clin Oncol*. 24(3):437-43.

Duncan CG, Killela PJ, Payne CA, **Lampson B**, Chen WC, Liu J, Solomon D, Waldman T, Towers AJ, Gregory SG, McDonald KL, McLendon RE, Bigner DD, Yan H. Integrated genomic analyses identify *ERF1* and *TACC3* as glioblastoma-targeted genes. *Oncotarget* 1(4):265-77.